INSTITUTO DE BIOCIÊNCIAS
PROGRAMA DE PÓS-GRADUAÇÃO EM BIOLOGIA ANIMAL

GUILHERME LAIZOLA FRAINER CORREA

O ÓRGÃO PRODUTOR DE SOM DOS GOLFINHOS (Odontoceti: Delphinida): FUNCIONALIDADE, ONTOGENIA E EVOLUÇÃO

PORTO ALEGRE
2019

GUILHERME LAIZOLA FRAINER CORREA

O ÓRGÃO PRODUTOR DE SOM DOS GOLFINHOS (Odontoceti: Delphinida): FUNCIONALIDADE, ONTOGENIA E EVOLUÇÃO

Tese apresentada ao Programa de Pós-Graduação em Biologia Animal, Instituto de Biociências da Universidade Federal do Rio Grande do Sul, como requisito parcial à obtenção do título de Doutor em Biologia Animal.

Área de concentração: Biologia Comparada
Orientador: Prof. Dr. Ignacio Benites Moreno

PORTO ALEGRE
2019

GUILHERME LAIZOLA FRAINER CORREA

O ÓRGÃO PRODUTOR DE SOM DOS GOLFINHOS (Odontoceti: Delphinida): FUNCIONALIDADE, ONTOGENIA E EVOLUÇÃO

Aprovado em ____ de _____ de 2019.

BANCA EXAMINADORA

_____
Dr. Aldo Mellender de Araújo
Departamento de Genética, Instituto de Biociências,
Universidade Federal do Rio Grande do Sul (UFRGS)

_____
Dr. Roberto Esser dos Reis
Laboratório de Sistemática de Vertebrados,
Pontificia Universidade Católica do Rio Grande do Sul (PUCRS)

_____
Dr. Cesar Leandro Schultz
Laboratório de Paleontologia de Vertebrados, Instituto de Geociências
Universidade Federal do Rio Grande do Sul (UFRGS)

AGRADECIMENTOS

Esse trabalho é fruto de uma educação de nível superior pública que culmina com essa tese de doutorado. Assim, agradeço de coração à Universidade Federal do Rio Grande do Sul por todas as oportunidades que me foram oferecidas durante a graduação e pós-graduação, aos mestres a mim designados, aos servidores e terceirizados dessa universidade e aos brasileiros em geral que contribuem para que tudo isso exista. Em especial, agradeço ao governo que implantou programas sociais e educacionais como o Programa Ciências sem Fronteiras (201709/2015-5), através do Conselho Nacional de Desenvolvimento Científico e Tecnológico (CNPq), que foi imprescindível para a realização desse trabalho e representou um marco na minha vida profissional. Ainda, agradeço a Coordenação de Aperfeiçoamento de Pessoal de Nível Superior (CAPES) pela bolsa de doutorado concedida durante os quatro últimos anos de formação. Esse trabalho reflete minha formação acadêmica que, em boa parte, é atrelada ao Departamento de Zoologia da Universidade Federal do Rio Grande do Sul, e principalmente aos laboratórios de Ictiologia e de Sistemática e Ecologia de Aves e Mamíferos Marinhos (LABSMAR) os quais sou muito agradecido. Agradeço de coração a todos os funcionários e professores do Centro de Estudos Costeiros, Limnológicos e Marinhos (CECLIMAR/UFRGS). Sou imensamente grato a todos os orientadores e co-orientadores que me acompanharam durante a formação acadêmica e foram importantes para que essa obra saísse dessa maneira, em especial à Prof. Dra. Clarice Fialho, Prof. Dr. Luiz Malabarba, Prof. Dr. Ignacio Moreno e Dr. Stefan Huggenberger. Agradeço a todos os colegas que passaram pelo LABSMAR durante essa minha formação. Um agradecimento muito especial também aos integrantes do Laboratório de Neurociências do Departamento II de Anatomia da Universidade de Colônia, que ajudaram a tornar esse trabalho possível, em especial ao Prof. Dr. Hannsjörg Schröder, Kirsten Pilz, Sigrun Kuhlage. Um agradecimento especial ao Prof. Dr. Ignacio Moreno e ao Dr. Stefan Huggenberger pela confiança no meu trabalho e por toda orientação e ajuda durante esse período. Agradeço a Dra. Stephanie Plön e ao Dr. Anders Galatius pela confiança e colaboração para com esse trabalho. Agradeço também aos curadores e técnicos do Museu de Zoologia de Copenhagen - Dinamarca, Museu de Porto Elizabeth - África do Sul, Museu de Ciências Naturais da UFRGS - Brasil, e da coleção científica do Grupo de Estudos de Mamíferos Aquáticos do Rio Grnde do Sul pelo disponibilidade do material analisado e auxílio durante a coleta de dados. Agradeço a todos que contribuíram com sugestões e ideias para que esse produto final fosse produzido, em especial ao Dr. Tiago Carvalho e ao Prof. Dr. Luiz R. Malabarba, bem como dois revisores anônimos do periódico *The Anatomical Record*. Agradeço muito à banca examinadora por aceitar o convite em julgar esse trabalho.

Meu maior agradecimento vão àquelas pessoas que mais importam na minha vida: minha família. Em especial à minha companheira de vida, minha flor Nathalia Serpa, pelo amor verdadeiro, amizade e carinho. Em especial, também, aos meus pais pelo incentivo, carinho e amizade de sempre; à família Serafini-Frainer e minha afilhada Helena por me ensinarem sentimentos únicos antes desconhecidos; à família Frainer-Coimbra pelo incentivo e amizade; à família Barbosa-Serpa pelo acolhimento e carinho, em especial pra Manuela que tem um espaço no meu coração; ao Giuliano Brusco, que também faz parte da família, pela amizade de sempre; e ao Julian Turm pela amizade e acolhimento em Köln. Por fim, agradeço aos meus poucos e verdadeiros amigos por compartilhar as alegrias da vida e às minhas fontes de inspiração naturais, como a música: a vida não tem movimento sem ritmo. Muito Obrigado!

SUMÁRIO

RESUMO

As estruturas envolvidas na produção do som para comunicação e ecolocalização em três grupos de odontocetos (i.e. Pontoporiidae, Phocoenidae and Delphinidae) foram investigados à luz da anatomia funcional, ontogenia e evolução. Odontocetos evoluíram um complexo sistema de ecolocalização para navegação e forrageio, o qual os permitiu ocupar ambientes pelágicos profundos, costeiros e em bacias hidrográficas. Sons produzidos para a ecolocalização (i.e. *clicks*) e socialização (e.g. *burst clicks* e assobios) são produzidos e modulados no complexo (nasal) epicranial dos golfinhos pelo lado direito e esquerdo, respectivamente. Embora a evolução dos odontocetos é inextricalvelmente relacionada com a habilidade de ecolocalizar, poucos estudos utilizam a anatomia do complexo epicranial - e seu desenvolvimento - à luz da anatomia comparada, filogenia e evolução. O principal objetivo desse estudo foi investigar a evolução das principais estruturas envolvidas na produção e modularidade do som em odontocetos, especialmente em grupos com produção de som com altas frequências e extremamente direcionais. A tese é dividida em quatro capítulos incluindo: uma introdução ao tópico (CAPÍTULO I - O SONAR BIOLÓGICO DOS ODONTOCETOS); a descrição das estruturas produtoras do som no *humpback dolphin* ("golfinho-corcunda") (*Sousa plumbea*) incluindo uma discussão geral sobre a anatomia funcional dessas estruturas em golfinhos (CAPÍTULO II - ANATOMIA FUNCIONAL); uma pesquisa original em que a anatomia comparada dos tecidos moles do nariz em estágios fetais, perinatais, neonatos e adultos dos três grupos de odontocetos citados foi investigada a fim de identificar transformações morfológicas ao longo da ontogenia, as quais foram úteis para identificar os processos heterocrônicos envolvidos na adaptação para a produção do som (CAPÍTULO III - ONTOGENIA E EVOLUÇÃO) a partir de uma análise cladística; um capítulo contendo os principais resultados e conclusões redigido em formato acessível com o intuito de divulgação científica (CAPÍTULO IV - A ORQUESTRA AMEAÇADA DOS ODONTOCETOS); e um capítulo conclusivo (CAPÍTULO V). O "golfinho-corcunda" representa um ótimo modelo comparativo ao golfinho-nariz-de-garrafa ou boto (*Tursiops* sp.) para subsidiar discernimentos sobre a anatomia funcional da produção do som em golfinhos, uma vez que são golfinhos costeiros, exibem tamanho corporal parecidos e apresentam similaridades no comportamento acústico. A análise de reconstrução ancestral de caracteres representou um método cladístico útil para presumir a morfologia dos tecidos moles do nariz de odontocetos extintos, e mapear as principais mudanças relacionadas com a evolução da produção e modulação do som nesses mamíferos altamente sociais e ecolocalizadores. A morfologia do trato nasal em odontocetos evoluiu a partir de processos heterocrônicos envolvidos na formação das estruturas que modulam o som. Demonstramos que, mapeando a evolução de distintas estruturas envolvidas na produção e modulação do som, formas ancestrais de todos os golfinhos conhecidos podem ter exibido morfologia única de tecidos moles adaptada para a produção de sons direcionais e de alta frequência. Em geral, a evolução das estruturas envolvidas na produção do som em odontocetos representa um exemplo didático dos recentes avanços em biologia evolutiva à luz da síntese evolutiva estendida. A evolução de sistema de sonares altamente sofisticados em pequenos golfinhos recentes pode estar relacionado com a vulnerabilidade desses grupos frente à perturbações no ambiente como petrechos de pesca ou de contenção de fauna.

Palavras-chave: anatomia funcional, comunicação, golfinhos, direcionalidade, ecolocalização, evolução, síntese evolutiva extendida, ontogenia, sistemática filogenética.

ABSTRACT

The sound generating structures involved in both communication and echolocation systems of three odontocete groups (i.e. Pontoporiidae, Phocoenidae and Delphinidae) were investigated in the light of the functinal anatomy, ontogeny and evolution. Odontocetes evolved a complex echolocation-based system for navigation and hunting which allowed them to explore deep, pelagic, shallow and freshwater environments. Echolocation (i.e. clicks) and social (e.g. burst-clicks and whistles) sounds are both produced and modulated in the epicranial (nasal) complex of dolphins, respectively at the right and left sides of the nasal passage. Although toothed whale evolution is inextricably related to the ability to echolocate and communicate, few studies have addressed the epicranial complex anatomy - and its development - in the light of comparative anatomy, phylogenetics and evolution. The aim of this thesis was to investigate the evolution of the sound production and modulation in toothed whales, specially those particular narrow-band high frequency species. The thesis is divided in four chapters including: an introduction for the topic (CHAPTER I - THE BIOSONAR OF ODONTOCETES, in Portuguese); a the description of the sound generating structures in the humpback dolphin (*Sounsa plumbea*) and with a general discussion on the functional anatomy of the sound generating structures in dolphins (CHAPTER II - FUNCTIONAL ANATOMY); an original research in which the comparative anatomy of the soft nasal tissues in fetuses, perinatals, neonates and adults of three related odontocete groups were investigated to identify morphological-based ontogenetic transformations. The methods used were useful to detect the heterochronic processes involved in major adaptations for sound production and modulation in dolphins (CHAPTER III - ONTOGENY AND EVOLUTION) in a cladistic point of view; a chapter containing the main results and conclusions in a non-technical style (in Portuguese) for science popularization purposes (CHAPTER IV - THE THREATEN DOLPHIN ORCHESTRY); and a conclusive chapter (CHAPTER V). The Indian Ocean humpback dolphin (*Sousa plumbea*) may represent a useful comparative model to the bottlenose dolphin (*Tursiops* sp.) to provide insights into the functional anatomy of the sound production in dolphins, since these coastal dolphins exhibit similar body size and share similarities on acoustic behavior. The ancestral character reconstruction analysis represented a cladistic method to presume the soft nasal morphology of extinct odontocetes and to map major changes linked with the evolution of the sound production and modulation in these complex echolocating and social mammals. The morphology of the nasal tract in odontocetes evolved under several heterochronic process linked to the development of main structures involved in the sound beam modulation. We demonstrated that, mapping the evolution of distinct structures involved in sound production, the ancestral forms of all known dolphins might have exhibited unique soft nasal tissue morphology adapted for narrow-band high frequency sounds. In general, the evolution of the sound generating structures in toothed whales represent a didactic example for the recent advances in the evolutionary biology. The evolution of specialized sonar systems in odontocetes might address the higher vulnerability of some of these groups in the face of human disturbances such as fishing activities and bather protections.

Keywords: communication, dolphins, directionality, echolocation, evolution, Extended Evolutionary Synthesis, functional anatomy, ontogeny, phylogenetic systematics.

CAPÍTULO I

O SONAR BIOLÓGICO DOS ODONTOCETOS

"*We suggest that echolocation in early odontocetes aided nocturnal feeding on cephalopods and other prey items, and that this early system was an exaptation for hunting deeper at light poor depths where abundant cephalopod resources were available 24 h a day*."

Lindberg e Pyenson (2007) *Lethaia*, 40: 335-343

O SONAR BIOLÓGICO DOS ODONTOCETOS

(Prefácio)

O aparecimento do comportamento de ecolocalização em diversas linhagens de vertebrados é frequentemente associado à mudanças ambientais e à evolução morfológica (Teeling et al., 2005, Lindberg & Pyenson, 2007). Lindberg e Pyenson (2007) sugerem que a origem da ecolocalização em odontocetos (Cetartiodactyla: Odontoceti) se dá no início do Oligoceno (33,9 - 28,4 Ma) e está relacionada aos hábitos noturnos de predação sobre cefalópodes e outros peixes demersais que migram das profundezas do oceano para a superfície todos os dias (migração vertical). Segundo os autores, as mudanças morfológicas relacionadas ao sonar biológico foram marcantes nesse período, como a transição da heterodontia para homodontia (Fordyce, 2003), a assimetria craniana (Cranford et al., 1996, Heyning, 1989) e o primeiro aumento significativo do cérebro (Marino et al., 2004, Marino et al., 2003). No entanto, a complexa relação social desses organismos - medida pela variabilidade de tipos de sons produzidos para comunicação - parece ter grande responsabilidade para o maior tamanho relativo do cérebro em relação aos ancestrais mais próximos (Fox et al., 2017).

Somente comprovado por Norris et al. (1961), o sonar biológico em odontocetos (Cetartiodactyla: Odontoceti) é um sistema complexo destinado à navegação e ao comportamento de forrageio (Au, 2000). Consiste na codificação de ecos e/ou reverberações como informações do ambiente ou presa, a partir de sons gerados pelo próprio animal que os assimila. O som é produzido através da passagem do ar ao longo das vias e sacos de ar presentes no complexo nasal, provocado por movimentos de abertura e fechamento da laringe (Houser et al., 2004), que, com o auxílio do ossos do hióide, mantém a alta pressão de ar necessária para realizar os sons ultrasônicos (Huggenberger et al., 2009). Cada passagem de ar possui uma estrutura chamada lábios-fônicos (phonic lips), onde o ar passa e cria “estalos” (ondas sonoras) em uma série de eventos, resultado da abertura e rápido fechamento da estrutura (Cranford & Amundin, 2003, Dubrovsky et al., 2004, Cranford et al., 2008b). Esses estalos produzidos são conduzidos pela bursa dorsal (Cranford 1988) até o melão, onde as ondas sonoras são colimadas para o ambiente (Evans & Prescott, 1962, Norris et al., 1961, Purves & Pilleri, 1983, Cranford et al., 1997, Aroyan, 2001). Esses pulsos são refletidos pelo ambiente e percebidos pela mandíbula que, através dos corpos gordurosos presentes na janela mandibular, são conduzidos para a bula timpânica e decodificados no cérebro (Norris, 1968, Bullock et al., 1968, Oelschläger, 1986, Huggenberger et al., 2009). Madsen et al. (2013) e Ridgway et al. (2015) sugerem que os dois lados do complexo epicranial produzem sons independentes, possibilitando a emissão de sons voltados para ecolocalização (i.e. lado direito) e comunicação (i.e. lado esquerdo) de maneira simultânea.

Os odontocetos, basicamente, produzem três principais tipos de sons: *clicks*, *burst clicks* e assobios. Os *clicks* são pulsos sonoros de maior frequência e estão relacionadas ao sistema do sonar biológico (Au, 2009). A estrutura física desses sons é única para cada espécie (Akamatsu et al., 2007) e proporcionou a irradiação de Odontoceti em diferentes tipos de ambientes como zonas costeiras, oceânicas e de bacias hidrográficas (Cassens et al., 2000) bem como a diferentes níveis de organização social (May-Collado et al., 2007). Os *burst clicks* são clicks com um intervalos curtos o suficiente para parecem sons contínuos, assim, muitas vezes, denominados "grunhidos" em outras línguas; são comuns a todos os odontocetos exceto cachalotes (*Physeter macrocephalus*), os quais se comunicam por *coda clicks* (i.e. um outro padrão de

pulso sonoro único para o grupo). Os assobios são sons com frequência modulada de curta duração e estão, também, associados à comunicação. A variabilidade morfológica encontrada nas estruturas produtoras do som em odontocetos reflete os diferentes tipos de modularidade sonora encontrada no grupo (Galatius et al., 2018): as propriedades direcionais ocasionadas pela interação do crânio, sacos de ar e dos principais corpos gordurosos do complexo epicranial com a fonte de som na cabeça dos odontocetos foram importantes para a adaptação no sistema de navegação e comunicação nos diferentes grupos. Alguns odontocetos (e.g. *Kogia* spec., *Phocoena phocoena*, *Cephalorhynchus commersonii* e *Pontoporia blainvillei*) evoluíram padrões de clicks com frequência muito superior à maioria dos odontocetos (i.e. frequências maiores que 150 KHz) junto à um feixe estreito de som, as espécies NBHF (*narrow-band high frequency*, espécies com produção de som com alta frequência e de banda estreita). Segundo Kyhn et al. (2010), a emissão de altas frequências por pequenos golfinhos pode estar associado a adaptações para evitar a predação por orcas (Orcinus orca), incapazes de perceber tais frequências; e a emissão múltipla de pulsos de *clicks* pode ser resultado de uma adaptação ao ambiente costeiro, o qual apresenta maior caracterização sonora (ambiente mais ruidoso) devido à ondas e maior concentração de vida comparado ao oceano aberto.

O principal objetivo desse trabalho foi investigar a origem, diversificação, e função (não necessariamente nessa ordem) do órgão responsável pela produção do som em golfinhos através da anatomia comparada. A investigação integrou a embriologia, paleontologia, anatomia comparada de recentes e seus aspectos da história de vida à luz das recentes adaptações da teoria evolutiva. A anatomia funcional das principais estruturas encontradas no complexo epicranial dos golfinhos (Cetartiodactyla: Delphinida) (Lambert et al., 2017) é discutida no Capítulo II da presente tese, uma vez que objetiva a caracterização do aparato emissor do som do "golfinho-corcunda" (sem tradução em português para o *humpback dolphin*) (Frainer et al., 2018): a comparação pertinente dessa espécie com o golfinho-nariz-de-garrafa ou boto (*Tursiops gephyreus*) se dá em virtude da possível distinção dos dois aparatos em relação às suas propriedades direcionais e um hábito de vida similar. A presença do ramo esquerdo em *S. plumbea* explica o porquê desse grupo apresentar maiores frequências na produção de sons para comunicação pois a gordura colima o som produzido de forma a facilitar a passagem de menores comprimentos de onda (Wei et al., 2017). O maior comprimento do rostro pode representar também um sonar biológico mais direcional em *S. plumbea* do que o encontrado em *T. gephyreus*, e, de certa forma, explica a maior mortalidade de adolescentes e adultos dessa espécie em redes de contenção de tubarão na costa da África do Sul (comparada à *Tursiops aduncus*).

O estudo do desenvolvimento do sonar biológico em odontocetos (Frainer et al., 2015, Rauschmann et al., 2006), juntamente com a massiva literatura a respeito da anatomia funcional do complexo epicranial (Cranford et al., 1996, Cranford et al., 2008a, Frainer et al., 2015, Huggenberger et al., 2014, Huggenberger et al., 2010, Huggenberger et al., 2009, Mead, 1975, Schenkkan, 1973) pode não apenas gerar subsídios para o entendimento de aspectos da história de vida e de suas principais ameaças (e.g. captura acidental em redes de emalhe) (Frainer et al., 2015), mas também ser útil como ferramenta taxonômica. Embora os odontocetos tenham evoluído por meio de um sistema de orientação e comunicação baseado na emissão de sons pelo complexo epicranial, poucos trabalhos avaliam a anatomia do sonar biológico - e seu desenvolvimento - à luz da taxonomia e da sistemática filogenética (Heyning, 1989, Kleinenberg & Yablokov, 1958, Mead, 1975, McKenna et al., 2012).

Segundo Kluge (1985), observações na ontogenia dos organismos incluem três usos básicos na sistemática filogenética: (1) podem fornecer subsídios para a determinação de homologias (Wiley, 1981); (2) servir como fonte adicional de informação para o julgamento de relações de parentesco; e (3) servir para a polarização da transformação de um caráter. O último, por sua vez, mais utilizado na cladística (de Queiroz, 1985, Kluge, 1985). de Queiroz (1985) propõe que a anatomia comparada, a paleontologia e a embriologia não são disciplinas distintas para a determinação da polaridade de um caráter (i.e. a direção da transformação) dentro do conceito de evolução. A principal questão dessa tese se deu na busca da origem e da evolução das principais estruturas envolvidas na produção e modulação do som em golfinhos e, para isso, a investigação das mudanças ontogenéticas dessas estruturas foram utilizadas para a criação de caracteres morfológicos a partir da idéia de Fink (1982), seguido de posterior aplicação em uma análise cladística (Geisler et al., 2011). A interpretação dos resultados foi dada á luz da síntese evolutiva estendida (extended evolutionary synthesis) de Laland et al. (2015).

Até pouco tempo atrás, aprendemos que a seleção natural de Charles Darwin (1859) era a única porção criativa da evolução biológica. A Síntese Moderna de Huxley (1942) agregou à Evolução Darwiniana (Bateson, 2017) os conceitos de herança mendeliana, porém não explicava como a forma se diferenciava. A década de 80 e 90 foram marcantes pelo crescimento de estudos voltados para o desenvolvimento e sua variação, bem como sua relação com a evolução dos organismos (evo-devo) e adaptações ecológicas adquiridas (eco-evo-devo) (West-Eberhard, 2003). Fatores epigenéticos como construção de nicho e herança cultural, atraves da transmissão social, são considerados fundamentais para a evolução das espécies (Laland et al., 2015). A teoria estendida de Laland e colaboradores (2015) retoma a idéia de que precisamos (metafisicamente) interpretar a evolução biológica como evolução de ontogenias (Klingenberg, 1998), sendo muitas características compartilhadas dependentes do processo de desenvolvimento do organismo.

O presente trabalho cria um exemplo de interpretação da teoria evolutiva em organismos complexos e carismáticos - o que auxilia nos propósitos de educação - ao mesmo tempo que sugere uma forma de identificar os processos evolutivos integrando áreas da paleontologia, embriologia, anatomia comparada e sistemática filogenética às novas propostas da teoria evolutiva. De maneira específica, propomos a distinção dos ramos direito e esquerdo do melão como estruturas independentes do melão principal (*Corpus adiposum nasalis terminalis*), visto à origem das estruturas nas fases fetais. Assim, ficam claras as diferenças nas transformações ontogenéitcas dessas estruturas através de mecanismos independentes de regulação entre os grupos estudados. Os ramos direito e esquerdo do melão exibem grande variedade de formas entre golfinhos, visto que há grupos em que os ramos são desconectados do melão principal (e.g. *Lagenorhynchus*), com apenas o direito ligado ao melão (e.g. *Pontoporia*), com o esquerdo ausente na fase adulta (e.g. *Tursiops*) ou ainda não são compostos por gordura especializada (e.g. *Phocoena*). A origem do melão em cetáceos corresponde aos grupos fósseis ancestrais a todos os odontocetos que exibem adaptação morfológica do ouvido especializada para a percepção de sons de alta frequência. Ainda, golfinhos atuais parecem apresentar sons mais brandos (i.e. menos direcionais porém com maior intensidade (dB)) em virtude de vários processos heterocrônicos que levaram a modificação das principais estruturas moduladoras do som. Assim, golfinhos que apresentam alta complexidade na modularidade do som, como as espécies NBHF, parecem representar resquícios evolutivos quase desconhecidos - e muito ameaçados - de sonares extremamente complexos.

O alinhamento das bursas com a porção posterior dos ramos do melão e do melão principal durante o desenvolvimento pós-natal é interpretado como um caráter homoplásico que evoluiu independentemente em linhagens evolutivas distintas dentro de Delphinida e podem estar relacionadas com especializações do sonar de alta frequência e direcional. Diferente da maioria dos delfinídeos (i.e. como *Tursiops gephyreus*), *Pontoporia blainvillei*, *Phocoena phocoena* e *Cephalorhynchus commersonii* apresentam elevação na porção posterior (nasal) do osso pré-maxilar, elevando o complexo epicranial e os principais corpos gordurosos logo à frente da passagem nasal. Embora não tenhamos analisado exemplares neonatos de *C. commersonii*, o indivíduo adulto também apresenta o mesmo alinhamento descrito para essas estruturas. Sendo assim, a conformação do sonar biológico encontrado em neonatos de *Phocoena* e *Pontoporia* sugerem uma imaturação morfológica do complexo epicranial nas primeiras fases de vida. Com hábitos estritamente costeiros, *P. blainvillei*, *P. phocoena* e *C. commersonii* tornam-se mais vulneráveis à ações antrópicas, sendo a pesca de emalhe a principal ameaça dessas espécies em que juvenis são capturados em maior número (Trippel et al., 1999, Tregenza et al., 1996, Iñiguez et al., 2003, Slooten et al., 2001, Stone & Yoshinaga, 2000, Secchi et al., 2004, Secchi et al., 1997, Reeves et al., 2013). A mudança na dieta ao longo da ontogenia de *C. commersonii* e *P. blainvillei* (Riccialdelli et al., 2013, Rodríguez et al., 2002) pode representar um período de maturação morfológica e comportamental do sonar biológico que, à luz da biologia da conservação, tornaria os animais juvenis mais suscetíveis à essas ações antrópicas (Frainer et al., 2015). Ainda, as propriedades direcionais do sonar biológico dessas espécies podem estar relacionadas com a mortalidade de adultos e seus críticos status de conservação (ver Capítulo II).

Foto da capa: Ignacio Moreno/CECLIMAR-UFRGS

REFERÊNCIAS BIBLIOGRÁFICAS

Akamatsu, T., Teilmann, J., Miller, L. A., Tougaard, J., Dietz, R., Wang, D., Wang, K., Siebert, U. & Naito, Y. 2007. Comparison of echolocation behaviour between coastal and riverine porpoises. *Deep Sea Research Part II: Topical studies in Oceanography* **54**: 290-297.

Aroyan, J. L. 2001. Three-dimensional modeling of hearing in *Delphinus delphis*. *The Journal of the Acoustical Society of America* **110**: 3305.

Au, W. L. (2000) Hearing in whales and dolphins: An overview. In: *Hearing by whales and dolphins*, (Au, W. L. & Richard, R. F., eds.). pp. 1-42. Springer, New York.

Au, W. L. (2009) Echolocation. In: *Encyclopedia of Marine Mammals*, Vol. 2 (Perrin, W. F., Wursig, B. & Thewissen, J. G. M., eds.). pp. 348-357. American Press, London.

Bateson, P. 2017. Adaptability and evolution. *Interface Focus* **7**: 20160126.

Bullock, T., Grinnell, A., Ikezono, E., Kameda, K., Katsuki, Y., Nomoto, M., Sato, O., Suga, N. & Yanagisawa, K. 1968. Electrophysiological studies of central auditory mechanisms in cetaceans. *Journal of Comparative Physiology A: Neuroethology, Sensory, Neural, and Behavioral Physiology* **59**: 117-156.

Cassens, I., Vicario, S., Waddell, V. G., Balchowsky, H., Van Belle, D., Ding, W., Fan, C., Mohan, R. L., Simões-Lopes, P. C. & Bastida, R. 2000. Independent adaptation to riverine habitats allowed survival of ancient cetacean lineages. *Proceedings of the National Academy of Sciences* **97**: 11343-11347.

Cranford, T. & Amundin, M. (2003) Biosonar pulse production in odontocetes: the state of our knowledge. In: *Echolocation in bats and dolphins. Chicago: The University of Chicago Press.* pp. 27-35.

Cranford , T. W. (1988) The anatomy of acoustic structures in the spinner dolphin forehead as shown by X-ray computed tomography and computer graphics. In: *Animal Sonar: Processes and Performance*, (Nactigall, P. E. & Moore, P. W. B., eds.). pp. 67-77. Plenum Publisher.

Cranford, T. W., Amundin, M. & Norris, K. S. 1996. Functional morphology and homology in the odontocete nasal complex: implications for sound generation. *Journal of Morphology* **228**: 223-285.

Cranford, T. W., Krysl, P. & Hildebrand, J. A. 2008a. Acoustic pathways revealed: Simulated sound transmission and reception in Cuvier's beaked whale (*Ziphius cavirostris*). *Bioinspiration & Biomimetics* **3**: 1-10.

Cranford , T. W., van Bonn, W. G., Chaplin, M. S., Carr, J. A., Kamolnick, T. A., Carder, D. A. & Ridgway, S. H. 1997. Visualizing dolphin sonar signal generation using high-speed video endoscopy. *Journal of Acoustic Society of America* **102**: 3123

Cranford, T. W. C. W., Krysl, P. & Hildebrand, J. A. 2008b. Acoustic pathways revealed: simulated sound transmission and reception in Cuvier's beaked whale (Ziphius cavirostris) using finite element modelling. *Faseb Journal* **22**.

Darwin, C. 1859. *On the origin of the species,* 1 ed. Routledge, London.

de Queiroz, K. 1985. The ontogenetic method for determining character polarity and its relevance to phylogenetic systematics. *Systematic Zoology* **34**: 280-299.

Dubrovsky, N. A., Gladilin, A., Møhl, B. & Wahlberg, M. 2004. Modeling of the dolphin's clicking sound source: The influence of the critical parameters. *Acoustical Physics* **50**: 463-468.

Evans, W. E. & Prescott, J. H. 1962. Observations of the sound production capabilities of the bottlenose porpoise: A study of whistles and clicks. *Zoologica* **47**: 121-128.

Fink, W. L. 1982. The conceptual relationship between ontogeny and phylogeny. *Paleobiology* **8**: 254-264.

Fordyce, R. E. (2003) Cetacean evolution and Eocene-Oligocene oceans In: *From greenhouse to icehouse, the marine Eocene-Oligocene transition*, (Prothero, D. R., Ivany, L. C. & Nesbitt, E. A., eds.). pp. 154-170.

Fox, K. C. R., Muthukrishna, M. & Shultz, S. 2017. The social and cultural roots of whale and dolphin brains. *Nature Ecology & Evolution* **1**: 1699-1705.

Frainer, G., Huggenberger, S. & Moreno, I. B. 2015. Postnatal development of franciscana's (*Pontoporia blainvillei*) biosonar relevant structures with potential implications for function, life history, and bycatch. *Marine Mammal Science* **31**: 1193-1212.

Frainer, G., Plön, S., Serpa, N. B., Moreno, I. B. & Huggenberger, S. 2018. Sound generating structures of the humpback dolphin *Sousa plumbea* (Cuvier, 1829) and the directionality in dolphin sounds. *The Anatomical Record* **0**: 1-12.

Galatius, A., Olsen, M. T., Steeman, M. E., Racicot, R. A., Bradshaw, C. D., Kyhn, L. A. & Miller, L. A. 2018. Raising your voice: evolution of narrow-band high-frequency signals in toothed whales (Odontoceti). *Biological Journal of the Linnean Society* **126**: 213-224.

Geisler, J. H., McGowen, M. R., Yang, G. & Gatesy, J. 2011. A supermatrix analysis of genomic, morphological, and paleontological data from crown Cetacea. *BMC Evolutionary Biology* **11**: 112.

Heyning, J. E. 1989. Comparative facial anatomy of beaked whales (Ziphiidae) and a systematic revision among the families of extant Odontoceti. *Contributions in Science* **405**.

Houser, D. S., Finneran, J., Carder, D., van Bonn, W. G., Smith, S., Hoh, C., Mattrey, R. & Ridgway, S. H. 2004. Structural and functional imaging of bottlenose dolphin (*Tursiops truncatus*) cranial anatomy. *Journal of Experimental Biology* **207**: 3657–3665

Huggenberger, S., André, M. & Oelschlager, H. A. 2014. The nose of the sperm whale: overviews of functional design, structural homologies and evolution. *Journal of the Marine Biological Association of the United Kingdom* **96**: 783-806.

Huggenberger, S., Vogl, T. J. & Oelschläger, H. H. A. 2010. Epicranial complex of the La Plata dolphin (*Pontoporia blainvillei*): Topographical and functional implications. *Marine Mammal Science* **26**: 471-481.

Huggenberger, S. M. A., Rauschmann, M. A. & Oelschläger, H. H. A. 2009. Functional morphology of the hyolaryngeal complex of the harbor porpoise (*Phocoena phocoena*): Implications for its role in sound production and respiration. *The Anatomical Records* **291**: 1262–1270

Huxley, J. 1942. *Evolution - The modern synthesis*. George Allen and Unwin, London.

Iñiguez, M. A., Hevia, M., Gasparrou, C., Tomsin, A. L. & Secchi, E. R. 2003. Preliminary estimate of incidental mortality of Commerson's dolphins (Cephalorhynchus commersonii) in an artisanal setnet fishery in La Angelina Beach and Ría Gallegos, Santa Cruz, Argentina. *Latin American Journal of Aquatic Mammals* **2**: 87-94.

Kleinenberg, S. C. & Yablokov, A. V. 1958. The morphology of the upper respiratory tract of whales. *Zoologichesk¨ zhurnal* **37**: 1091-1099.

Klingenberg, C. P. 1998. Heterochrony and allometry: the analysis of evolutionary change in ontogeny. *Biological Reviews* **73**: 79-123.

Kluge, A. 1985. Ontogeny and phylogenetic systematics. *Cladistics* **1**: 13-27.

Kyhn, L. A., Jensen, F. H., Beedholm, K., Tougaard, J., Hansen, M. & Madsen, P. T. 2010. Echolocation in sympatric Peale's dolphins (*Lagenorhynchus australis*) and Commerson's dolphins (*Cephalorhynchus commersonii*) producing narrow-band high-frequency clicks. *Journal of Experimental Biology* **213**: 1940-1949.

Laland, K. N., Uller, T., Feldman, M. W., Sterelny, K., Müller, G. B., Moczek, A., Jablonka, E. & Odling-Smee, J. 2015. The extended evolutionary synthesis: its structure, assumptions and predictions. *Proceedings of the Royal Society B: Biological Sciences* **282**: 20151019.

Lambert, O., Bianucci, G., Urbina, M. & Geisler, J. H. 2017. A new inioid (Cetacea, Odontoceti, Delphinida) from the Miocene of Peru and the origin of modern dolphin and porpoise families. *Zoological Journal of the Linnean Society* **179**: 919-946.

Lindberg, D. R. & Pyenson, N. D. 2007. Things that go bump in the night: evolutionary interactions between cephalopods and cetaceans in the tertiary. *Lethaia* **40**: 335-343.

Madsen, P. T., Lammers, M., Wisniewska, D. & Beedholm, K. 2013. Nasal sound production in echolocating delphinids (*Tursiops truncatus* and *Pseudorca crassidens*) is dynamic, but unilateral: clicking on the right side and whistling on the left side. *The Journal of Experimental Biology* **216**: 4091-41102.

Marino, L., McShea, D. & Uhen, M. D. 2004. The origin and evolution of large brains in toothed whales. *Anatomical Record-Advances in Integrative Anatomy and Evolutionary Biology* **281A**: 1247–1255.

Marino, L., Uhen, M. D., Pyenson, N. D. & Frohlich, B. 2003. Reconstructing cetacean brain evolution using computed tomography. *Anatomical Record-Advances in Integrative Anatomy and Evolutionary Biology* **272B**: 107–117.

May-Collado, L. J., Agnarsson, I. & Wartzok, D. 2007. Phylogenetic review of tonal sound production in whales in relation to sociality. *BMC Evolutionary Biology* **7**: 136.

McKenna, M. F., Cranford, T. W., Berta, A. & Pyenson, N. D. 2012. Morphology of the odontocete melon and its implications for acoustic function. *Marine Mammal Science* **28**: 690-713.

Mead, J. G. 1975. Anatomy of the external nasal passages and facial complex in the Delphinidae (Mammalia: Cetacea). *Smithsonian Contributions to Zoology* **207**: 1-35.

Norris, K. 1968. The evolution of acoustic mechanisms in odontocete cetaceans. *Evolution and environment*: 297-324.

Norris, K. S., Prescott, J. H., Asa-Dorian, P. V. & Perkins, P. 1961. An experimental demonstration of echo-location behavior in the porpoise, *Tursiops truncatus* (Montagu). *Biological Bulletin* **120**: 163-176.

Oelschläger, H. H. A. 1986. Tympanohyal bone in toothed whales and the formation of the timpano-periotic complex (Mammalia: Cetacea). *Journal of Morphology* **188**: 157-165.

Purves, P. & Pilleri, G. 1983. *Echolocation in whales and dolphins*. Academic Press London.

Rauschmann, M. A., Huggenberger, S., Kossatz, L. S. & Oelschläger, H. H. A. 2006. Head morphology in perinatal dolphins: a window into phylogeny and ontogeny. *Journal of Morphology* **267**: 1295–1315.

Reeves, R. R., McClellan, K. & Werner, T. B. 2013. Marine mammal bycatch in gillnet and other entangling net fisheries, 1990 to 2011. *Endangered Species Research* **20**: 71-97.

Riccialdelli, L., Newsome, S. D., Dellabianca, N. A., Bastida, R., Fogel, M. L. & Goodall, R. N. P. 2013. Ontogenetic diet shift in Commerson's dolphin (*Cephalorhynchus commersonii commersonii*) off Tierra del Fuego. *Polar biology* **36**: 617-627.

Ridgway, S. H., Dibble, D. S., Van Alstyne, K. & Price, D. 2015. On doing two things at once: dolphin brain and nose coordinate sonar clicks, buzzes and emotional squeals with social sounds during fish capture. *Journal of Experimental Biology* **218**: 3987-3995.

Rodríguez, D., Rivero, L. & Bastida, R. 2002. Feeding ecology of the franciscana (*Pontoporia blainvillei*) in marine and estuarine waters of Argentina. *Latin American Journal of Aquatic Mammals* **1**: 77-94.

Schenkkan, E. J. 1973. On the comparative anatomy and function of the nasal tract in odontocetes (Mammalia, Cetacea). *Bijdragen tot de Dierkunde* **43**: 127-159.

Secchi, E. R., Kinas, P. G. & Muelbert, M. 2004. Incidental catches of franciscana in coastal gillnet fisheries in the Franciscana Management Area III: period 1999-2000. *Latin American Journal of Aquatic Mammals* **3**: 61-68

Secchi, E. R., Zerbini, A. N., Bassoi, M., Dalla-Rosa, L., Moller, L. M. & Rocha-Campos, C. C. 1997. Mortality of franciscanas, Pontoporia blainvillei, in coastal gillnetting in southern Brazil: 1994-1995. *Report of the International Whaling Commission* **47**: 653-658

Slooten, E., Fletcher, D. & Taylor, B. L. 2001. Accounting for Uncertainty in Risk Assessment: Case Study of Hector's Dolphin Mortality due to Gillnet Entanglement. *Conservation Biology* **14**: 1264-1270.

Stone, G. S. & Yoshinaga, A. 2000. Hector's Dolphin '*Cephalorhynchus hectori*' Calf Mortalities May Indicate New Risks from Boat Traffic and Habituation. *Pacific Conservation Biology* **6**: 162-170.

Teeling, E. C., Springer, M. S., Madsen, O., Bates, P., O'Brien, S. J. & Murphy, W. J. 2005. A molecular phylogeny for bats illuminates biogeography and the fossil record. *Science* **307**: 580-584.

Tregenza, N. J. C., Berrow, S. D., Hammond, P. S. & Leaper, R. 1996. Harbour porpoise (Phocoena phocoena L.) by-catch in set gillnets in the Celtic Sea. *ICES Journal of Marine Science* **54**: 896-904.

Trippel, E. A., Strong, M. B., Terhune, J. M. & Conway, J. D. 1999. Mitigation of harbour porpoise (Phocoena phocoena) by-catch in the gillnet fishery in the lower Bay of Fundy. *Canadian Journal of Fisheries and Aquatic Sciences* **56**: 113-123.

Wei, C., Au, W. W. L., Ketten, D. R., Song, Z. & Zhang, Y. 2017. Biosonar signal propagation in the harbor porpoise's (*Phocoena phocoena*) head: The role of various structures in the formation of the vertical beam. *The Journal of the Acoustical Society of America* **141**: 4179-4187.

West-Eberhard, M. J. 2003. *Developmental plasticity and evolution*. Oxford University Press, New York.

Wiley, E. O. 1981. *Phylogenetics: the theory and practice of phylogenetic systematics*. Wiley, New York.

CAPÍTULO II

ANATOMIA FUNCIONAL

"A harmonicidade na comunicação dos golfinhos, promovida pelo timbre de seus instrumentos produtores de som e pela maneira como é manipulado, é crucial para a caça em grupo: os golfinhos são coordenados em movimento pelo líder, o qual produz sons com múltiplos harmônicos a fim de demonstrar sua posição junto à informação da tática de caça para os outros membros do grupo."

ver Discussão pág. 26

*Manuscrito submetido e publicado no periódico *The Anatomical Record*


VOL. 302 NO. 6 JUNE 2019
The Anatomical Record
Advances in Integrative Anatomy and Evolutionary Biology
AN OFFICIAL PUBLICATION OF THE AMERICAN ASSOCIATION OF ANATOMISTS
KURT H. ALBERTINE • EDITOR-IN-CHIEF
Celebrating
OVER
100 YEARS
of Excellence in
ANATOMICAL
PUBLICATION

Sound Generating Structures of the Humpback Dolphin *Sousa plumbea* (Cuvier, 1829) and the Directionality in Dolphin Sounds

GUILHERME FRAINER,[1,2,3*] **STEPHANIE PLÖN**,[4] **NATHALIA B. SERPA**,[1,2] **IGNACIO B. MORENO**,[1,2] **AND STEFAN HUGGENBERGER**[3]

[1]Programa de Pós-Graduação em Biologia Animal, Departamento de Zoologia, Universidade Federal do Rio Grande do Sul, 91540-000, Porto Alegre, Brazil
[2]Centro de Estudos Costeiros, Limnológicos e Marinhos (CECLIMAR/UFRGS), Campus Litoral Norte, Universidade Federal do Rio Grande do Sul, 95625-000, Imbé, Brazil
[3]Department II of Anatomy, University of Cologne, 50924, Cologne, Germany
[4]African Earth Observation Network (AEON) -Earth Stewardship Science Research Institute (ESSRI), Nelson Mandela University, 6031, Port Elizabeth, South Africa

ABSTRACT

The macroscopic morphology of structures involved in sound generation in the Indian Ocean humpback dolphin (*Sousa plumbea*) were described for the first time using computed tomography imaging and standard gross dissection techniques. The Indian Ocean humpback dolphin may represent a useful comparative model to the bottlenose dolphin (*Tursiops* sp.) to provide insights into the functional anatomy of the sound production in dolphins, since these coastal dolphins exhibit similar body size and share similarities on acoustic behavior. The general arrangement of sound generating structures, that is, air sacs and muscles, was similar in both the bottlenose dolphin and the Indian Ocean humpback dolphin. The main difference between the two species existed in a small left posterior branch of the melon in the Indian Ocean humpback dolphin, which was not found in the bottlenose dolphin and might reflect an adaptation of directionality for high frequency communication sounds as seen in some other delphinids (e.g., *Lagenorhynchus* sp., *Grampus griseus*). Thus, this may be the main reason for the asymmetry of the sound production structures in dolphins. Additionally, the longer rostrum in Indian Ocean humpback dolphins might suggest a more directional echolocation beam compared to the Lahille's bottlenose dolphin. Anat Rec, 2018. © 2018 Wiley Periodicals, Inc.

Key words: humpback dolphin; sound production; communication; mixed-directionality; echolocation

Grant sponsor: Cetacean Society International; Grant sponsor: Conselho Nacional de Desenvolvimento Científico e Tecnológico; Grant number: 201709/2015-5; Grant sponsor: Coordenação de Aperfeiçoamento de Pessoal de Nível Superior; Grant sponsor: Society for Marine Mammalogy.

*Correspondence to: Guilherme Frainer, Programa de Pós-Graduação em Biologia Animal, Departamento de Zoologia, Universidade Federal do Rio Grande do Sul, 91540-000 Porto Alegre, Brazil. Tel: 55 51 33081267

E-mail: gui.frainer@gmail.com

Received 22 February 2018; Revised 1 June 2018; Accepted 14 July 2018.

DOI: 10.1002/ar.23981

Published online 00 Month 2018 in Wiley Online Library (wileyonlinelibrary.com).

Humpback dolphins, genus *Sousa* Grey 1866 (Odontoceti: Delphinidae), are a poorly known genus of cetaceans divided into four species and restricted to tropical and subtropical near-shore coastal waters of the Eastern Atlantic (*S. teutzi*), Indian (*S. plumbea*), and western Pacific (*S. chinensis, S. sahulensis*) Oceans (Ross *et al.,* 1994; Jefferson and Karczmarski, 2001; Parra and Ross, 2009; Rice, 2009; Mendez *et al.,* 2013). They are adapted to live in bay and estuarine habitats, hunting mainly reef-associated, estuarine and demersal fishes (Barros and Cockcroft, 1991; Ross *et al.,* 1994).

Indian Ocean humpback dolphins off South Africa, *S. plumbea*, measure between 97 and 108 cm at birth and reach 280 cm total length in adult males (Ross *et al.,* 1994; Plön *et al.,* 2015), which makes them the largest of all *Sousa* species (Jefferson and Rosenbaum, 2014). Their comparatively small organ weights indicate that humpback dolphins are shallow divers and relative slow moving delphinids (Plön *et al.,* 2012). Although, they are commonly sighted solitary or in groups with a mean size of only seven individuals (Guissamulo and Cockcroft, 2004), recent studies demonstrated a significant decrease in both mean and maximum group size in South African waters (Plön *et al.,* 2015; Koper *et al.,* 2016). The main threat for this species is the accidental entanglement in shark nets (Atkins *et al.,* 2013, 2016), which is the main catalyst for this work as it seems to indicate that these animals cannot sense these nets.

In the present study, the general morphology of the main structures involved in echolocation and social sound generation of the poorly known humpback dolphin is investigated. The detailed descriptions of the main acoustic fat bodies of the Indian Ocean humpback dolphin with additional comparisons to bottlenose dolphin (*Tursiops* sp.) (see Mead, 1975) were useful in interpreting its function, especially regarding social sounds in dolphins.

Sound generation in dolphins takes place in the center of the epicranial (nasal) complex at the MLDB (monkey-lips dorsal bursae) complex, a structure consisting of a lip-like valve of the nasal passage (monkey lips) and accompanying small fat bodies (posterior and anterior dorsal bursae). Air pressure variation in the nasal cavity promotes repeatedly opening and closing movements of these lips, generating a single click each cycle due to vibrations within the associated MLDB complexes (Cranford *et al.,* 1996, 2011). The sound beam seems to be primarily formed by interactions of the MLDB with the skull and the air sacs to form its directional nature (Aroyan *et al.,* 1992; Au *et al.,* 2010; Wei *et al.,* 2017). Accordingly, the sound travels into a large rostral fat body (melon) which acts as an acoustic wave guide by collimating the sound produced by each MLDB complex anteriorly and contributing to narrow the resultant biosonar beam (Wei *et al.,* 2017). In addition, the heterogeneous composition of the fatty melon attenuates the sound to effectively transmit it into the aquatic environment by impedance matching (Harper *et al.,* 2008; McKenna *et al.,* 2012). In this respect, the shape of the melon seems to play a significant role in refining and collimating the sound produced for echolocation (McKenna *et al.,* 2012; Wei *et al.,* 2017).

Besides the echolocation clicks for hunting and navigation/orientation, dolphins commonly produce pulsed calls (e.g., burst pulses and buzzes) (Henderson *et al.,* 2011) and tonal sounds (i.e., whistles) for communication (May-Collado *et al.,* 2007). Pulsed calls are sequences of clicks characterized by the high repetition rate and low interpulse interval and represent the primary mode of communication of some non-whistling odontocetes (e.g., of the genus *Physeter*, *Kogia*, *Platanista*, *Phocoena*, *Cephalorhynchus*) and as common as whistles in dolphins that produce both (Au, 2000). These sounds are associated with several behavioral contexts, such as socializing, aggression, male alliance, affiliative behaviors, play, social feeding, courtship, and others (Herzing, 2000). Dolphin whistles are narrow-band frequency-modulated signals (Au, 2000) and seem to increase in complexity within Delphinoidea due to the evolution of social signals for group cohesion (May-Collado *et al.,* 2007). Both types of communication sounds are known to be made up of harmonics, which may play a role in group navigation due to the mixed-directionality of these sounds (Miller, 2002; Lammers and Au, 2003).

Experimental studies have demonstrated singularities on the sound emission of dolphins in which both echolocation and communication sounds are emitted simultaneously (Ridgway *et al.,* 2015) and with specific source locations: the echolocation signals were produced in the right side of the epicranial complex, while the left side was used for communication sounds, such as whistles and pulsed calls (Madsen *et al.,* 2013). Although, it has been demonstrated that the biosonar beam originates more or less at the center in *T. truncatus* (Moore *et al.,* 2008; Finneran *et al.,* 2014), the source center of the right sound beam may be adjusted by means of the mobility of the nasal plugs by retraction of the nasal plug muscles during vocalizing (Mead, 1975; Heyning and Mead, 1990). Herein, we discuss this asymmetry comparing the biosonar structures *bauplan* of two delphinids with additional comparisons of anatomical and behavioral (acoustic) studies of selected odontocetes from the literature.

MATERIALS AND METHODS

Two Indian Ocean humpback dolphins (Port Elizabeth Museum accession number PEM N5094—female, total length 198.8 cm, condylobasal length 51.50 cm, frozen, carcass condition code 2 (Geraci and Lounsbury, 1993); and PEM N5096—male, total length 262.0 cm, frozen, carcass condition code 3), incidentally caught in shark nets off KwaZulu-Natal (KZN), South Africa, were analyzed at the KwaZulu-Natal Sharks Board facilities, Durban-KZN. It is noteworthy that the Indian Ocean humpback dolphin is a rare and endangered species and obtaining fresh samples from South African waters is not easy due to the climatic conditions. Thus, the scientific collaboration with the KwaZulu-Natal Sharks Board represents a unique opportunity to access the freshest material available. In this context, McKenna *et al*. (2007) have demonstrated that the morphology of the deep soft tissues of the epicranial complex in the dolphin head remain without significant changes postmortem or due to freezing effects (i.e., live, fresh, or thawed). However, superficial soft tissues could exhibit a slight displacement forward due to disarticulation of the head from the body (McKenna *et al.,* 2007). Since the arrangement of the sound emission apparatus appears to have very minor morphological variations at genus level (Mead, 1975; Cranford *et al.,* 1996), we

TABLE 1. List of anatomical abbreviations including the old/usage nomenclature (when applied), the current terminology and the reference used

Abbreviation	Old/usage nomenclature	Current nomenclature	Reference
Bl	Left branch of the melon	*Corpus adiposum nasalis terminalis*	Cranford *et al*. (1996), Huggenberger *et al*. (2014)
Br	Right branch of the melon	*Corpus adiposum nasalis terminalis*	Cranford *et al*. (1996), Huggenberger *et al*. (2014)
Cana	Anterior dorsal bursae	*Corpus adiposum nasalis anterior*	Cranford *et al*. (1996), Huggenberger *et al*. (2014)
Canp	Posterior dorsal bursae	*Corpus adiposum nasalis posterior*	Cranford *et al*. (1996), Huggenberger *et al*. (2014)
melon	Melon	*Corpus adiposum nasalis terminalis*	Mead (1975), Huggenberger *et al*. (2014)
M	Maxillary bone	*Maxilla*	Mead and Fordyce (2009), Nomina Anatomica Veterinaria (2017)
MLDB	Monkey lips dorsal bursae complex	-	Cranford *et al*. (1996)
Mm	-	*Musculus maxillonasolabialis*	Huber (1934), Huggenberger *et al*. (2009)
OI	Premaxillary bone	*Os incisivum*	Mead and Fordyce (2009), Nomina Anatomica Veterinaria (2017)
ON	Nasal bone	*Os nasale*	Mead and Fordyce (2009), Nomina Anatomica Veterinaria (2017)
Snn	Nasofrontal air sacs	*Saccus nasalis nasofrontalis*	Murie (1874), Huggenberger *et al*. (2014)
Snp	Premaxillary air sacs	*Saccus nasalis praemaxillaris*	Murie (1874), Huggenberger *et al*. (2014)
Snv	Vestibular air sacs	*Saccus nasalis vestibularis*	Lawrence and Schevill (1956), Huggenberger *et al*. (2014)
Vnd	Lip of blowhole	*Valva nasalis dorsalis*	Rodionov and Markov (1992), Huggenberger *et al*. (2014)
Vni	Monkey lips	*Valva nasalis intermedia*	Cranford *et al*. (1996), Huggenberger *et al*. (2014)
Vnv	Nasal plugs	*Valva nasalis ventralis*	Cranford *et al*. (1996), Rodionov and Markov (1992)

discuss our findings based on what is known about the sound production in *Sousa* spp.

The analyses of the anatomical topography of the biosonar-related structures were based on a transverse computed tomography scan (CT-scan) of the female´s head (N5094) using Toshiba Aquilion (120 KV, 225 mAs). The head was aligned longitudinally with the bed of the CT-scan and dorsoventrally at 90° to avoid distortions promoted by gravity during scanning. The CT-scan generated a sequence of images (1 mm slice thickness, 0.724 mm pixel edge length) in all three planes (i.e., coronal, sagittal, and axial) that were analyzed using 3D-Slicer (http://slicer.org/). The main biosonar-related components were identified using the segmentation technique (Cranford *et al.,* 2008). In short, images were analyzed and edited voxel by voxel on the three planes accomplished with a threshold assistance tool. Then, a 3D model of each fat and bone structure was generated, and the respective volumes and dimensions were calculated. The size of the brain was characterized by the height of the cranial vault for comparative purposes (Huggenberger *et al.,* 2010). Both heads were dissected, removing tissues layer by layer following the procedure of Schenkkan (1972). Photos of the dorsal view from the female (N5094) were taken to measure and demonstrate the surface area of the air sacs (i.e., vestibular, nasofrontal, and premaxillary) using ImageJ (https://imagej.nih.gov/ij) and Photoshop (www.adobe.com), respectively. The air sacs were collapsed during dissection and, therefore, do not represent the shape of this dynamic structure while *in vivo.* However, the data provided here address a comparative approach with other odontocetes whose air sac morphology has been investigated using gross dissection technique (Schenkkan, 1973).

In addition, one existing CT-scan series (1 mm slice thickness, 0.912 mm pixel edge length) of a male Lahille's bottlenose-dolphin, *Tursiops gephyreus*, (*Grupo de Estudos de Mamíferos Aquáticos do Rio Grande do Sul* accession number GEMARS 1447, total length 248.0 cm, condylobasal length: 51.13 cm, frozen, carcass condition code 2) was used to compare the head morphology of the Indian Ocean humpback dolphin with this well described delphinid (Schenkkan, 1973; Mead, 1975; Rodionov and Markov, 1992; Cranford *et al.,* 1996). Terminology follows Mead (1975) and Huggenberger *et al*. (2014) for soft tissues and Mead and Fordyce (2009), adapted to Nomina Anatomica Veterinaria (2017), for the skull (see the list of abbreviations in Table 1). In this contribution, we assumed the terminology "posterior branch" for all fat bodies between the main body of the melon (connected to it or not) and the dorsal bursae complexes to address a comparative approach.

RESULTS

In general, the epicranial complex of the Indian Ocean humpback dolphin specimens (Figs. 1 and 2) exhibited a similar arrangement to that of other delphinids (see Schenkkan, 1973; Mead, 1975), such as the Lahille's bottlenose dolphin (Fig. 2). However, specific features regarding the position, shape, and asymmetry of the specialized fat bodies in the epicranial complex of the Indian Ocean humpback dolphin were remarkably distinct and will be described in detail.

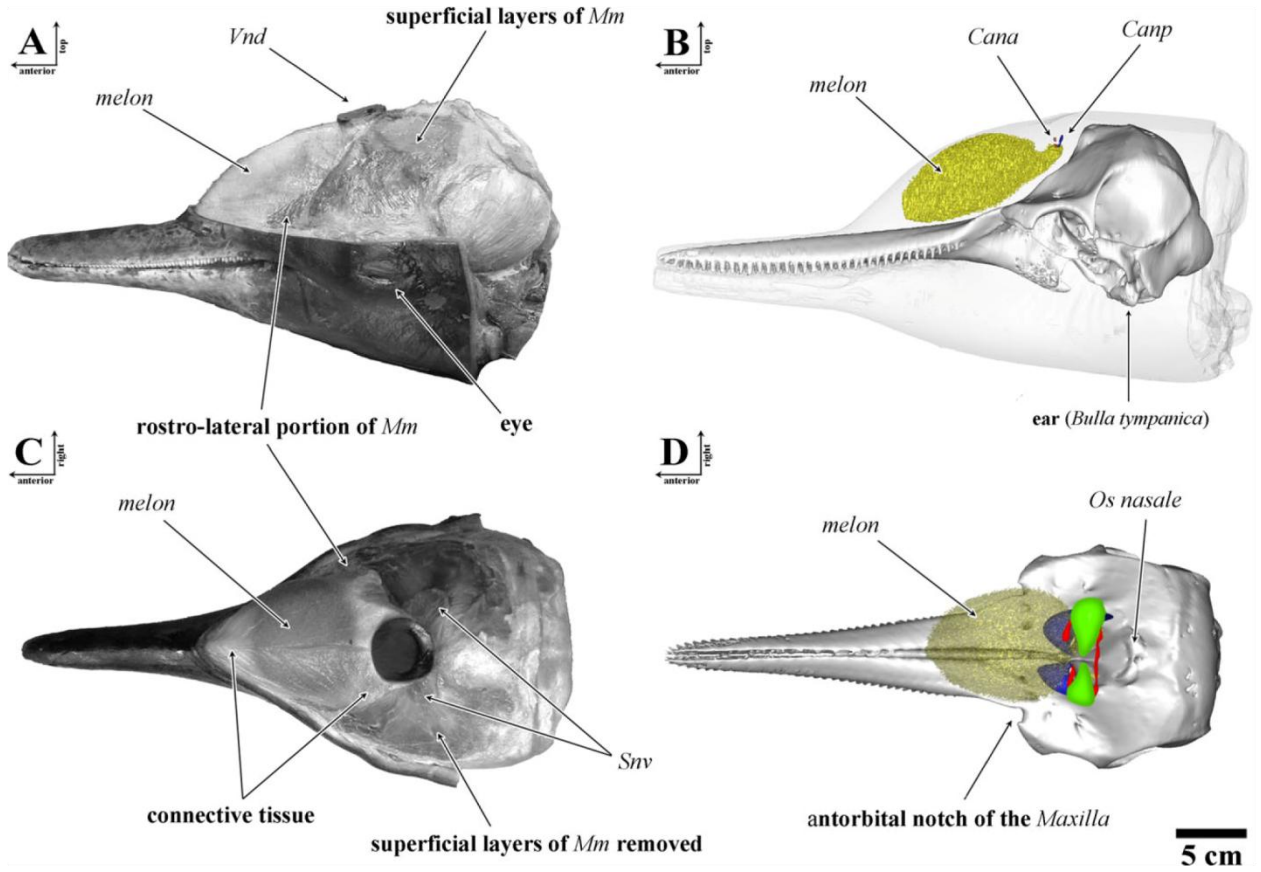

Fig. 1. General topography of the main structures involved in the sound production of a juvenile female (PEM N5094, total length 198.8 cm, condylobasal length 51.5 cm) Indian Ocean humpback dolphin, *Sousa plumbea*. **A**, **C.** Dissected head showing the *Valva nasalis dorsalis* (*Vnd*, lips of the blowhole) and the main body of the *Corpus adiposum nasalis terminalis* (*melon*) and the arrangement of the superficial layers of the *Musculus maxilonasolabialis* (*Mm*) and its rostro-lateral portion in dorsal and lateral view, respectively. **B**, **D**. 3D reconstructions of the specialized fat bodies in the epicranial complex of the same specimen by computed tomography assistance (*melon, Corpus adiposum nasalis terminalis* (yellow); *Cana, Corpus adiposum nasalis anterior* (red); *Canp, Corpus adiposum nasalis posterior* (blue). In **D**, the nasal air sacs were demonstrated at dorsal view (*Saccus nasalis vestibularis*, green; *Saccus nasalis nasofrontalis*, red; *Saccus nasalis praemaxillaris*, blue).

Monkey lips (*Valva nasalis intermedia, Vni*)—These flat lips characterized by small wrinkles on the anterior and posterior side of the epithelium of the nasal passage were placed below the ventral opening of the vestibular air sacs (*Snv*, *Saccus nasalis vestibularis*, see below) and aligned with the dorsal bursae (*Cana*, *Corpus adiposum nasalis anterior* and *Canp*, *Corpus adiposum nasalis posterior*, see below). The wrinkles were surrounded by a thin and light pale pigmentation on both the left- and right-hand side which delimits the structure. On the right *Vni*, the pigmentation was more intense than on the left side (Fig. 3). In both Indian Ocean humpback dolphin specimens, the right *Vni* exhibited deeper and clear wrinkles compared to the left structures where the wrinkles were not clear to the naked eye without shifting the tissue.

Posterior dorsal bursae (*Corpus adiposum nasalis posterior, Canp*)—This pair of small ellipsoid fat bodies were situated posteriorly to each nasal passage and aligned axially 16.03 mm and 14.41 mm in front to the right and left distal-most mesethmoid margin of the nasal bone (*ON*, *Os nasale*), respectively (Fig. 2). The right and left *Canp* were not aligned symmetrically from the mid-sagittal plane, since the left *Canp* was shifted ("skewed") to the right (Figs. 1 and 2). The right *Canp*, instead, was aligned perpendicularly to the mid-sagittal plane and exhibited larger dimensions than the left one (right *Canp* maximum width: 12.84 mm, height: 6.48 mm, axial length: 3.10 mm; left *Canp* max. width: 10.50 mm, height: 3.26 mm, axial length: 2.14 mm). The same size asymmetry between the right and left *Canp* was more evident in the Lahille's bottlenose dolphin (Fig. 2).

Anterior dorsal bursae (*Corpus adiposum nasalis anterior, Cana*)—This second pair of ellipsoid fat bodies were placed anteriorly to each nasal passage just in front of the respective right and left *Canp*. Both *Cana* were aligned to the corresponding *Canp*. The right *Cana* also exhibited larger dimensions than the left one (right *Cana* maximum width: 9.30 mm, height: 3.28 mm, axial length: 2.54 mm; left *Cana* max. width: 6.51 mm, height: 3.33 mm, axial length: 2.33 mm). However, both *Cana* were smaller than the corresponding *Canp* (Fig. 2).

Melon (*Corpus adiposum nasalis terminalis*)—The greatest fat structure in the epicranial complex of the

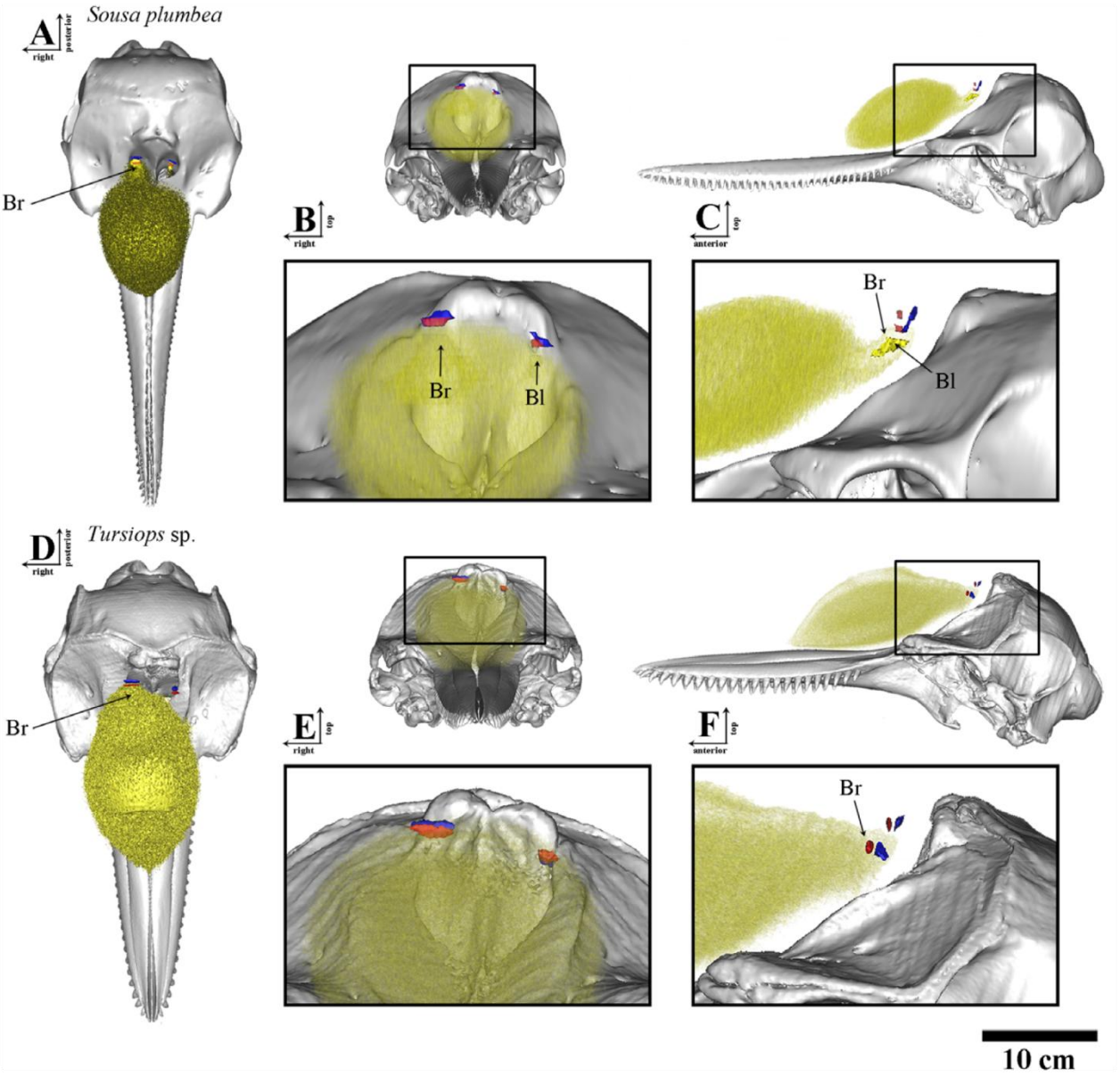

Fig. 2. General topography of the epicranial fat bodies in the Indian Ocean humpback dolphin, *Sousa plumbea* (PEM N5094, total length 198.8 cm, condylobasal length 51.5 cm) (**A–C**) and *Tursiops gephyreus* (GEMARS 1447, total length 248.0 cm, condylobasal length: 51.13 cm) (**D–F**) in dorsal (**A** and **D**), frontal (**B** and **E**), and lateral (**C** and **F**) view (*melon, Corpus adiposum nasalis terminalis* (yellow); left branch of the melon (opaque yellow) *Cana, Corpus adiposum nasalis anterior* (red); *Canp, Corpus adiposum nasalis posterior* (blue); Br, right posterior branch of *melon*; Bl, left posterior branch of the *melon*).

Indian Ocean humpback dolphin resembled the condition found in other delphinids. The anterior portion of the epicranial complex of the Indian Ocean humpback dolphin was nearly totally composed by fat and connective tissues of the *melon*. The rostral musculature of the *Musculus maxilonasolabialis* (*Mm*) was restricted to the lateral borders of the *melon* (Fig. 1). The *melon* originated from both sides of the nasal passage into the nasal plug (*Vnv*, *Valva nasalis ventralis*), where the right and left caudal branches of the *melon* were placed ventral to each *Cana*.

The posterior tip of the right branch of the *melon* in the Indian Ocean humpback dolphin was positioned 2.97 mm and 2.99 mm below to the right *Canp* and *Cana*, respectively (when the nasal passage was collapsed). The width of the right branch of the *melon* at its dorsoposterior portion was 13.90 mm. It extended ventrally 10.52 mm, where it became larger (maximum width at this point: 22.16 mm) and switched its orientation anteriorly, following the skull concavity, until it connected to the main body of the *melon* (maximum width at this point:

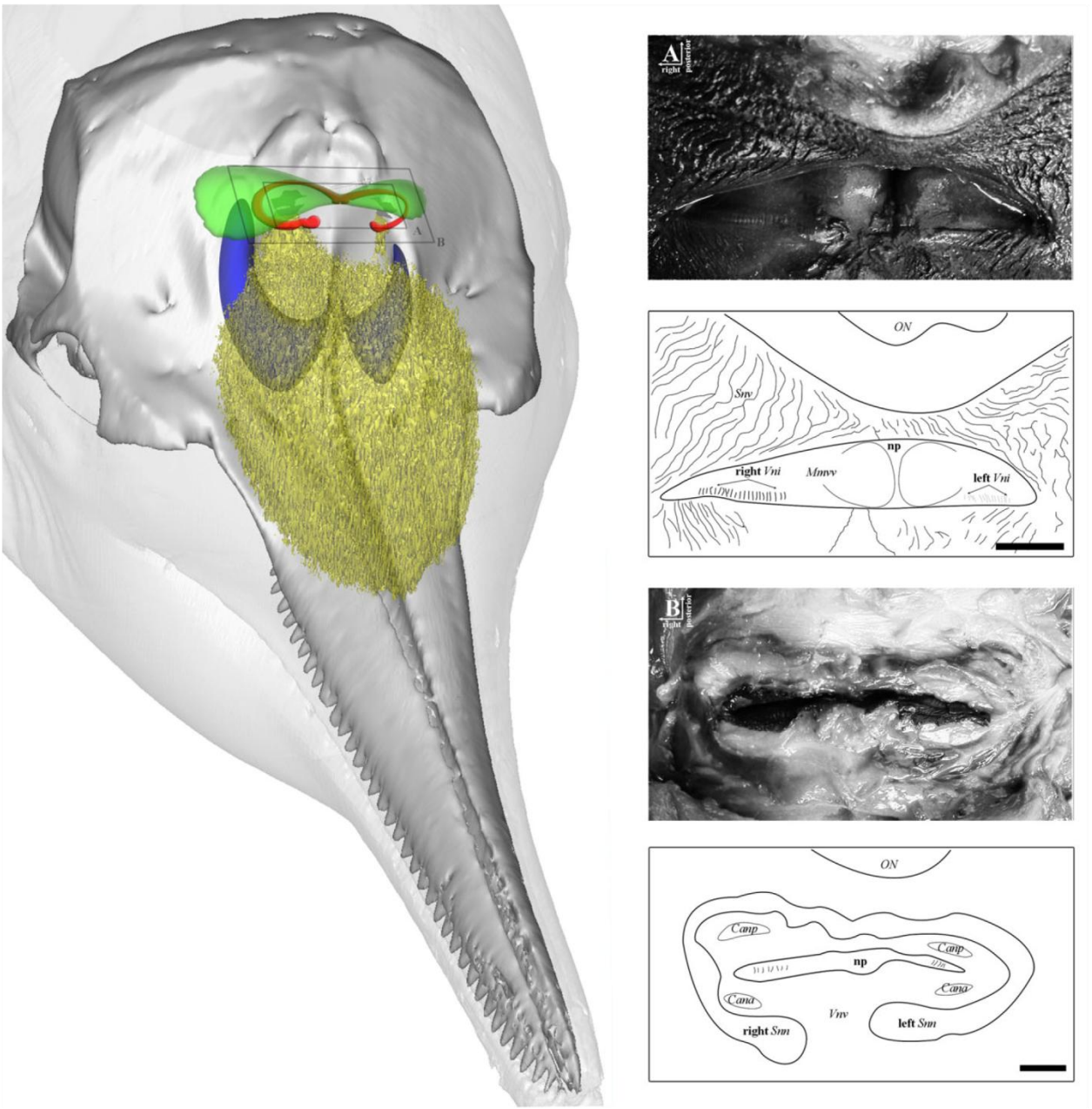

Fig. 3. The general arrangement of the main biosonar-related fat structures (*Corpus adiposum nasalis terminalis*, *melon*, yellow; *Corpus adiposum nasalis posterior*, *Canp*, gray; and *Corpus adiposum nasalis anterior*, *Cana*, gray) of the female Indian Ocean humpback dolphin, *Sousa plumbea* (PEM N5094, total length 198.8 cm, condylobasal length 51.5 cm) relative to the nasal air sacs (schematic representation) (*Saccus nasalis vestibularis, Snv*, green; *Saccus nasalis nasofrontalis*, *Snn*, red; *Saccus nasalis praemaxillaris*, *Snp*, blue). In detail, the nasal passage of the dissected viewed from above at two levels: **A.** Inside the *Snv* showing both right and left-hand side *Valva nasalis intermedia* (*Vni*); and **B.** Below to the *Snv*, showing the (*Snn*) surrounding the nasal passage (np) and the *Canp* and *Cana* into the *Valva nasalis ventralis* (*Vnv*), just in front of the *Os nasale* (*ON*, nasal bone). Scale bars: 1 cm.

45.46 mm; Fig. 2). The length of the right branch of the *melon* (i.e., from its posterior tip to the posteriormost point of the main body of the *melon*) in the Indian Ocean humpback dolphin was 25.60 mm. The left branch of the *melon* was smaller than the right one and did not connect to the main body of the *melon*. Instead, it extended ventrally while entering in the dense connective tissue of the nasal plug. It was positioned 4.33 mm and 3.91 mm ventrally to the left *Canp* and *Cana*, respectively. The width of the left branch of the *melon* at its dorsoposterior

TABLE 2. Morphometric parameters of the specialized fat bodies (*Canp*, *Cana*, and *melon*) of *Sousa plumbea* (PEM 5094, total length 198.8 cm) and *Tursiops gephyreus* (GEMARS 1447, total length 248.0 cm) in mm and relative to the condylobasal length (CBL)

		Sousa		*Tursiops*	
Condylobasal length		515	%CBL	511.3	%CBL
Distance between the *Canp* and the ventrolateral mesethmoid margin of the *ON*	Right	16.03	3.11	18.55	3.63
	Left	14.41	2.80	20.36	3.98
Maximum width of the *Canp*	Right	12.84	2.49	20.22	3.95
	Left	10.50	2.04	10.82	2.12
Height of the *Canp*	Right	6.48	1.26	8.31	1.63
	Left	3.26	0.63	6.30	1.23
Axial length of the *Canp*	Right	3.10	0.60	3.70	0.72
	Left	2.14	0.42	6.39	1.25
Maximum width of the *Cana*	Right	9.30	1.81	20.67	4.04
	Left	6.51	1.26	10.26	2.01
Height of the *Cana*	Right	3.28	0.64	6.77	1.32
	Left	3.33	0.65	5.48	1.07
Axial length of the *Cana*	Right	2.54	0.49	2.36	0.46
	Left	2.33	0.45	3.57	0.70
Distance between the *Canp* and *Cana* complexes and the branches of the *melon*	Right	2.97/2.99	0.57/0.58	1.24/0.73	0.24/0.14
	Left	4.33/3.91	0.84/0.75	-	-
Largest width of the branches of the *melon*	Right	45.46	8.82	69.90	13.67
	Left	4.77	0.93	-	-
Maximum width of the *melon*		100.02	19.42	136.06	26.61
Length of the *melon* with its right branch		159.04	30.88	242.46	47.42
Epicranial complex length	Point to point	160.78	31.21	235.30	46.02
	In parallel	137.08	26.61	223.21	43.66
Elevation angle of the *Canp* and *Cana* complexes	Right	24.35°	-	20.11°	-
	Left	23.45°	-	19.51°	-
Height of the cranial vault		103.5	20.09	128.27	25.08

portion was 4.77 mm. The length of the left branch of the *melon* (i.e., from its posterior tip to the anterior end of this fat body) was 17.67 mm.

The right branch of the *melon* in the Lahille's bottlenose dolphin extended anteriorly, gradually enlarging its diameter to became continuous with the main body of the *melon*. Thus, it was not possible to distinguish the anterior and posterior limits of the right branch of the *melon* in the Lahille's bottlenose dolphin. Additionally, in contrast to the humpback dolphin, there was no evidence of a fat tissue area just anterior to the left *Cana* in the Lahille's bottlenose dolphin. However, a fat protuberance from the axis of the main body of the *melon* on the left side was found (Fig. 2).

The main body of the *melon* of the Indian Ocean humpback dolphin, in dorsal view, was a big triangular fat body with the largest base positioned at 17.19 mm and 19.27 mm in front of both right and left *Cana*, respectively. The largest width of the *melon* was 100.02 mm, just at the line that passed vertically 23.58 mm in front of the antorbital notches of the maxillary bone (*M*, *Maxilla*) in dorsal view. At this point, the *melon* started to taper abruptly from its lateral sides and the top to its anteriormost tip, positioned at the line that passed vertically through the eighth (counted from proximal) tooth of both right and left *M*. The anterior portion of the *melon* was surrounded anteriorly by a connective tissue which gradually lost its fat composition until it reached the skin (Fig. 1). The length of the *melon*, including its right branch (i.e., length between the posterior tip of the *melon* terminus and its anterior tip), was 160.63 mm (32.5% of the condylobasal length). The asymmetry of this structure was evident since the right antorbital notch was almost totally covered by the *melon* in dorsal view, while it covered only the proximal portion of the left antorbital notch (Fig. 1).

The epicranial complex length, that is, distance from the rostroventral tip of the *melon* to the nasal passage between both *Canp* and *Cana* complexes (Huggenberger *et al.,* 2010), of the Indian Ocean humpback dolphin was 194.21 mm from point to point and 167.64 mm in parallel to the sagittal plane. The elevation angle of the *Canp* and *Cana* complexes, determined as the angle between the axis of the skull and the line that passes through the tip of the *melon* to each nasal passage between both MLDB complexes (Huggenberger *et al.,* 2010), was 24.35° on the right and 23.45° on the left side. The association between specialized fat tissues and skull elements in the humpback dolphins was similar to the Lahille's bottlenose dolphin, in contrast to the relative size between the *Canp* and *Cana* complexes which seemed to be more asymmetric in the Lahille's bottlenose dolphin (Table 2).

Vestibular air sacs (*Saccus nasalis vestibularis, Snv*) – The pair of *Snv* were placed just below the blowhole and dorsally covered the posterior portion of the epicranial complex completely. These outpockets of the nasal tract extended laterally (right: 73.2 mm, left: 57.5 mm) from the blowhole forming two rounded and flattened air spaces between the superficial layers of the *Mm* (Fig. 1). In dorsal view, the lateral extension of both *Snv* surpassed the distal borders of the posterior projection of the premaxillary bones (*Os incisivum*, *OI*). The dorsal border of the *Snv* opening was placed posterior to the nasal passage and partially surrounded the vestibulum below the blowhole. The ventral border of the *Snv* opening totally covered the horizontal nasal passage just above the nasal plug muscle (*Musculus maxilonasolabialis valvae ventralis*) and the *Vni*. The size asymmetry between both *Snv*

was evident since the dorsal surface area of the left *Snv* was 13.04 cm^2, about 0.6 times smaller than the right *Snv* (21.27 cm^2). Both *Snv* exhibited a dark coloration of their folded epithelium, in which the folds were oriented in parallel to the axes of the maximum diameter of each *Snv* (Fig. 3).

Nasofrontal air sacs (*Saccus nasalis nasofrontalis, Snn*)—The pair of *Snn* originated on the proximal portion of the posterior walls of each nasal passage, just below the *Snv*. Both sacs surrounded the nasal passage bordering the *Canp* and *Cana* complexes anteriorly, laterally, and posteriorly (Fig. 1). Its epithelium was thin with a dark pigmentation and exhibited small longitudinal folds. The right *Snn* was larger than the left one. Their dorsal surface areas were 6.91 cm^2 and 6.55 cm^2, respectively. The right *Snn* extended 5.43 mm laterally from its medialmost origin, while the left *Snp* extended 4.82 mm laterally. An accessory air sac was not found during the dissections of the two specimens.

Premaxillary air sacs (*Saccus nasalis premaxillaris, Snp*)—As in the bottlenose dolphin, the pair of *Snp* were the largest air sacs in the epicranial complex of the Indian Ocean humpback dolphin (Fig. 1). They were positioned below the *Vnv* and covered 19.59 cm^2 and 9.68 cm^2 of the right and left premaxillary sac fossa of the *OI*, respectively. The maximum width of each sac (i.e., by the line that passed horizontally through the anterior border of each nasal passage) was 5.08 cm for the right and 3.3 cm for the left *Snp*. Thus, the left *Snp* was smaller and narrower compared to the right one, although its anterior tip was placed 0.64 mm in front of the right *Snp* anterior tip. The length of the anterior portion of each *Snp* (i.e., between the anterior border of each nasal passage to the anterior tip of each sac) was 2.65 cm and 3.17 cm for the right and left *Snp*, respectively. Both *Snp* and their opening slits extended laterally around the border of the bony nasal passages. In this way, the right *Snp* opening surrounded the anterior and the lateral border of the naris reaching its posterior limits. The left one extended laterally only half way to the center of the left naris (Fig. 1).

DISCUSSION

The general arrangement of sound generating structures described here for the Indian Ocean humpback dolphin is similar to those described for bottlenose dolphins (*T. gephyreus* and *T. truncatus*, cf. Schenkkan, 1973; Mead, 1975; Rodionov and Markov, 1992; Cranford *et al.,* 1996, this study), that is, the shape of the air sacs as well as the nasal muscles resemble each other in both genera. However, a remarkable difference to bottlenose dolphins exists in the small left posterior branch of the *melon,* which ends anteroventrally to the left bursae complex in the Indian Ocean humpback dolphin.

The shape of the posterior end of the *melon*, which connects the MLDB complex with the melon, attracted some attention in the literature: posterior "rami" or "branches" of the melon were firstly mentioned by Cranford (1988) in the spinner dolphin, *Stenella longirostris*, as small bulbous projections, posterior to the main portion of the melon, which ends on each side of the nasal plug. However, Cranford *et al*. (1996) also described a fat tissue protuberance diverging from the main axis of the melon in the common dolphin, *Delphinus delphis*, as the left branch of the melon, similar to the Lahille's bottlenose dolphin (this study) and the common bottlenose dolphin (*Tursiops truncatus*) (Harper *et al.,* 2008). In this case, the left branch ends posteriorly in the connective tissue and is, thus, not in direct contact to the sound generating structures of the nasal passage (dorsal bursae). Cranford *et al*. (1996) also described "enlarged fatty basins, located between the main body of the melon and (both) MLDB complex(es)" in the Pacific white-sided dolphin (*Lagenorhynchus obliquidens*) and noticed it for the white-beaked dolphin (*Lagenorhynchus albirostris*), Risso's dolphin (*Grampus griseus*), and a neonate northern right whale dolphin (*Lissodelphis borealis*). McKenna *et al*. (2012) used the term "branch" for this *fatty basin* in the Pacific white-sided dolphin. Similar structures were described anterior to the left MLDB complexes in the Franciscana dolphin, *Pontoporia blainvillei*, as "fatty melon branches" (Cranford *et al.,* 1996), but differed from that of the Pacific white-sided dolphin. The right branch connects to the main body of the melon in the Franciscana dolphin, as in most odontocetes, and on the left side is a smaller isolated triangular fat body just anterior to the left anterior dorsal bursa (Cranford *et al.,* 1996; Frainer *et al.,* 2015). Although it seems that this structure was independently acquired in these lineages, it is evident that there is a functional connection between species with this fat body structure connected to the left bursae complex and their sound repertoire:

1. The spinner dolphin is known to produce a high fundamental frequency (~69 kHz) in its whistles compared to other members of the Delphininae subfamily, containing harmonic elements close to 80 kHz (Au *et al.,* 1999b; Lammers and Au, 2003);
2. The Risso's dolphin is known to produce a higher overall frequency in its whistle repertoire compared to other *Globicephala* species and present a high number of harmonics in the barks (ranging from 1 to 28 harmonics) and buzzes (ranging from 20 to 36 harmonics; Corkeron and Van Parijs, 2001);
3. The white-beaked dolphin produces fundamental frequencies of up to 35 kHz with a harmonic element up to 50 kHz, and Rasmussen *et al.* (2006) proposed that whistle production in this species is more directional than seen in the bottlenose dolphin (Rasmussen *et al.,* 2004).
4. Recently, broad band acoustic tags have been able to record high frequency and complex whistles with maximum frequency at 82 kHz for the Franciscana dolphin with up to eight harmonics, a species that ever since was believed to not produce modulated sounds (Cremer *et al.,* 2017).

Humpback dolphins are known to produce broadband clicks for echolocation, ranging from 12 to at least 22 kHz, as well as pulsed calls (i.e., barks, quacks, and grunts) and whistles (Zbinden *et al.,* 1977; Schultz and Corkeron, 1994; Van Parijs and Corkeron, 2001; Weir, 2010; Sims *et al.,* 2012). Schultz and Corkeron (1994) demonstrated that Pacific humpback dolphins produce a higher overall frequency for communication sounds

compared to bottlenose dolphins, and Van Parijs and Corkeron (2001) showed that the barks (i.e., a type of burst-pulses) produced by the Australian humpback dolphin exhibit higher frequencies compared to other delphinids, such as the Atlantic spotted dolphin, *Stenella frontalis*, and the orca, *Orcinus orca* (Ford, 1991; Herzing, 1996), with a number of harmonics ranging from 1 to 22. Sims *et al*. (2012) have recorded barks of the Indo-Pacific humpback dolphin ranging from 4.1 kHz to 24.9 kHz with closely spaced harmonics; in contrast, whistles were simple in structure, with a lower overall frequency compared to barks and a wide spacing between harmonics. However, Weir (2010) have recorded whistles from the Atlantic humpback dolphin with a harmonic structure reaching, at least, 44 kHz.

The acoustic repertoire described for humpback dolphins should be interpreted with caution due to the nature of sampling wild animals (*e.g.,* animal distance/angle from the hydrophone and limitation on recording equipment) and may not represent the whole sound spectrum produced by these animals (Van Parijs and Corkeron, 2001; Weir, 2010). However, the high frequency of burst-pulses and harmonic energy together with the elevated number of harmonics described for burst pulses of humpback dolphins may be a general feature of this genus.

Harmonic social sounds in dolphins are supposed to play a role in group coordination during traveling and hunting since it may provide cues of the moving emitter due to the mixed-directionality of communication sounds (Miller, 2002; Lammers and Au, 2003). Accordingly, higher frequency harmonics are transmitted forward, while lower frequency components are known to be more omnidirectional (Blomqvist and Amundin, 2004). The directionality of the sound produced by dolphins seems to vary between delphinid species (Au *et al.,* 1999a; Rasmussen *et al.,* 2004) and it has been associated with the morphology of the main structures involved in sound emission including the head and rostrum size and the shape of the air sacs (Au *et al.,* 1999a; Song *et al.,* 2016; Wei *et al.,* 2017). Given that fat bodies in the dolphin head are important for absorbing and collimating small wave lengths (i.e., high frequency) and since the heterogeneity of tissue density in the nasal plug may allow for complex timbre across Odontoceti species (Amundin and Andersen, 1983; Cranford *et al.,* 1996; Madsen *et al.,* 2013), we suggest that the asymmetry in the nasal soft tissues found in the Indian Ocean humpback dolphin (i.e., the small left posterior branch of the melon), may indicate one cause among others for adaptation of the high frequency communication sounds reported in this species.

Directionality in dolphin echolocation sounds seems to have evolved to increase the source level (dB) in the forward direction, where click energy presents its elevated center frequency (kHz), thus, increasing the range of target detection and reducing reflection from the periphery (Jensen *et al.,* 2009; Koblitz *et al.,* 2012; Finneran *et al.,* 2014). The directional biosonar beam is formed by interactions with the skull, dense connective tissue surrounding the posterior portion of the melon, air sacs through the right branch of the melon and the melon. (Figs. 1 and 2) (Au *et al.,* 2006; Finneran *et al.,* 2016; Wei *et al.,* 2017). However, dolphins can steer and modify the width of the echolocation beam by changing the frequency emitted (Au *et al.,* 1995; Madsen *et al.,* 2004) and by modulating the shape of the associated soft tissue (*e.g.,* air sacs and melon) through contraction and retraction of the rostral musculature of the *Mm* (Fig. 1) (Moore *et al.,* 2008; Koblitz *et al.,* 2012). Additionally, head movements may allow dolphins to manipulate the sound beam while scanning for prey (Herzing, 1996).

Interestingly, independent toothed whale lineages have evolved convergent (i.e., nonhomologous) specializations for a highly directional echolocation beam production at higher frequencies (i.e., above 120 kHz) and lower source levels compared to other dolphins, the so called NBHF (Narrow-Band High Frequency) species (*e.g.,* pygmy and dwarf sperm whales, *Kogia* spp.; the harbor porpoises, *Phocoena* spp.; the Franciscana dolphins; *Cephalorhynchus* species, *Cephalorhynchus* spp.; and the hourglass dolphin, *Lagenorhynchus cruciger*) (Madsen *et al.,* 2005; Kyhn *et al.,* 2010; Tougaard and Kyhn, 2010). Harbor porpoises, *Cephalorhynchus* species and Franciscana dolphins are small toothed whales inhabiting similar habitats (i.e., coastal waters) and, therefore, the morphological variation found in the biosonar apparatus of these species may reflect the complex factors promoting the directional properties of the sound beam across odontocetes (Wei *et al.,* 2017). However, convergent morphologies in the biosonar apparatus of these species might be useful to interpret meticulous differences between the sound production in the Indian Ocean humpback dolphin and the Lahille's bottlenose dolphin.

Harbor porpoises and *Cephalorhynchus* species are small, non-whistling odontocetes (May-Collado *et al.,* 2007) exhibiting short rostra and a discontinuity between the main body of the melon and the MLDB complex (i.e., the right branch of the melon is absent) which only the dense connective fibers of the nasal plug are remaining and are covered dorsally by the pair of *Snv* (i.e., more developed in the harbor porpoises) (Mead, 1975; Huggenberger *et al.,* 2009). In contrast, the small Franciscana dolphin exhibits the right branch of the melon connected to the main body, while presenting a narrow and long rostrum that, together with the large size of the right *Snv* and the cylindrical melon, may be responsible for the directional properties of the biosonar in this species (Cranford *et al.,* 1996; Huggenberger *et al.,* 2010; Song *et al.,* 2016). Despite the obvious convergence for riverine habitats, the broad-banded clicking Ganges river dolphin (*Platanista gangetica*) exhibits similar morphological adaptations for a directional sound compared to Franciscana dolphins, as this species also presents a long and narrow rostrum and maxillary bony crests acting as sound reflectors above the epicranial complex (Jensen *et al.,* 2013). Harbor porpoises and Franciscana dolphins (and *Cephalorhynchus*, unpublished data by GF) exhibit the MLDB complex aligned in the axial plane with the posterior portion of the melon (Huggenberger *et al.,* 2009; Frainer *et al.,* 2015). This might be related to sound production convergence in these species, since the dorsocaudally position of these structures relative to the melon seems to be a conserved character in delphinids (Fig. 2).

In the present study, we demonstrated that despite the Indian Ocean humpback dolphin exhibiting a continuous melon (i.e., connecting the main body of the melon and the right MLDB complex), it represents a more heterogeneous tissue than the one found in Lahille's bottlenose dolphin. Since there are transverse connective tissue fibers of the nasal plug between the posterior portion of

the right branch of the melon and its main body in the Indian Ocean humpback dolphin (Fig. 2), this could address a distinct sound collimation mechanism. Additionally, the general topography of the biosonar relevant structures differ between both species, which is reflected by the steeper epicranial complex of the Indian Ocean humpback dolphin (i.e., based on the higher values of the elevation angle of the MLDB complex) and its relative longer rostrum compared to the Lahille's bottlenose dolphin. In this way, the data for the Indian Ocean humpback dolphin may challenge previous knowledge that steeper epicranial complexes are related to larger brains (Table 2; Huggenberger *et al.,* 2010). In addition, the longer rostrum in Indian Ocean humpback dolphins might suggest a more directional echolocation beam compared to the Lahille's bottlenose dolphin (Fig. 2; Song *et al.,* 2016).

Coastal NBHF species are not only known to have sophisticated (directional) biosonar systems but also highly negative interaction with fisheries due to accidental entanglement in gill nets (Jefferson and Curry, 1994; Secchi *et al.,* 1997; Iñíguez *et al.,* 2003; Secchi *et al.,* 2004). Despite the fact that mainly calves are captured in these nets, the high mortality of adults may address the higher vulnerability of these particular groups toward gill nets (Reeves *et al.,* 2013). In the same way, the population of Indian Ocean humpback dolphin from the east coast of South Africa has been in decline due to the continued bycatch in shark nets off the KwaZulu-Natal coast (KZN) (Atkins *et al.,* 2013; Plön *et al.,* 2015). Interestingly, the higher bycatch rates are not only due to juveniles being caught, but also males between 2.2 and 2.5 m in length. Another related delphinid, the Indian Ocean bottlenose dolphin (*Tursiops aduncus*), is also threatened by the presence of shark nets, but for this species mostly calves are caught (Cockcroft, 1990; Peddemors, 1999). In the latter species, 30% of all captured calves presented fresh tooth marks indicative of epimeletic behavior (Cockcroft and Sauer, 1990). Thus, lactating females might detect gill nets, but cannot prevent the entanglement of their calves.

Frainer *et al*. (2015) proposed that young individuals of the endangered Franciscana dolphin might be more susceptible to entanglement in fishery gill nets than adults, due to, among other causes, an immature anatomy of biosonar-relevant structures and premature behavior skills related to echolocation. In this respect, the cause of why adolescent male Indian Ocean humpback dolphins exhibit higher bycatch rates is still a matter of speculation. However, we suspect that coastal dolphins with specialized directional echolocation beam are more susceptible to die in gill nets, because they are limited on performing wide range adjustments of their directional properties while pursuing prey or avoiding obstacles (Moore *et al.,* 2008). Franciscana dolphins, for example, do not exhibit rostral musculature of the *Mm*, so the melon axis might be steered mainly by movements of the neck while echolocating. In this way, scanning movements of the head promoted to amplify the inspected area surrounding the animal (Herzing, 1996) might represent a disadvantageous condition for species with a long rostrum, such as Franciscana dolphins and Indian Ocean humpback dolphins. Nevertheless, directional echolocation beams are, theoretically, more restricted to a straightly frontal inspection, while omitting surrounding obstacles. In this way, sudden encounters at short range with a low reflective material (such as the monofilaments of fishing and shark nets) may characterize the bycatch phenomenon of these species specialized in directional echolocation beam generation.

ACKNOWLEDGEMENTS

Our special thanks to Dr. Greg Hofmeyr (Port Elizabeth Museum at Bayworld) and staff of the KwaZulu-Natal sharks board for assistance during dissections and to Dr. Wedderburn-Maxwell (Uhmlanga Hospital, Durban) for his help during CT-image acquisition. We also thank IFAW for financial support to SP. This is a contribution of the Research Group "*Evolução e Biodiversidade de Cetáceos*/CNPq" and an AEON publication no. 178.

LITERATURE CITED

Amundin M, Andersen SH. 1983. Bony nares air pressure and nasal plug muscle activity during click production in the harbour porpoise, *Phocoena phocoena*, and the bottlenosed dolphin, *Tursiops truncatus*. J Exp Biol 105:275–282.

Aroyan JL, Cranford TW, Kent J, Norris KS. 1992. Computer modeling of acoustic beam formation in *Delphinus delphis*. J Acoust Soc Am 92:2539–2545.

Atkins S, Cantor M, Pillay N, Cliff G, Keith M, Parra GJ. 2016. Net loss of endangered humpback dolphins: integrating residency, site fidelity, and bycatch in shark nets. Mar Ecol Prog Ser 555:249–260.

Atkins S, Cliff G, Pillay N. 2013. Humpback dolphin bycatch in the shark nets in KwaZulu-Natal, South Africa. Biol Conserv 159: 442–449.

Au WL. 2000. Hearing in whales and dolphins: an overview. In: Au WL, Richard RF, editors. *Hearing by whales and dolphins*. New York: Springer. p 1–42.

Au WL, Kastelein RA, Benoit-Bird KJ, Cranford TW, McKenna MF. 2006. Acoustic radiation from the head of echolocating harbor porpoises (*Phocoena phocoena*). J Exp Biol 209:2726–2733.

Au WWL, Houser DS, Finneran JJ, Lee W, Talmadge LA, Moore PW. 2010. The acoustic field on the forehead of echolocating Atlantic bottlenose dolphins (*Tursiops truncatus*). J Acoust Soc Am 128:1426–1434.

Au WWL, Kastelein RA, Rippe T, Schooneman NM. 1999a. Transmission beam pattern and echolocation signals of a harbor porpoise (*Phocoena phocoena*). J Acoust Soc Am 106:3699–3705.

Au WWL, Lammers MO, Aubauer R. 1999b. A portable broadband data acquisition system for field studies in bioacoustics. Mar Mamm Sci 15:526–531.

Au WWL, Pawloski JL, Nachtigall PE, Blonz M, Gisner RC. 1995. Echolocation signals and transmission beam pattern of a false killer whale (*Pseudorca crassidens*). J Acoust Soc Am 98:51–59.

Barros NB, Cockcroft VG. 1991. Prey of humpback dolphins (*Sousa plumbea*) stranded in eastern Cape Province. South Africa Aquat Mamm 17:134–136.

Blomqvist C, Amundin M. 2004. An acoustic tag for recording, directional, pulsed ultrasounds aimed at free-swimming Bottlenose dolphins (*Tursiops truncatus*) by conspecifics. Aquat Mamm 30: 345–356.

Cockcroft VG. 1990. Dolphin catches in the Natal shark nets, 1980 to 1988. Afr J Wildl Res 20:44–51.

Cockcroft VG, Sauer W. 1990. Observed and inferred epimeletic (nurturant) behaviour in bottlenose dolphins. Aquat Mamm 16:31–32.

Corkeron PJ, Van Parijs SM. 2001. Vocalizations of eastern Australian Risso's dolphins, *Grampus griseus*. Can J Zool 79: 160–164.

Cranford TW. 1988. The anatomy of acoustic structures in the spinner dolphin forehead as shown by X-ray computed tomography and computer graphics. *Animal Sonar*. Springer, New York. p 67–77.

Cranford TW, Amundin M, Norris KS. 1996. Functional morphology and homology in the odontocete nasal complex: implications for sound generation. J Morphol 228:223–285.

Cranford TW, Elsberry WR, Van Bonn WG, Jeffress JA, Chaplin MS, Blackwood DJ, Carder DA, Kamolnick T, Todd MA, Ridgway SH. 2011. Observation and analysis of sonar signal generation in the bottlenose dolphin (*Tursiops truncatus*): evidence for two sonar sources. J Exp Mar Biol Ecol 407:81–96.

Cranford TW, McKenna MF, Soldevilla MS, Wiggins SM, Goldbogen JA, Shadwick RE, Krysl P, Leger JAS, Hildebrand JA. 2008. Anatomic geometry of sound transmission and reception in Cuvier's beaked whale (*Ziphius cavirostris*). Anat Rec 291:353–378.

Cremer MJ, Holz AC, Bordino P, Wells RS, Simões-Lopes PC. 2017. Social sounds produced by franciscana dolphins, *Pontoporia blainvillei* (Cetartiodactyla, Pontoporiidae). J Acoust Soc Am 141:2047–2054.

Finneran JJ, Branstetter BK, Houser DS, Moore PW, Mulsow J, Martin C, Perisho S. 2014. High-resolution measurement of a bottlenose dolphin's (*Tursiops truncatus*) biosonar transmission beam pattern in the horizontal plane. J Acoust Soc Am 136:2025–2038.

Finneran JJ, Mulsow J, Branstetter BK, Moore P, Houser S. 2016. Nearfield and farfield measurements of dolphin echolocation beam patterns: no evidence of focusing. J Acoust Soc Am 140:1346–1360.

Ford JKB. 1991. Vocal traditions among resident killer whales (*Orcinus orca*) in coastal waters of British Columbia. Can J Zool 69: 1454–1483.

Frainer G, Huggenberger S, Moreno IB. 2015. Postnatal development of franciscana's (*Pontoporia blainvillei*) biosonar relevant structures with potential implications for function, life history, and bycatch. Mar Mamm Sci 31:1193–1212.

Geraci JR, Lounsbury VJ. 1993. *Marine mammals ashore—a field guide for strandings*. Texas: Texas A&M University Sea Grant Publication.

Guissamulo A, Cockcroft VG. 2004. Ecology and population estimates of Indo-Pacific humpback dolphins (*Sousa chinensis*) in Maputo Bay, Mozambique. Aquat Mamm 30:94–102.

Harper C, McLellan W, Rommel S, Gay D, Dillaman R, Pabst D. 2008. Morphology of the melon and its tendinous connections to the facial muscles in bottlenose dolphins (*Tursiops truncatus*). J Morphol 269:820–839.

Henderson EE, Hildebrand JA, Smith MH. 2011. Classification of behavior using vocalizations of Pacific white-sided dolphins (*Lagenorhynchus obliquidens*). J Acoust Soc Am 130:557–567.

Herzing DL. 1996. Vocalizations and associated underwater behavior of free-ranging Atlantic spotted dolphins, *Stenella frontalis* and bottlenose dolphins, *Tursiops truncatus* Aquat Mamm 22:61–80.

Herzing DL. 2000. Acoustics and social behavior of wild dolphins: implications for a sound society. In: Au WL, Richard RF, editors. *Hearing by whales and dolphins*. New York: Springer. p 225–272.

Heyning JE, Mead JG. 1990. Evolution of the nasal anatomy of cetaceans. In: Thomas JA, Kastelein RA, editors. *Sensory abilities of cetaceans*. Boston, MA: Springer. p 67–79.

Huber E. 1934. Anatomical notes on Pinnipedia and Cetacea. Carnegie Inst Wash Publ 447:105–136.

Huggenberger S, André M, Oelschlager HA. 2014. The nose of the sperm whale: overviews of functional design, structural homologies and evolution. J Mar Biol Assoc U K 96:783–806.

Huggenberger S, Rauschmann MA, Vogl TJ, Oelschläger H. 2009. Functional morphology of the nasal complex in the harbor porpoise (*Phocoena phocoena* L.). Anat Rec 292:902–920.

Huggenberger S, Vogl TJ, Oelschläger HHA. 2010. Epicranial complex of the La Plata dolphin (*Pontoporia blainvillei*): topographical and functional implications. Mar Mamm Sci 26:471–481.

Iñíguez MA, Hevia M, Gasparrou C, Tomsin AL, Secchi ER. 2003. Preliminary estimate of incidental mortality of Commerson's dolphins (*Cephalorhynchus commersonii*) in an artisanal setnet fishery in La Angelina Beach and Ria Gallegos, Santa Cruz, Argentina. Lat Am J Aquat Mamm 2:87–94.

Jefferson TA, Curry BE. 1994. A global review of porpoise (Cetacea: Phocoenidae) mortality in gillnets. Biol Conserv 67:167–183.

Jefferson TA, Karczmarski L. 2001. *Sousa chinensis*. Mammal Species 655:1–9.

Jefferson TA, Rosenbaum HC. 2014. Taxonomic revision of the humpback dolphins (*Sousa* spp.), and description of a new species from Australia. Mar Mamm Sci 30:1494–1541.

Jensen FH, Bejder L, Wahlberg M, Madsen PT. 2009. Biosonar adjustments to target range of echolocating bottlenose dolphins (*Tursiops* sp.) in the wild. J Exp Biol 212:1078–1086.

Jensen FH, Rocco A, Mansur RM, Smith BD, Janik VM, Madsen PT. 2013. Clicking in shallow rivers: short-range echolocation of Irrawaddy and Ganges river dolphins in a shallow, acoustically complex habitat. PLoS One 8:e59284.

Koblitz JC, Wahlberg M, Stilz P, Madsen PT, Beedholm K, Schnitzler HU. 2012. Asymmetry and dynamics of a narrow sonar beam in an echolocating harbor porpoise. J Acoust Soc Am 131: 2315–2324.

Koper RP, Karczmarski L, Preez D, Plön S. 2016. Sixteen years later: occurrence, group size, and habitat use of humpback dolphins (*Sousa plumbea*) in Algoa Bay, South Africa. Mar Mamm Sci 32: 490–507.

Kyhn LA, Jensen FH, Beedholm K, Tougaard J, Hansen M, Madsen PT. 2010. Echolocation in sympatric Peale's dolphins (*Lagenorhynchus australis*) and Commerson's dolphins (*Cephalorhynchus commersonii*) producing narrow-band high-frequency clicks. J Exp Biol 213:1940–1949.

Lammers MO, Au WL. 2003. Directionality in the whistles of Hawaiian spinner dolphins (*Stenella longirostris*): a signal feature to cue direction of movement? Mar Mamm Sci 19:249–264.

Lawrence B, Schevill WE. 1956. The functional anatomy of the delphinid nose. Bull Mus Comp Zool 114:103–151.

Madsen P, Carder DA, Bedholm K, Ridgway SH. 2005. Porpoise clicks from a sperm whale nose—convergent evolution of 130 KHz pulses in toothed whale sonars? Bioacoustics 15:195–206.

Madsen PT, Kerr I, Payne R. 2004. Echolocation clicks of two free-ranging, oceanic delphinids with different food preferences: false killer whales *Pseudorca crassidens* and Risso's dolphins *Grampus griseus*. J Exp Biol 207:1811–1823.

Madsen PT, Lammers M, Wisniewska D, Beedholm K. 2013. Nasal sound production in echolocating delphinids (*Tursiops truncatus* and *Pseudorca crassidens*) is dynamic, but unilateral: clicking on the right side and whistling on the left side. J Exp Biol 216: 4091–41102.

May-Collado LJ, Agnarsson I, Wartzok D. 2007. Phylogenetic review of tonal sound production in whales in relation to sociality. BMC Evol Biol 7:136.

McKenna MF, Cranford TW, Berta A, Pyenson ND. 2012. Morphology of the odontocete melon and its implications for acoustic function. Mar Mamm Sci 28:690–713.

McKenna MF, Goldbogen JA, Leger JS, Hildebrand JA, Cranford TW. 2007. Evaluation of postmortem changes in tissue structure in the bottlenose dolphin (*Tursiops truncatus*). Anat Rec 290:1023–1032.

Mead JG. 1975. Anatomy of the external nasal passages and facial complex in the Delphinidae (Mammalia: Cetacea). Smithson Contrib Zool (207):1–35.

Mead JG, Fordyce RE. 2009. The therian skull: a lexicon with emphasis on the odontocetes. Smithson Contrib Zool (627):1–248.

Mendez M, Jefferson TA, Kolokotronis S, Krützen M, Parra GJ, Collins T, Minton G, Baldwin R, Berggren P, Särnblad A. 2013. Integrating multiple lines of evidence to better understand the evolutionary divergence of humpback dolphins along their entire distribution range: a new dolphin species in Australian waters? Mol Ecol 22:5936–5948.

Miller PJ. 2002. Mixed-directionality of killer whale stereotyped calls: a direction of movement cue? Behavioral Ecol Sociobiol 52: 262–270.

Moore PW, Dankiewicz LA, Houser DS. 2008. Beamwidth control and angular target detection in an echolocating bottlenose dolphin (*Tursiops truncatus*). J Acoust Soc Am 124:3324–3332.

Murie J. 1874. On the organization of the caaing whale, Globicephalus melas. Trans Zool Soc London 8:236–302.

Nomina Anatomica Veterinaria. 2017. *International Committee on Veterinary Gross Anatomical Nomenclature*. 6th ed. Columbia, MO: World Association of Veterinary Anatomists.

Parra GJ, Ross G. 2009. The Indo-Pacific humpback dolphin, *Sousa chinensis*. In: Perrin WF, Wursig B, Thewissen JGM, editors. *Encyclopedia of marine mammals*. London: American Press. p 576–581.

Peddemors VM. 1999. Delphinids of southern Africa: a review of their distribution, status and life history. J Cetacean Res Manag 1:157–165.

Plön S, Albrecht KH, Cliff G, Froneman PW. 2012. Organ weights of three dolphin species (*Sousa chinensis*, *Tursiops aduncus* and *Delphinus capensis*) from South Africa: implications for ecological adaptation. J Cetacean Res Manag 12:265–276.

Plön S, Cockcroft VG, Froneman WP. 2015. The natural history and conservation of Indian Ocean humpback dolphins (*Sousa plumbea*) in South African waters. In: Jefferson TA, Curry BE, editors. *Advances in marine biology*. Oxford: Academic Press. p 143–162.

Rasmussen MH, Lammers MO, Beedholm K, Miller LA. 2006. Source levels and harmonic content of whistles in white-beaked dolphins (*Lagenorhynchus albirostris*). J Acoust Soc Am 120:510–517.

Rasmussen MH, Wahlberg M, Miller LA. 2004. Estimated transmission beam pattern of clicks recorded from free-ranging white-beaked dolphins (*Lagenorhynchus albirostris*). J Acoust Soc Am 116:1826–1831.

Reeves RR, McClellan K, Werner TB. 2013. Marine mammal bycatch in gillnet and other entangling net fisheries, 1990 to 2011. Endanger Species Res 20:71–97.

Rice DW. 2009. Classification (Overall). In: Perrin WF, Wursig B, Thewisse JGM, editors. *Encyclopedia of marine mammals*. 2nd ed. Academic Press, United States of America. p 234–238.

Ridgway SH, Dibble DS, Van Alstyne K, Price D. 2015. On doing two things at once: dolphin brain and nose coordinate sonar clicks, buzzes and emotional squeals with social sounds during fish capture. J Exp Biol 218:3987–3995.

Rodionov VA, Markov VI. 1992. Functional anatomy of the nasal system in the bottlenose dolphin. In: Thomas JA, Kastelein RA, Supin AY, editors. *Marine mammal sensory systems*. New York: Plenum Press. p 147–177.

Ross GJB, Heinsohn GE, Cockcroft VG. 1994. Humpback dolphins *Sousa chinensis* (Osbeck, 1,765), *Sousa plumbea* (G. Cuvier, 1829) and *Sousa teuszii* (Kukenthal, 1892). Handbook Mar Mamm 5: 23–42.

Schenkkan EJ. 1972. On the nasal tract complex of *Pontoporia blainvillei* Gervais and d'Orbigny 1844 (Cetacea, Platanistidae). Invest Cetacea 4:83–90.

Schenkkan EJ. 1973. On the comparative anatomy and function of the nasal tract in odontocetes (Mammalia, Cetacea). Bijdr Dierk 2:127–159.

Schultz KW, Corkeron PJ. 1994. Interspecific differences in whistles produced by inshore dolphins in Moreton Bay, Queensland, Australia. Can J Zool 72:1061–1068.

Secchi ER, Kinas PG, Muelbert M. 2004. Incidental catches of franciscana in coastal gillnet fisheries in the Franciscana Management Area III: period 1999-2000. Lat Am J Aquat Mamm 3:61–68.

Secchi ER, Zerbini AN, Bassoi M, Dalla-Rosa L, Moller LM, Rocha-Campos CC. 1997. Mortality of franciscanas, *Pontoporia blainvillei*, in coastal gillnetting in southern Brazil: 1994-1995. Rep Int Whal Commn 47:653–658.

Sims PQ, Vaughn R, Hung SK, Würsig B. 2012. Sounds of Indo-Pacific humpback dolphins (*Sousa chinensis*) in west Hong Kong: a preliminary description. J Acoust Soc Am 131:EL48–EL53.

Song Z, Zhang Y, Wei C, Wang X. 2016. Inducing rostrum interfacial waves by fluid–solid coupling in a Chinese river dolphin (*Lipotes vexillifer*). Phys Rev E 93:012411.

Tougaard J, Kyhn LA. 2010. Echolocation sounds of hourglass dolphins (*Lagenorhynchus cruciger*) are similar to the narrow band high-frequency echolocation sounds of the dolphin genus *Cephalorhynchus*. Mar Mamm Sci 26:239–245.

Van Parijs SM, Corkeron PJ. 2001. Vocalizations and behaviour of Pacific humpback dolphins *Sousa chinensis*. Ethology 107:701–716.

Wei C, Au WWL, Ketten DR, Song Z, Zhang Y. 2017. Biosonar signal propagation in the harbor porpoise's (*Phocoena phocoena*) head: the role of various structures in the formation of the vertical beam. J Acoust Soc Am 141:4179–4187.

Weir CR. 2010. First description of Atlantic humpback dolphin *Sousa teuszii* whistles, recorded off Angola. Bioacoustics 19:211–224.

Zbinden K, Pilleri G, Kraus C, Bernath O. 1977. Observations on the behaviour and underwater sounds of the plumbeous dolphin (*Sousa plumbeous* G. Cuvier 1829) in the Indus Delta region. Invest Cetacea 8:259–286.

Foto da capa: Ignacio Moreno/CECLIMAR-UFRGS

CAPÍTULO III

ONTOGENIA E EVOLUÇÃO

"Organisms are not billiard balls, propelled by simple and measurable external forces to predictable new positions on life's pool table. Sufficiently complex systems have greater richness. Organisms have a history that constrains their future in myriad, subtle ways."
Stephen Jay Gould (1980) *The Panda's Thumb*, p. 16

*Manuscrito formatado nas normas do periódico *Journal of Evolutionary Biology*

ECHO-EVO-DEVO: ONTOGENY AND EVOLUTION OF THE SOUND GENERATING STRUCTURES IN INFRAORDER DELPHINIDA (ODONTOCETI: DELPHINIDA)

Guilherme Frainer[1,2,3], Ignacio B. Moreno[1,2], Nathalia Serpa[1,2], Anders Galatius[4], Stefan Huggenberger[3]

[1]Programa de Pós-Graduação em Biologia Animal, Departamento de Zoologia, Universidade Federal do Rio Grande do Sul, 91540-000, Porto Alegre, Brazil.

[2]Centro de Estudos Costeiros, Limnológicos e Marinhos (CECLIMAR/UFRGS), Campus Litoral Norte, Universidade Federal do Rio Grande do Sul, 95625-000, Imbé, Brazil.

[3]Department II of Anatomy, University of Cologne, 50924, Cologne, Germany.

[4]Department of Bioscience, Aarhus University, 4000 Roskilde, Denmark

ABSTRACT

The ontogeny of the main structures involved in sound generation and modulation in dolphins was investigated through the comparison of the soft nasal structures between fetal, perinatal, neonate and adult specimens of three families (Pontoporiidae, Phocoenidae and Delphinidae). Fetal samples were sectioned at 10 µ in saggital and coronal view, and stained. Existing CT and MRI-scan series were combined with new data to represent the ontogenetic stages of the three groups. The image series were analyzed in 3D-Slicer to characterize the topographical arrangement of the tissues surrounding the nasal passage. The muscles and connective tissues surrounding the blowhole region were dissected, layer by layer, to describe and lay out the nasal soft tissues. Morphological ontogenetic-based transformations were used to create transformational characters for phylogenetic inference. The morphogenesis of the soft nasal tissues in dolphins was remarkable for its transformation during early fetal stages: the origins of the melon and the vestibular air sac were detected between Carnegie stages C16 and F22. The three groups analyzed presented distinct formation of the nasal plug and nasal plug muscles, mainly on the loss of fat pathways (or their maintenance in Pontoporiidae) and the hyperdevelopment of the nasal plug muscles in both sides (e.g. during perinatal development of Phocoenidae) or just on the left side (e.g. during postnatal development in Delphinidae). We suggest that ancestral forms of all known delphinidans might have exhibited unique soft nasal tissue morphology capable of producing highly directional sounds as known for some narrow-band high frequency species. Thus, broad-band vocalizing delphinidans, such as most delphinids, might have evolved under heterochronic events acting on the formation of the rostrum and vestibular air sacs formation, as well as on the transformation of the branches of the melon, in turn leading to a reduced directionality of the sonar beam.

Keywords: character transformation; directionality; echolocation; heterochrony; toothed whales; systematics.

INTRODUCTION

A substantial part of the shape variation among biological organisms are due to changes in the ontogenetic processes (Alberch *et al.*, 1979; Gould, 1977) promoted by variations in the regulation of gene expression domains during development (Laland *et al.*, 2015). According to Huxley (1942), modern evolutionary synthesis combine mendelian inheritance with Darwin's (1859) prerogative for natural selection, but the shape (i.e. character) transformation remained unexplained until recent advances in the field of evolutionary developmental biology (evo-devo). Only few studies have integrated this topic into systematics (de Pinna, 1991; De Queiroz, 1985; Fink, 1982; Kluge, 1985). Kluge (1985) pointed out that observations on ontogeny could support homology determinations and also polarize the character transformation by defining the direction of such changes (De Queiroz, 1985; Kluge, 1985). Although cetaceans may represent didactic organisms for interpreting the evolutionary theory (Moran *et al.*, 2011; Thewissen *et al.*, 2006), the evolution of specialized organs composed of soft tissue, such as the sonar beam for echolocation in odontocetes, is largely unknown (Galatius *et al.*, 2018; Morisaka & Connor, 2007).

Odontocetes evolved a complex echolocation-based system for navigation and hunting which allowed them to explore deep, pelagic, shallow and freshwater environments (Au, 2000). Lindberg and Pyenson (2007) proposed that the origin of echolocation in this group dates from the early Oligocene (33.9 – 28.4 m.y.) and is related to nocturnal epipelagic feeding on cephalopods and demersal fishes that perform diel migration from deep to surface waters at night. The authors (Lindberg & Pyenson, 2007) pointed out that morphological innovations related to the advent of echolocation in fossils were found as, e.g., the transition from heterodont to homodont forms, the origin of an asymmetric skull (Cranford *et al.*, 1996; Heyning, 1989), and the enlargement of the brain (Huggenberger, 2008; Marino *et al.*, 2004; Oelschläger *et al.*, 2010). Recent studies have proposed that echolocation arose about 32 Mya ago evidenced by decreasing body size and cochlear length in some stem odontocetes presumably capable of perceiving ultrasonic sounds (Churchill *et al.*, 2016; Geisler *et al.*, 2014). Additionally, even more complex echolocating odontocetes living 18 Mya seems to have evolved inner ear morphology specialized at perceiving narrow-band high frequency (**NHBF**) sounds as observed in some odontocetes (Galatius *et al.*, 2018). However, it seems that not only the echolocation system was responsible for the enlargement of the brain in odontocetes but also challenges in social life, evidenced by the richness of their social repertoire, particularly in delphinids (Fox *et al.*, 2017). Here, acoustic communication was probably a very important function to establish complex social societies in the aquatic environment (Au, 2000).

Echolocation (i.e. clicks) and social (e.g. burst-clicks and whistles) sounds are both produced and modulated in the epicranial (nasal) complex of dolphins, respectively at the right and left (Madsen *et al.*, 2013) **MLDB** (monkey/phonic-lips dorsal bursae) complexes. These lip-like valves of the nasal passage (phonic lips, or *Valva nasalis intermedia*) and small fat bodies (posterior, *Corpus adiposum nasalis posterior*, and anterior, *Corpus adiposum nasalis anterior*, dorsal bursae) are positioned on both sides of the nasal passage, a few centimeters below the blowhole in dolphins and porpoises (Cranford *et al.*, 1996). The initial sound waves of both vocalisations interact with the skull, a dense connective tissue theca, and an air sac system surrounding the acoustic apparatus (Wei *et al.*, 2017). The sound is collimated forward through first the tissue of or near the nasal plugs (*Valva nasalis ventralis*), i.e. paired masses of connective tissue interspersed with muscle

fibers just anterior to each nasal passage (Harper *et al.*, 2008), and then the **melon** (*Corpus adiposum nasalis terminalis*) into the environment (Wei *et al.*, 2017).

In this study, the comparative anatomy of the soft nasal tissues in fetuses, perinatals, neonates and adults of three related odontocete groups were investigated to identify morphology-based ontogenetic transformations and, from a cladistic point of view, to determine the heterochronic processes involved in major adaptations for sound production in these echolocating marine mammals. Although toothed whale evolution is inextricably related to the ability to echolocate, few studies have addressed the biosonar anatomy - and its development - in the light of phylogenetics and evolution (Heyning, 1989; Kleinenberg & Yablokov, 1958; McKenna *et al.*, 2012; Mead, 1975).

MATERIAL AND METHODS

The development of the main soft nasal structures involved in sound generation were investigated through the comparison of fetal, perinatal, neonate and adult specimens of three odontocete families (Pontoporiidae, Phocoenidae and Delphinidae), as indicated in Table 1. Fetuses were classified according to the Carnegie/Fetal stages proposed by Thewissen and Heyning (2007). In this study, different morphological techniques were used to investigate the nasal tissue transformation throughout ontogeny as described below.

Microscopic analysis

All fetuses were fixed in 10% formalin, dehydrated and embedded in paraffin for processing. The samples were sectioned at 10 µ in saggital or coronal view, and stained with Azan, and Hematoxylin and Eosin (H&E). Except for the sections of *Delphinus* (TBS 199) and *Pontoporia* (MM 35) all sections were housed in the extended cetacean embryological collection located at the *Dr. Senckenbergische Anatomie* (SAI) of the *Johann Wolfgang Goethe Universität* in Frankfurt am Main, Germany. The sections were scanned at 3200 dpi using an EPSON L220 digital scanner, then edited and aligned in Adobe Photoshop ©. The image series were converted to DICOM format using DICOM import and export plugin for ImageJ (https://imagej.nih.gov/ij/) and analyzed in 3D-Slicer (http://slicer.org/) to characterize and demonstrate the topographical arrangement of the early tissues surrounding the nasal cartilage (for 3D reconstruction, see below). Additional information from the morphogenesis of the narwhal's (*Monodon monoceros*) head were taken from (Comtesse-Weidner, 2007).

Computed tomography (CT) and Magnetic Resonance Imaging (MRI)

Existing CT and MRI-scan series (see Table 1) were combined with new data representing different ontogenetic stages of these three specific groups. CT-scans were performed in the Department of Radiology of the Uniklinik, University Hospital of Cologne, Germany, resulting in a sequence of images (1 mm slice thickness) in all three planes (i.e. coronal, sagittal and horizontal). Conventional MRI and 7-Tesla MRI-scans were performed in the Max-Planck Institute for Metabolism Research, in Cologne, Germany, using a Siemens © Magnetom Prisma and a Bruker © BioSpin machine, respectively. The CT and MRI image series were analyzed using 3D-Slicer. The structures were identified using the segmentation technique (Cranford *et al.*, 2008) for which the images were edited voxel by voxel on the three planes, accomplished with a threshold assistance tool. Each fat tissue and bone structure was built as a 3D model to characterize the general topography, as well as to perform allometric comparisons. The epicranial complex length (**ECL**) was calculated in parallel, by the line that passes vertically through the anterior tip of the **melon** and between the

bursae complexes; and from point to point, from the tip of the melon to the middle point between both dorsal bursae complexes.

Gross dissection and cross sections

The muscles and connective tissues surrounding the blowhole region were dissected, layer by layer, to describe and demonstrate the nasal soft tissues (Schenkkan, 1972). A brain-sectioning blade was used to perform horizontal cross sections of ~1 cm slice thickness in the epicranial complex of perinatal specimens. The neonate *Tursiops truncatus* was cross-sectioned ~30 mm slice thickness in the horizontal plane to visualize and demonstrate the arrangement of the main fat structures in the nose.

Terminology and general description

Terminology follows Klima (1999) for the early nasal cartilage in fetal specimens and Comtesse-Weidner (2007) for most early soft nasal tissues; Mead (1975), Rodionov and Markov (1992), and Huggenberger *et al.* (2014) for soft tissues in adults; and Mead and Fordyce (2009), adapted to NAV (2017), for the skull. The *bauplan* orientation of the fetuses follow (NAV, 2017). The melon (*Corpus adoposum nasalis terminalis*) was defined as its main body definition (compare Discussion). The precursor tissues of the main structures involved in sound production such as the dorsal bursae complex, the rostrum and facial skull, the nasal diverticula, melon and the branches of the melon, connective tissue theca, etc. were identified by comparing the topographical position and composition of the structures as found in adults. Some important structures such as the phonic lips (*Valva nasalis intermedia*) were not examined due to samples fixation. The fetal tissues were described to elucidate the development and formation to the mature and well-known general adult morphology (see references in Discussion).

Phylogenetic approach

The main developmental changes in the soft nasal tract in dolphins were used to create transformational characters (de Pinna, 1991) as proposed by Fink (1982) (see **Supplementary file - S1**), in which, theoretically, ordered states represented ontogenetic-based transformations and, thus, state transformation and reversions were considered heterochronic changes. Conventional characters were also created with non-ontogenetically based transformations, and additional descriptions were compiled from the literature to represent the morphological variation among odontocetes. All seven characters were constructed following Sereno (2007) and added to the list of Peredo *et al.* (2018), which is a modified version from (Lambert *et al.*, 2017). We included the new data (**Supplementary file - S2**) using the matrix of Kimura and Hasegawa (2019), which added a new taxon into the supermatrix. The phylogenetic analysis was conducted with TNT (Goloboff *et al.*, 2008) using the New Technology Search with default values, except the application was tasked with shortest tree 1,000 times. The consistence index (CI) and retention index (RI) of each added character and the Character 100 of Lambert *et al.* (2017) were calculated and shown in the character description. The morphology of extinct groups were inferred using the parsimony method for the ancestral character reconstruction (**Supplementary file - S1**) in Mesquite v.3.40 (Maddison & Maddison, 2018). Developmental process in heterochronic terms were classified according Gould (1977) and Alberch *et al.* (1979), as summarized by Klingenberg (1998).

Table 1. List of examined specimens in this study. **Length of fetuses are expressed in total length/crown-hump length (mm) followed by its Carnegie/Fetal system defined by Thewissen and Heyning (2007). SAI, Dr. Senckenbergische Anatomie (Department of Anatomy III, Johann Wolfgang Goethe-University, Frankfurt a.M., Germany); GEMARS, *Grupo de Estudos de Mamíferos Aquáticos do Rio Grande do Sul*; FTZ, Forschungs- u.

Technologiezentrum Westküste, Büsum, Germany; GEMM, Grupo de Estudo de Mamíferos Marinhos da Região dos Lagos, Araruama/RJ, Brazil; MUCIN, Museu de Ciências Naturais - Universidade Federal do Rio Grande do Sul, Imbé/RS, Brazil. Methods applied: CT, Computed tomography; 7-MRI, 7-Tesla Magnetic Resonance; MRI, Magnetic Resonance Imaging; MD, Macroscopical Dissection; CS, Cross section.

Species	Code	Structure	Stage	Size** (mm)	Fixation	Method applied
FAMILY PLATANISTIDAE						
Platanista gangetica	SAI no number	Head	adult	?	?	CT
FAMILY ZIPHIIDAE						
Mesoplodon sp.	SAI no number	Head	adult	?	?	CT
FAMILY INIIDAE						
Inia geoffrensis	SAI no number	Head	adult	?	?	CT
FAMILY PONTOPORIIDAE						
Pontoporia blainvillei	GEMARS 1465	Head	adult	1381	frozen	CT/MRI/DS
Pontoporia blainvillei	GEMARS 1472	Head	neonate	755	frozen	MRI/DS
Pontoporia blainvillei	GEMM 220	Head	neonate	689	frozen	CT/DS
Pontoporia blainvillei	GEMARS no number	Body	perinatal	200	formalin	MRI
Pontoporia blainvillei	MUCIN (MM 36)	Body	fetus	?/90 (F20)	formalin	7- MRI*
Pontoporia blainvillei	MUCIN (MM35)	Head	fetus	66/54 (F20)	formalin	7- MRI*/HIS*
FAMILY PHOCOENIDAE						
Phocoena phocoena	SAI no number	Head	adult	?	frozen	CT/MRI
Phocoena phocoena	FTZ 1366	Head	adult	?	frozen	MRI
Phocoena phocoena	SAI (CN) 905	Head	adult	?	frozen	CT*
Phocoena phocoena	SAI 2000-32	Head	adult	?	frozen	CT
Phocoena phocoena	FTZ 1281	Head	subadult	?	frozen	MRI
Phocoena phocoena	SAI(SNG)1903	Head	neonate	?	frozen	CT/MRI
Phocoena phocoena	FTZ 903	Head	neonate	?	frozen	MRI
Phocoena phocoena	FTZ 898	Head	neonate	?	frozen	MRI
Phocoena phocoena	SAI 7613	Body	perinatal	700	formalin	DS*
Phocoena phocoena	SAI 903	Head	perinatal	620	frozen	CT*
Phocoena phocoena	SAI (CN)138	Head	perinatal	?	frozen	CT
Phocoena phocoena	SAI (MK)76	Head	fetus	134/60 (F22)	formalin	HIS
Phocoena phocoena	SAI (MK)69	Head	fetus	107/46 (C19)	formalin	HIS
Phocoena phocoena	SAI (MK)61	Body	fetus	95/45 (C19)	formalin	HIS
Phocoena phocoena	SAI (MK)19	Head	fetus	?/36 (C18)	formalin	HIS
Phocoena phocoena	SAI (MK)62	Body	fetus	70/28.6 (C18)	formalin	HIS
Phocoena phocoena	SAI (MK)64	Body	fetus	60/24 (C18)	formalin	HIS
Phocoena phocoena	SAI (MK)70	Body	fetus	42/18 (C16)	formalin	HIS
Phocoena phocoena	SAI (MK)71	Head	fetus	28/11.5 (C14)	formalin	HIS
FAMILY DELPHINIDAE						
Cephalorhynchus sp.	SAI no number	Head	adult	?	frozen	MRI
Tursiops gephyreus	GEMARS 1447	Head	adult	2480	frozen	CT/DS*
Tursiops truncatus	SAI no number	Head	neonate	?	formalin	CT/MRI/CS
Stenella longirostris	SAI (PGT) 037	Head	perinatal	761	formalin	CT*/MRI*/DS*
Grampus griseus	SAI (PEN) 842	Head	perinatal	649	formalin	7 - MRI*
Stenella attenuata	SAI (RXM) 056	Head	perinatal	550	formalin	7 - MRI*/CS*
Delphinus delphis	SAI (DBH)161	Body	fetus	432/- (F23)	formalin	7 - MRI*/CS*
Delphinus delphis	SAI (TBS)199	Head	fetus	233.81/- (F22)	formalin	7 - MRI*/HIS*
Lagenorhynchus albirostris	SAI (MK)77	Head	fetus	107/46 (C18)	formalin	HIS

RESULTS

General features of fetal development of the soft nasal structures

The morphogenesis of the soft nasal tissues in dolphins was remarkable for its transformation early in ontogeny: the smallest fetus we analyzed (MK 71, *P. phocoena*, crown-hump length=11.5 mm, Carnegie stage C14) presented a loose-like connective tissue containing mesemchymal cells with a large amount of intercellular substance dorsally (future posteriorly, see below) to each fetal nasal passage and surrounded by undifferentiated cells anteriorly and posteriorly (**Fig. 1A', B**). On its ventral portion (future anterior portion, see below), the fetal nasal passage exhibited more heterogeneous tissue since it was primarily composed of undifferentiated mesenchymal cells along its ventral surface and lightly stained cells with brighter nuclei at the anterior tip of the face. Undifferentiated mesenchymal cell at a point just below the ventral surface of each fetal nasal passage showed cells with inter-cellular substance and few collagen fibers, which ran downwards, and anteriorly over the loose-like connective tissue at the tip of the rostrum. This was also observed in the slightly larger fetus MK 70 (*P. phocoena*, crown-hump length=18 mm, Carnegie stage C16) (**Fig. 1A', C**). At this stage, the external naris were separated in two nasal passages by the *septum nasi* (**sn**) (see **Fig. 3**), which reached the distal portion of the nasal apertures, and was positioned at the snout tip (not shown in figures). The primitive nasal passages were aligned horizontally to the *septum nasi* and both sides presented similar morphology in tissue organization.

Fetal tissue maturation

Changes were observed between Carnegie stage C16 and C19 in *P. phocoena* specimens as the body´s curvature slightly changed from the typical “C” shaped form to a less concave condition. The head streched relative to the body axis; and the posterior portion of the body changed its orientation as observed by the alignment of the lumbar vertebrae with the main axis of the body in late Carnegie stage C18 specimens (**Fig. 1**). In all specimens classified as Carnegie stage C18 (MK 62, MK 64, MK 77), the nasal cartilage developed anteroventrally by the elongation of the *rostrum nasi* (**rn**); and dorsally (i.e. to the vertex of the skull) by the *tectum nasi* (**tn**) and projections of the *cupula nasi anterior* (**ca**) (see below) (**Fig. 1A'', A''', A''''**). At this stage, the external nasal passages became adjacent to each other by the anterodorsal extension of the *cupula nasi anterior* in parallel to the nasal passages. Thus, the cartilage sustained the associated soft tissue dorsally/posteriorly positioned relative to each nasal passage which surpassed the level of the *septum nasi* (**Fig. 1A''', A'''', Fig. 2**). The loose connective tissue dorsal/posterior to each nasal passage (herein topographical area 1, **TA1**) was surrounded by another tissue composed of a mesenchymal cells disposed in line. The latter developed from the projections of the *cupula nasi anterior* between Carnegie stages C16 and C18, running distally and posteriorly thus surrounding part of **TA1**, while muscle and collagen fibers started to grow concentrically in parallel (e.g. **Fig 1D**, **Fig. 2E,2I**).

The anterior portion of the primitive epicranial complex exhibited undifferentiated mesenchymal cells (herein topographical area 2, **TA2**) extending from the lips of the blowhole (*Valva nasalis dorsalis*) to a point between the *rostrum nasi* tip and its midline, where it reaches the loose-like connective tissue covering the dorsal surface of the *rostrum nasi* (**Fig 1A''**). The **TA2** covered dorsally the heterogeneous loose connective tissue positioned just below/anterior to the nasal passage (herein topographical area 3, **TA3**) dividing the anterior portion of the primitive epicranial complex in **TA3** posteriorly/below and a loose connective tissue (herein topographical area 4, **TA4**) rostrally. At these stages, **TA4** resembled the blubber precursor tissue

found around the fetus body (**Fig. 1A'''**), i.e. composed of light cells with great vacuoles below the *epidermis*. Increasing collagen fibers within fibroblasts horizontally oriented relative to the axis of the *rostrum nasi* appeared in **TA4** at late Carnegie stage 18 - as it was observed in *P. phocoena* (MK 62, crown-hump length=28.6 mm) and *L. albirostris* (MK 77, crown-hump length=46 mm). It covered dorsally the premaxillary (*os incisivum*, **OI**) and maxillary (**M**) bones, i.e. their anterior portions. In all specimens classified as Carnegie stage 18, including *L. albirostris*, muscle fibers from the *Musculus maxillonasolabialis rostralis* (**mr**) - or *Musculus maxillonasolabialis partes profundus, lateralis et medialis* in adults - were observed attached to **TA4** laterally on both sides of the primitive epicranial complex. The fibers extended from the anterior portion of the **premaxillary** and **maxillary bones** to the posterior end of the **maxillary bone**, which was positioned posteriorly to the nasal passage and rostrolaterally to the braincase (**Fig. 2**).

Interspecific variation was noticed in late fetal development although no direct comparisons were possible between each of the Carnegie stages of all three studied odontocete groups. The main difference took place in the size and proportions of the *rostrum nasi* cartilage which well prominent in Carnegie stage F20 in *P. blainvillei* compared to later stages in *D. delphis and P. phocoena* (**Fig. 3**), reaching almost three times the braincase width in *P. blainvillei*. *P. blainvillei* was the only species exhibiting a rostrum surpassing the anterior limits of the epicranial complex during fetal stages. However, the epicranial complex remained similar in composition and proportion compared to the other species, except by the size of the invaginations of the nasal complex. These invaginations became relatively larger from stage to stage (**Fig. 4**).

Bony tissues were detected for the first time, ontogenetically, at Carnegie stage C18 specimens: MK 64 (*P. phocoena*, crown-hump length=24 mm) was the smallest specimen presenting bone formation. It was only found in the head region, i.e. in the frontal bone (*os frontale*, **OF**), originating posteriorly to the lateral tip of the *septum interorbitale* (**si**) and running dorsolaterally while covering both sides of the anterior forebrain (not shown in figures). The **maxillary bone** presented ossification at its posterior portion just in front of the frontal bone (i.e. posterior to the nasal passage), building an ossified plate on both sides of the *septum nasi* with little bony tissue surrounding the *rostrum nasi*, posteriorly. The premaxillary bone originated from both sides of the *lamina transversalis anterior* cartilage (**lta**) and extended anteriorly through the *rostrum nasi* while surpassing the anterior limits of the ossified portion of the **maxillary bone**. The *Mandibula* (**Ma**), laterally covered the Meckel's cartilage from a line that passes vertically through the eye posteriorly and extending anteriorly to a point anterior to the tip of the Meckel's cartilage. In fetal stages, the *septum nasi* was a thin cartilage surrounded by the maxillary and premaxillary bones, posteriorly. In *P. phocoena*, the inner ear started ossification later than the nasal structures, at early Carnegie stage C19, by the tympanic bone (*os tympanicum*) characterizing the morphogenesis of the tympanic cavity.

The connective tissue found in the topographical areas (**TA**'s) at early stages in *P. phocoena* (**Fig. 1**, **Fig. 2**) was topographically positioned in the same regions of the primitive epicranial complex as in the other studied species, and was mainly composed of **TA3** anterior to the nasal passages. The **TA3** in late fetal stages (i.e. Carnegie stages F20 to F22), consisted of concentric muscle and collagen fibers anterior to each nasal passage between the deepest nasal invagination - placed just above the *lamina transversalis anterior* cartilage - and the **TA2**, that covered the epicranial complex dorsally (**Fig. 2**, **Fig. 3**). **TA3** composition exhibited clear association with the nasal cartilage, specifically with the dorsal portion of the *septum nasi*: the heterogeneous composition of this tissue was due to the loose connective tissue composed of lightly stained

mesenchymal cells with rounded nuclei. These cells were disposed in a matrix supported by dense extra-cellular substances colored in blue and irrigated by blood vessels (**Fig. 2**). The shapes of these loose connective tissue structures varied between species and ontogenetic stages since they became elongated in early stages such as in *L. albirostris* (MK 77, crown-hump length=46 mm, Carnegie stage C18) and in *P. blainvillei* (MM 35, crown-hump length=54 mm, Carnegie stage F20). Here, they laterally surrounded the *septum nasi* and dorsally covered the *lamina transversalis anterior* cartilage and the deepest nasal invaginations (**Fig. 2**). In late fetuses, such as in *P. phocoena* (MK 76, total length=134 mm, Carnegie stage F22) and *D. delphis* (TBS 199, total length=233.81 mm, Carnegie stage F22), the *septum nasi* was reduced to a thin cartilage that separated both right and left **TA3**'s, which presented loose connective tissues embedded into concentric collagen and muscle fibers of the **TA3** (**Fig. 2, Fig. 3, Fig. 4**). Additionally, in the late *D. delphis* (TBS 199), the loose connective tissue from **TA3** exhibited increased collagen and muscle fibers from the nasal plug muscles (**npm**).

Dorsolaterally of each **TA3** and placed just anteriorly to the nasal passage at the distal border of the nasal diverticula, a pair of small loose connective tissue structures (herein topographical area 5, **TA5**) were found from Carnegie stage C19 onwards (**Fig. 2**). These structures exhibited similar arrangements to those found in **TA3**, with dense extra-cellular matrix sustaining the light stained cells (**Fig. 4A**). In the late *D. delphis* (TBS 199) fetus, both **TA5** exhibited increased collagen fibers. Anteriorly, **TA5** was attached by the axially oriented collagen and muscle fibers originating from **TA3** and was surrounded dorsally by the **TA2** and ventrally by a dense connective tissue that covered the anterior portion of the nasal passage. The **TA2** was primarily composed of dense collagen and muscle fibers disposed concentrically around **TA3** at later fetal stages (i.e. F20 to F22) in all three groups. The collagen fibers were attached ventrally to a thin and oblique membrane of connective tissue between the anterior portion of the *lamina transversalis anterior* and the *rostrum nasi* cartilages, just at the rostrum base, and dorsally at the blowhole ligament.

Major changes in *P. phocoena* between Carnegie stages C16 to C18 included the blubber differentiation that covered the whole fetus body, which coincided with the anterior development of the *rostrum nasi* and the displacement of the external naris towards the top of the head (**Fig. 1A, A'', A''', A''')**. Simultaneously, in *P. phocoena* (MK 76, **Fig. 2**), **TA4** originated ventrally from the loose connective tissue covering the dorsal surface of the *rostrum nasi* tip, where collagen fibers concentrically converged from each side of the cartilage connecting anterior muscle fibers from each side of the *Musculus maxillonasolabialis rostralis*. The concentric collagen fibers from **TA4** were thicker just anterior to the primitive epicranial complex, where the fibers extended horizontally from both sides of the blubber precursor tissue anchoring the medial portion of the *Musculus maxillonasolabialis rostralis*. The collagen fibers ended dorsally at a line intersecting the level of both loose connective tissues in the **TA3** and the dorsal tip of the *spina mesethmoidalis*. Few fibroblasts and muscle fibers from the *Musculus maxillonasolabialis rostralis* were embedded into the loose connective tissue of the blubber precursor tissue covering **TA4** dorsally. Additionally, **TA4** presented gradual composition since strong collagen fibers were found close to **TA2** posteriorly, while these fibers decreased in number and size rostralwards where **TA4** reached the blubber precursor tissue (**Fig. 2D**).

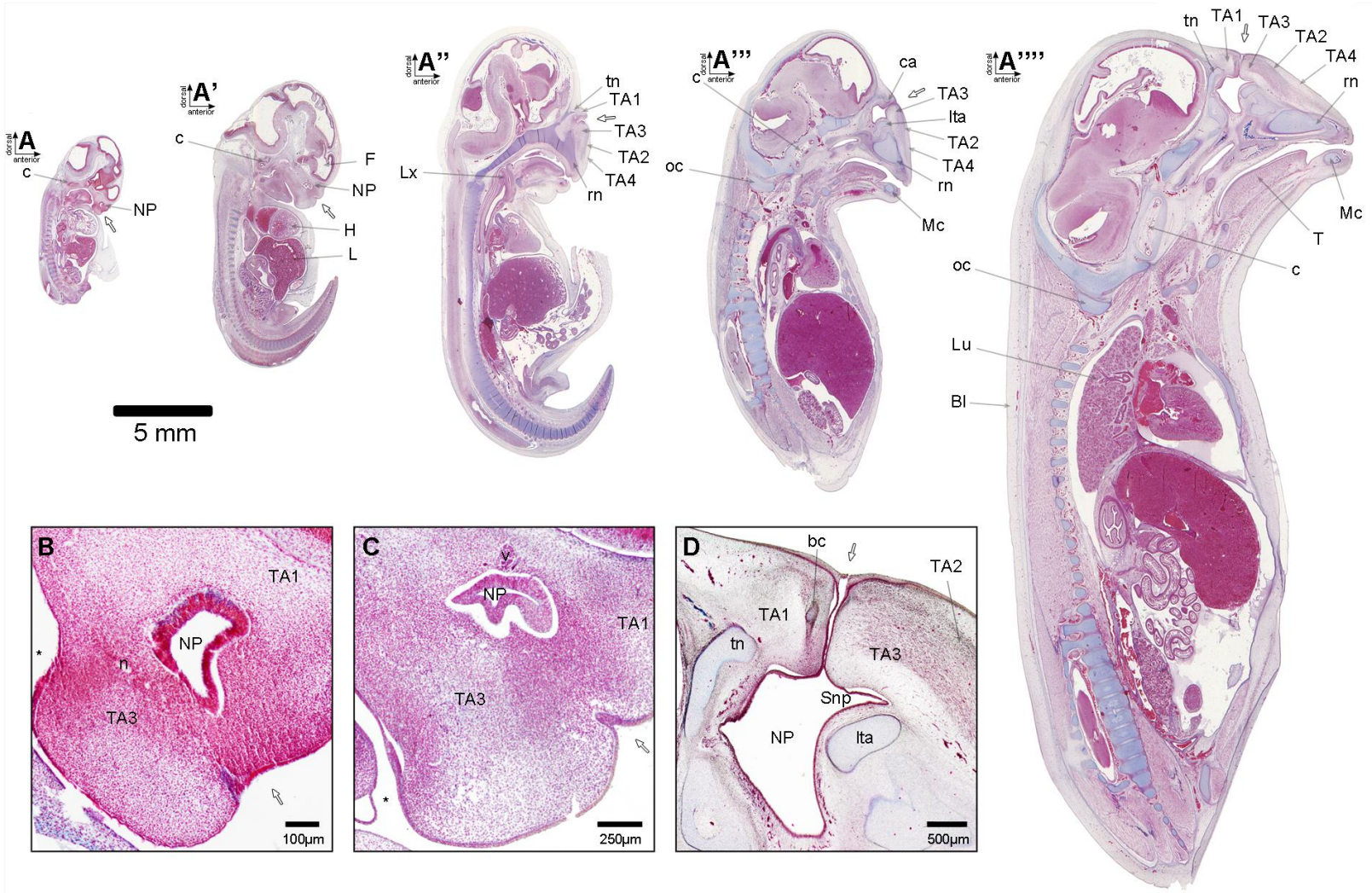

Fig. 1. Early development of *Phocoena phocoena* in saggittal sections. **A**. MK 71 crown-hump length=11.5 mm, Carnegie stage 14. **A'**. MK 70 crown-hump length=18 mm, Carnegie stage 16. **A''**. MK 64 crown-hump length=24 mm, Carnegie stage 18. **A'''**. MK 62 crown-hump length=28.6 mm, Carnegie stage 18. **A''''**. MK 61 crown-hump length=45 mm, Carnegie stage 19. **B**. MK 71. **C**. MK 70. **D**. MK 61. Blubber precursor tissue, **Bl**; cochlea, **c**; *cupula nasi anterior* cartilage, **ca**; forebrain, **F**; heart, **H**; liver, **L**; *lamina transversalis anterior* cartilage, **lta**; larynx, **Lx**; lungs, **Lu**; Meckelian cartilage, **Mc**; nerve, **n**; nasal passage, **NP**; rostrum nasi cartilage, **rn**; occipital condyle, **oc**; tongue, T; *tectum nasi* cartilage, **tn**; umbilical cord, **U**; vessel, **v**. For **TA1** to **TA4** see main descriptions. Mouth and external nasal passage position are indicated by asterisks and white arrows, respectively.

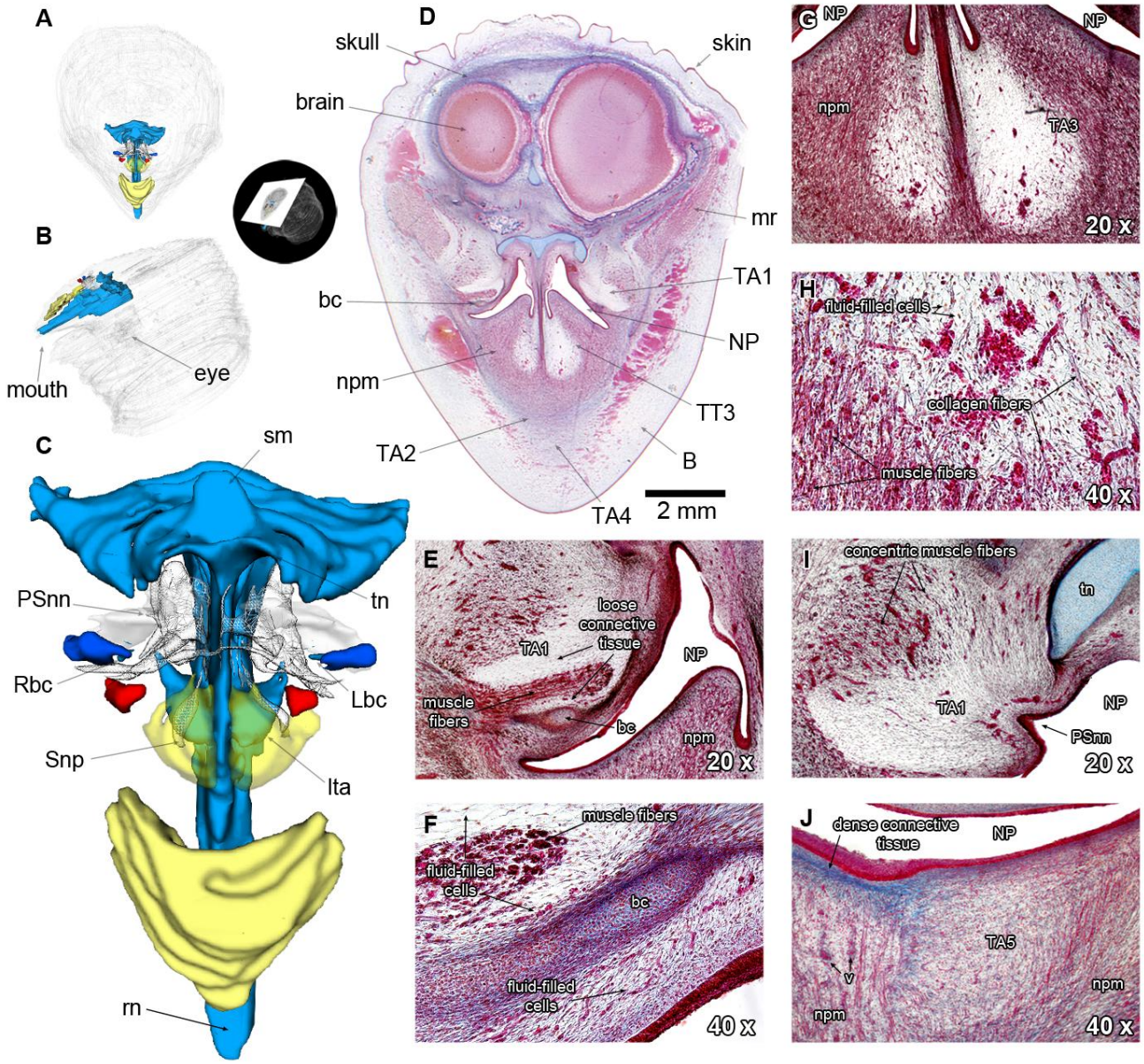

Fig. 2. Anatomy of the nasal structures precursor tissues in a late *Phocoena phocoena* fetus (MK 76, total length = 134 mm, Carnegie stage F22). (**A**-**C**) 3D reconstructions from histological slides (**D**-**J**) demonstrating general head (**translucent white**) and nasal cartilages (**cyan**) morphology, including the bursae cartilage (**bc**). The main precursor tissues and structures of the sound production apparatus were labeled in 3D (**C**) (anterior dorsal bursae, **red**; branches of the melon, **translucent yellow**; loose connective tissue covering the posterior Snn, **white**; melon, **yellow**; nasal passage and nasal air sacs, **white wireframe**; posterior dorsal bursae, **blue**) and demonstrated by focal microscopy photographs (**E**-**J**). Blubber precursor tissue, **B**; *lamina transversalis anterior* cartilage, **lta**; left bursae cartilage, **Lbc**; *Musculus maxillonasolabialis rostralis*, **mr**; nasal plug muscle, **npm**; posterior *Saccus nasalis nasofrontalis*, **PSnn**; right bursae cartilage, **Rbc**; *rostrum nasi* cartilage, **rn**; spina mesethmoidalis, **sm**; *Saccus nasalis praemaxillaris*, **Snp**; *tectum nasi* cartilage, **tn**. For **TA1** to **TA5** see main descriptions.

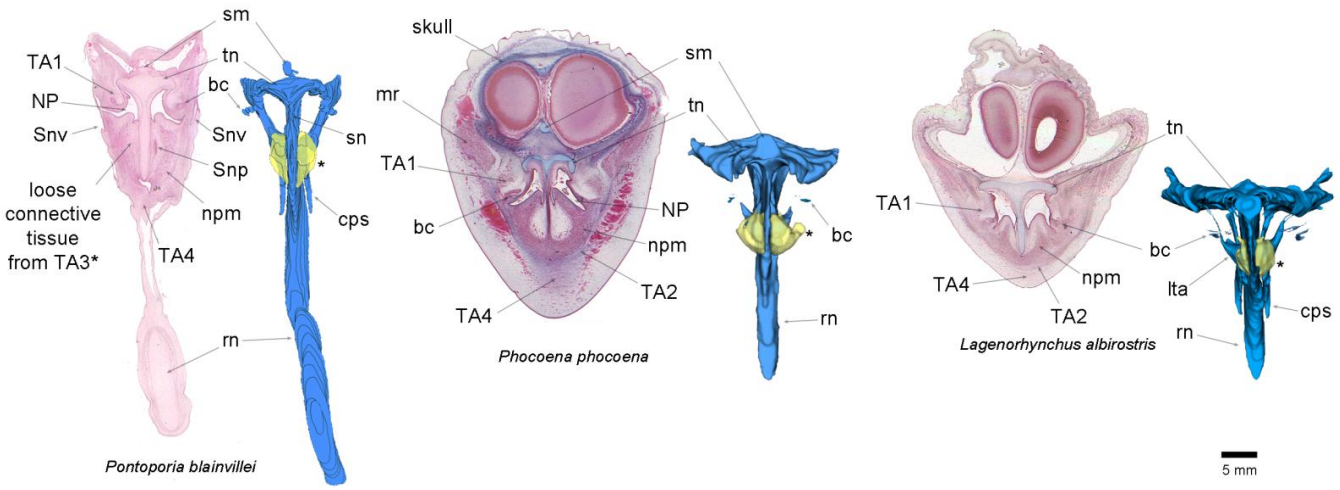

Fig. 3. 3D reconstructions from histological slices of the nasal cartilages (cyan) and the loose connective tissue from **TA3** (translucent yellow) in late fetuses of *Pontoporia blainvillei* (**MM 35**, crown-hump length=54 mm, Carnegie stage F20), *Phocoena phocoena* (MK 76, total length=134 mm, Carnegie stage F22), and *Lagenorhynchus albirostris* (MK 77, crown-hump length=46 mm, Carnegie stage F18) in dorsal view. Bursae cartilage, **bc**; *cartilago paraseptalis*, **cps**; *lamina transversalis anterior* cartilage, **lta**; *Musculus maxillonasolabialis rostralis*, **mr**; nasal passage, **NP**; nasal plug muscle, **npm**; *rostrum nasi* cartilage, **rn**; *Saccus nasalis praemaxillaris*, **Snp**; *Saccus nasalis vestibularis*, **Snv**; *spina mesethmoidalis*, **sm**; *tectum nasi* cartilage, **tn**. For **TA1** to **TA5** see main descriptions.

The nasal cartilages were increasingly surrounded by osteological tissues from Carnegie stage C19 onwards, except the dorsal and lateral projections of the *cupula nasi anterior* (**Fig. 1A", A"', A""**, **Fig. 2**): all fetuses classified as between Carnegie stages C18 to F23 presented those cartilage projections sustaining the loose connective tissue posterior to both sides of the nasal passage (i.e. **TA1**). These cartilages (**bc**) (**Fig. 4A", B", C"**) were connected to the *cupula nasi anterior* by their medial portion, as mentioned before. The **bc** extended ventrally (i.e. in parallel to the nasal passage) as a cylindrical shape through the anterior portion of **TA1**, ending sharply at its anteroventral portion. Below and attached to each of those cartilages, a pair of undifferentiated mesenchymal cell tissues ran ventrally (laterally within the epicranial complex) and followed the diverticula into the distalmost portion of the premaxillary air sacs, at the posterior portion of the premaxillary bones. These cartilages anchored concentric muscle and collagen fibers inserted into the **TA1**'s loose connective tissue, while anchoring a small portion of loose connective tissue (see blue structure in **Fig. 2C**, becoming the posterior dorsal bursae, see below) on its dorsal half. Posteriorly, it was surrounded by muscle fibers from the *Musculus maxillonasalis* (**mmn**). In the late fetus we analyzed histologically (*D. delphis* - TBS 199, total length=233.81 mm, Carnegie stage F22), the connective tissue linking the mentioned cartilage (**bc)** to *cupula nasi anterior* was reduced to a thin layer of fibroblast cells, and the *Musculus maxillonasalis* exhibited increased muscle fiber posterior to **TA1**.

Development of nasal diverticulae

The nasal air sacs morphogenesis was detected during the fetal development, starting at Carnegie stage 18 (**Fig. 1D**, **Fig. 2C**, **2I**). The premaxillary air sacs (*Saccus nasalis praemaxillaris*, **Snp**) formation was characterized by two invaginations of the nasal passage epithelium that covered dorsolaterally each *lamina transversalis anterior* cartilage on both sides of the epicranial complex at early Carnegie stage C18 (although it seems a cilindric rostrally-oriented air space in the 3D model in **Fig. 2C** due to distortions between histological slices). At this stage, the nasofrontal air sacs (*Saccus nasalis nasofrontalis*, **Snn**) were detected

as a pair of lateral bifurcated invaginations, in which the anterior portion was positioned anteriorly to the ventral portion of **TA1**, and its lateral tip followed the connective tissue running ventrally to the **bc** (as cited above). The posterior portion was smaller and exhibited associated collagen and muscle fibers from the posterior portion of **TA1**. The premaxillary air sacs of fetal specimens from Carnegie stages C19 to F20 exhibited increased relative size, but their anterior position was still dorsal to the *lamina transversalis anterior* cartilage. At this stage, the nasal passage was positioned more posteriorly compared to earlier stages. Additionally, the posterior portion of the nasofrontal air sacs increased relatively in size in fetal specimens of Carnegie stages F20 to F22 since it extended posteriorly and distally (i.e. laterally) as in the late *D. delphis* fetus (TBS 199, total length=233.81 mm, Carnegie stage F22), thus surrounding **TA1** posteriorly (not shown in images). The morphogenesis of the vestibular air sacs (*Saccus nasalis vestibularis*, **Snv**) was detected between Carnegie stages C18 to F22 as invaginations of the *epidermis* at both lateral sides of the blowhole (**Fig. 4**). Thus, they formed the distalmost diverticula in the dolphin head. The timing of development of the vestibular air sacs varied between the three groups analyzed since in *P. phocoena* it started to differentiate late in Carnegie stage F22 onwards while in *L. albirostris* (MK 77), at Carnegie stage C18, the pair of vestibular air sacs were present forming small invaginations from the *epidermis* at the future blowhole. In *P. blainvillei* (MM 35), the vestibular air sacs exhibited relatively larger dimensions compared to the other specimens as they extended posteriorly and anteriorly to the nasal passage, covering the lateral sides of the epicranial complex just at the level of the **bc**. Although a similar condition was found in *P. phocoena* and *L. albirostris*, their vestibular air sacs did not extend anteriorly to the nasal passage.

Perinatal development of the soft nasal structures

The perinatal development of the soft nasal structures were characterized by topographic and compositional changes in the epicranial complex, remarkably distinct between the three groups analysed in this study. Nevertheless, perinatal specimens exhibited similar general features to those found in adults, such as the straight alignment of the rostrum with the axial skeleton, the complete skin pigmentation and a similar arrangement of the structures involved in the sound generation (except for the monkey lips at the *Valva nasalis intermedia*). In delphinids, the epicranial complex asymmetry was perceived by the larger size of the right nasal plug muscle and the right dorsal bursae complex, that exhibited larger dimensions and was positioned more dorsally compared to the left one in all species analyzed (Table 1; **Fig. 5**). In the following, the main soft nasal structures and their respective topographical/compositional correspondence with early fetal tissues are described.

Posterior dorsal bursae (*Corpus adiposum nasalis posterior*, **Canp**). This pair of small ellipsoid fat bodies were positioned just posteriorly to each nasal passage, below the vestibular air sacs and surrounded posteriorly by the nasofrontal air sacs. In the early perinatal *D. delphis* (DBH 161, total length: 432 mm), the posterior dorsal bursae complexes were associated to the anterior loose-like connective tissue found posteriorly to **bc** in **TA1** in late fetal specimens (**Fig. 2C**,**2F** and **Fig 5**).

Anterior dorsal bursae (*Corpus adiposum nasalis anterior*, **Cana**). This pair of small ellipsoid fat bodies were positioned just anteriorly to each nasal passage, surrounded by a thin and dense connective tissue, just dorsally to the nasal plug (**Vnv**) and the nasal plug muscles (**npm**) (see below). Dense collagen and muscle fibers from the **npm** border were located anteriorly to each anterior dorsal bursae (**Fig. 5A**), in a similar condition as the loose connective tissue described as **TA5** in late fetal specimens (**Fig. 2J**).

Fig. 4. Histological sections of the primitive epicranial complex in (**A, A', A''**) *Pontoporia blainvillei* (**MM 35**, crown-hump length=54 mm, Carnegie stage F20), (**B, B'', B''**) *Phocoena phocoena* (MK 76, total length=134 mm, Carnegie stage F22), and *Lagenorhynchus albirostris* (**C, C', C''**) (MK 77, crown-hump length=46 mm, Carnegie stage F18), in dorsal view, demonstrating the early formation of the vestibular air sacs (*Saccus nasalis vestibularis*, **Snv**) (**A, A', B, B', C, C'**), and interespecific morphological variation of the bursae cartilage (**bc**) (**A'', B'', C''**). Nasal passage, **NP**; *Saccus nasalis nasofrontalis*, **Snn**; *septum nasi* cartilage, **sn**; *Saccus nasalis vestibularis*, **Snv**; nasal plug muscle, **npm**.

Nasal plugs (*Valva nasalis ventralis*, **Vnv**) **and nasal plug muscles** (*Musculus maxillonasolabialis*, *pars valvae nasalis ventralis*, **npm**). The nasal plug was characterized by dense connective tissue covering the nasal passage from anteriorly in the epicranial complex, just below the anterior dorsal bursae and dorsally to the premaxillary air sacs. The topographical position of the nasal plug resembled the growing dense connective tissue found at the same position in late fetuses (**Fig. 2D, 2G,2J**). The nasal plug muscle exhibited remarkable variation during the perinatal development among the three groups analysed in this study. In the investigated delphinids, the right-hand side nasal plug muscle became larger and composed of dense and concentric muscle fibers surrounding two small fatty tissue structures that extended posteriorly from the nasal passage to the concentric muscle fibers to the *Musculus maxillolabialis* (**mml**), anteriorly (**Fig. 5**). The nasal

plug muscle arrangement resembled the **TA3** found in fetal specimens due to the topographical position of both tissues. Moreover, in delphinids, the muscle fibers from the nasal plug muscles were disposed in the same orientation as in **TA3**, while the fat pathways, which can be described as branches of the melon, were placed at both sides of the epicranial complex. These branches were embedded into the muscle and collagen fibers of the nasal plug muscles and were topographically positioned at the same position as the loose connective tissue found in **TA3** during the fetal development (**Fig. 2**, **Fig. 3**).

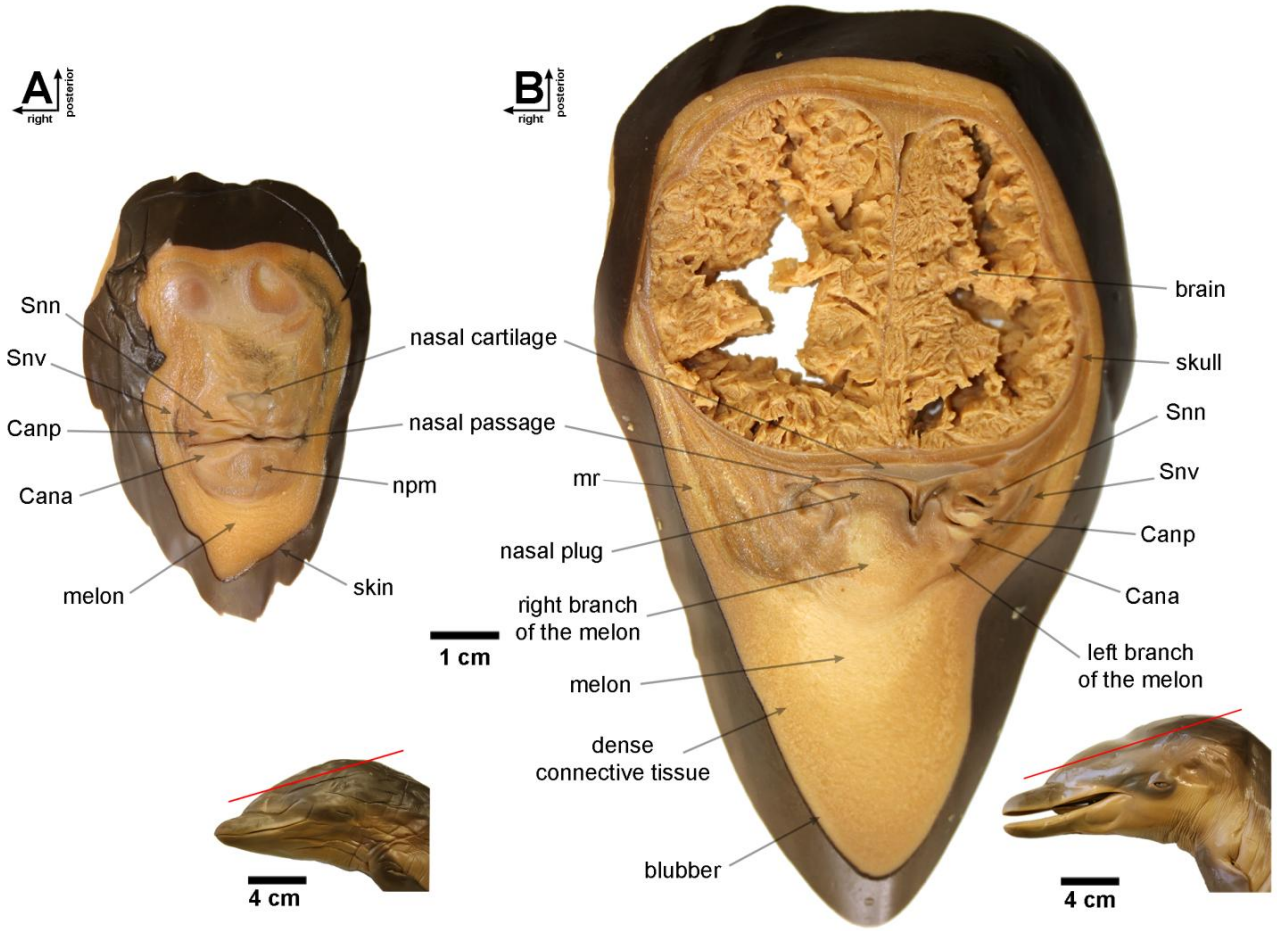

Fig. 5. Soft nasal structures in perinatal delphinid specimens. (**A**) *Delphinus delphis* (DBH 161, total length=43.2 cm); (**B**) *Stenella longirostris* (PGT 037, total length=76.1 cm). Anterior dorsal bursal (*Corpus adiposum nasalis anterior*) **Cana**; *Corpus adiposum nasalis terminalis*, **melon**; *Musculus maxillonasolabialis rostralis*, **mr**; nasal plug muscle (*Musculus maxillonasolabialis*, *pars valvae nasalis ventralis*), **npm**; nasofrontal air sac (*Saccus nasalis nasofrontalis*), **Snn**; posterior dorsal bursae (*Corpus adiposum nasalis posterior*), **Canp**; vestibular air sacs (*Saccus nasalis vestibularis*), **Snv**.

Despite the clear asymmetry of the nasal plug and the nasal plug muscles during the perinatal development in delphinids, promoted by the increased timing of development of the right portion of these structures, major differences in the composition of the nasal plug muscles were found between the three groups analyzed in this study. In delphinids, the right nasal plug muscle was expanded by an increased number of collagen and muscle fibers with a large amount of fat between the layers (**right branch of the melon, rm**). In comparison, the left branch of the melon (lm) (**Fig. 5**), positioned just ventrally to the anterior

dorsal bursae and surrounded by collagen and muscle fibers, was much smaller. In *P. phocoena*, the nasal plug muscles were nearly symmetrical tissues composed of dense collagen and muscle fibers on each side of the epicranial complex, and there was no evidence of fat tissues within the fibers. In *P. blainvillei*, the nasal plug muscles were also nearly symmetrical and composed of collagen and muscle fibers surrounding fat tissues at both sides, as seen in adults (see below). In delphinids, the *Musculus maxillolabialis* was embedded in the fat tissue, thus forming a continued fat pathway from the anterior portion of the nasal passage into the **melon**, as seen in adults (see below).

Melon (*Corpus adiposum nasalis terminalis*, **melon**). The largest fat tissue structure in the dolphin head was composed of concentrically oriented collagen fibers, anchored on both sides of the medial portion of the *Musculus maxillonasolabialis rostralis* (**mr**), with a large amount of adipose tissue between the layers (**Fig. 5**). Late perinatal specimens exhibited increased adipose tissue between the collagen fibers and started to shape the rounded curvature of this structure (**Fig. 5B**). The melon clearly resembled the **TA4** described in fetal stages (**Fig. 1, Fig. 2, Fig. 3, Fig. 5**).

Nasal air sacs. The nasal diverticula exhibited continued topographical transformation due to the formation of the vestibular air sacs and the nasofrontal air sacs, while the premaxillary air sacs presented similar shape compared to adults during perinatal development. The pair of premaxillary air sacs were positioned at both posterior projections of the premaxillary bones as observed in late fetal specimens. They extended from the nasal passage to the anterior border of the nasal/posterior portion of the premaxillary bones. They are thus asymmetric in the investigated delphinids, while in *P. phocoena* and *P. blainvillei* they were nearly symmetric. The nasofrontal air sacs originated on the posterior wall of the nasal passage, surrounded posteriorly by connective tissue at the position of TA1 in early fetuses (**Fig. 2**, **Fig. 3**, **Fig. 4**, **Fig. 5**). In the early perinatal *D. delphis* (DBH 161, total length=432 mm), the nasofrontal air sacs were not pigmented. In delphinids and *P. phocoena*, it developed anteriorly while surrounding the nasal passage and the anterior dorsal bursae, while in *P. blainvillei*, the anterior portion of the nasofrontal air sacs was absent. In *P. phocoena* and *P. blainvillei*, the connective tissue surrounding the posterior portion of the nasofrontal air sacs has differentiated to a dense and rigid connective tissue composed of concentric fibers on each side of the nasal passage.

The pair of vestibular air sacs was the distalmost invagination of the nasal passage, starting at the early fetal blowhole slit and present in all perinatal specimens. In the perinatal *D. delphis* (DBH 161), the vestibular air sacs covered dorsally and laterally the posterior dorsal bursae complex with shallow invaginations at its anterior portion. These invaginations were more pronounced in larger perinatals such as in *S. longirostris* (PGD 037, total length=761 mm). In this specimen, the vestibular air sacs presented this feature in the whole structure. In late *P. phocoena* perinatals - such as SAI **7613** (total length=700 mm) - the vestibular air sacs were the biggest structure in the epicranial complex (except for the **melon**), and exhibited a higher degree of invaginations.

Postnatal development of the soft nasal structures

At birth, all specimens exhibited all structures involved in the sound generation process. However, despite allometric changes related to the increased size (**Supplementary file - S3**), topographical and compositional transformations occurred during the postnatal development of the epicranial complex (**Fig. 6**, **Fig. 7**) as the final steps to a mature (i.e. adult looking) sound generating apparatus. Topographical changes of the epicranial complex occurred in parallel to the skull formation. The posterior portion of the premaxillary

bone exhibited great variation among the species analyzed in this study. In *P. blainvillei* and *P. phocoena*, the elevation of the dorsal surface of the posterior (nasal) portion of this bone during the postnatal development directly elevated the premaxillary air sacs and all the soft nasal tissues positioned anterior to the nasal passage in relation to the length axis of the skull (**Fig. 7**). In these groups, the posterior and anterior dorsal bursae were aligned with the posterior portion of the main body of the **melon** along this length axis (**Fig. 7**). In *Tursiops* spec., the posterior (nasal) portion of the **premaxillary bone** was concave and without major shape transformations during postnatal development, differing from the situation in *P. blainvillei*, *P. phocoena*, and *C. commersonii*, where the posterior end of the right branch of the **melon** was situated anteriorly to the anterior dorsal bursa.

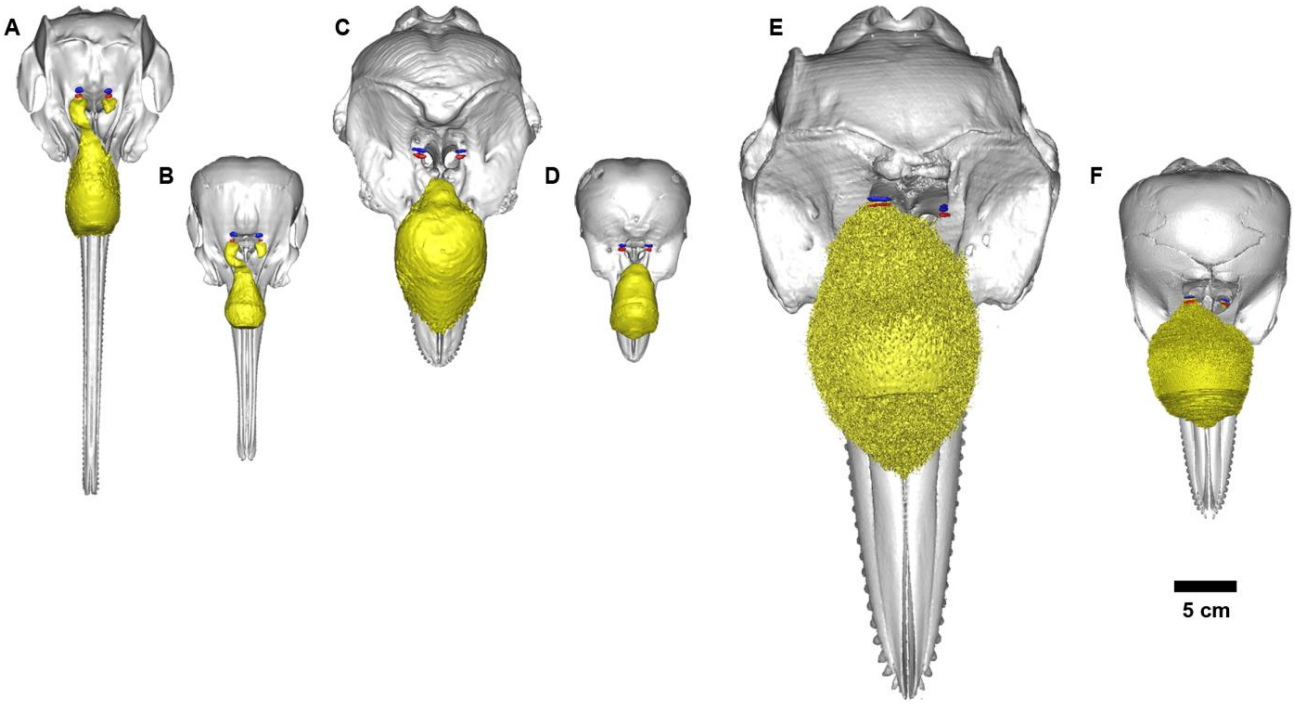

Fig. 6. 3D reconstructions of the main fat pathways (posterior dorsal bursae, **blue**; anterior dorsal bursae, **red**; melon and the branches of the melon, **yellow**) and the skull of (**A**-**B**) *Pontoporia blainvillei*, (**C**-**D**) *Phocoena phocoena* (**E**-**F**) *Tursiops* spp., in dorsal view.

The bursae complex (i.e. right and left anterior dorsal bursae and posterior dorsal bursae) presented similar allometric changes (**Supplementary file - S3**), and in their relative position in the three groups analyzed, since in all neonate specimens, the posterior dorsal bursae were dorsocaudally positioned relative to the anterior dorsal bursae while they were aligned axially in adults (**Fig. 7**). The caudal movements of both posterior portions of the maxillary and premaxillary bones and associated facial muscles plus connective tissues resulted in a topographical rearrangement of these structures relative to the bursae complex in adults. The steeper vertex of the skull in *Tursiops* spec. reflected the distinct arrangement of the posterior melon in most delphinids: the right branch of the melon extended posteriorly while following the skull shape development (**Fig. 7**). In *P. blainvillei*, the dorsal movement of the posterior (nasal) portion of the premaxillary bone, described above, and the caudal movements of the maxillary and the nasal bones resulted in a flattened dorsal surface of the adult skull, serving as the base of the epicranial complex (**Fig. 8A**). Additionally, adult *P. blainvillei* displayed an elongated right branch of the melon compared to the neonate (**Fig. 6, Fig. 7**).

The rostrum developed in three, remarkably distinct, group-specific ways: in delphinids, the rostrum developed anteriorly and increased in size relative to the melon (**Supplementary file - S3**) while the **melon** exhibited less convexity of its anterior portion in adults compared to neonates. In *P. blainvillei*, the rostrum developed slightly anteroventrally, while presenting a more convex dorsal surface, also apparent in the anterior shape of the **melon**. In *P. phocoena*, the rostrum and the melon presented a constantly similar shape and relative size throughout postnatal ontogeny. Compositional changes were observed during the postnatal development of the **left branch of the melon** (**lm**) in *Tursiops* spec.: the neonate specimen analyzed, as also observed in all perinatal delphinids, presented a fat pathway (ending in the nasal plug just below the left anterior dorsal bursae. In the adult, the left nasal plug was composed of dense connective tissue with concentric collagen fibers (**Fig. 8C, 8D**). On the other hand, *P. phocoena* did not exhibit the right and left **branches of the melon**, but in their place, concentric dense collagen fibers and muscle fibers (**Fig. 8B**). The ontogenetic dorsal movement of the posterior portion of the premaxillary bones elevated the left premaxillary air sacs and changed the orientation of the left branch of the melon to a more anterodorsal alignment relative to the axis of the skull in *P. blainvillei* and *P. phocoena* (**Fig. 7**).

Plylogenetic analysis

Seven new characters (325 to 331) represented the main features related to the directional properties of the sound production in odontocetes (Aroyan *et al.*, 1992; Au *et al.*, 2010; Wei *et al.*, 2017). The phylogenetic analysis resulted in four shortest trees with a length of 4,565,997 steps, a consistency index of 0.587, and a retention index of 0.498. Independent changes in ontogenetic patterns of the sound generating structures in odontocetes led to morphological diversity of biosonar designs found in this group. The evolution of the vestibular air sacs (trait only) (Character 100, **Supplementary file - S1**) may have two explanations: 1) An acceleration of the formation of the tissues surrounding the blowhole between Carnegie stages C18 to F22 could have independently evolved in Physeteroidea and Delphinida (i.e. homoplasic condition); or 2) These changes in the blowhole formation at fetal stages might have evolved in a common ancestor of crown cetaceans, thus, consequently, paedomorphic (post-displacement) events might have occurred in a common ancestor of Ziphiidae and Platanistidae for its loss (**Supplementary file - S1**).

Although the rostrum size, relative to the epicranial complex length (ECL) (Character 330, **Supplementary file - S1**), may have evolved under more than one heterochronic proccess (e.g. rostrum increased/decrased and increasing melon development), we perceived that, within Delphinida, the decreased size of the rostrum relative to the ECL supports the Delphinoidea clade: Delphinidae + (Phocoenidae + Monodontidae). Changes in relative size of the rostrum occurred early in development in *P. phocoena* and *L. albirostris* compared to *P. blainvillei*, thus representing a post-displacement process reducing the size of the rostrum at fetal stages or a pre-displacement process in the Pontoporiidae line. All perinatal and postnatal ontogenies studied here presented increased size of the rostrum, thus representing a distinct, shared, process of the three groups analyzed. Interestingly, some small dolphins such as *Delphinus* exhibit increased rostrum representing an undefined peramorphic process.

The left branch of the melon seems to be one of the most variable structures in all cetaceans. In odontocetes except for Physeteroidea, this structure might have be useful for collimating sounds in all delphinidan families except in Phocoenidae and some Delphinidae. Particularly in Delphinidae, this character exhibited two reversions (**Fig. 9**). The absence of the left fat pathway is intrinsically related to the acceleration

process of the left nasal plug muscle development (Fig. 4, Fig. 8). In this way, delphinids exhibiting this structure such as *G. griseus* evolved under a neotenic proccess (especially in the postnatal development) in the formation of the left side of the epicranial complex. Delphinids also exhibited a distinct configuration compared to all odontocetes except Physeteroidea, in which the bursae complex is not aligned with the posterior portion of the melon (Character 325, state=1). Since dorsalwards extensions of the posterior premaxillary bones were observed in the postnatal development of *P. blainvillei* and *P. phocoena*, it would be plausible to assume that delphinids, lacking this extension, present a progenetic process in the formation of the posterior portion of the premaxillary and maxillary, resulting in a distinct arrangement of the soft tissues (**Fig. 6**, **Fig. 7**, **Fig. 9**). Additionally, delphinids exhibited a distinct arrangement of the nasal diverticula as the premaxillary air sacs became larger than the vestibular air sacs (Character 328, state=1). In this case, independent processes might have occurred on the size regulation of each structure such as a progenesis process in the development of the vestibular air sacs in delphinids (i.e. during perinatal and postnatal development); followed by a hypermorphic proccess in the premaxillary air sacs.

DISCUSSION

Cetacean *bauplan* evolution is linked to the adaptations of these top predators to subsist throughout all life phases in the aquatic environment. The transition from terrestrial to aquatic organisms has lead to a great number of developmental-based changes of individual organ systems (Berta *et al.*, 2014; Thewissen & Williams, 2002). Besides evolutionary novelties related to hydrodynamic locomotion and propulsion (Fish, 2002; Thewissen *et al.*, 2009), stem cetaceans from the Eocene (56 – 33.9 m.y.) evolved unique arrangements of the sound receiving structures due to adaptation for directional underwater hearing (Nummela *et al.*, 2004; Oelschläger, 1990). A gradual shift of the external naris to the top of the head occurred in concert with the so-called "telescoping" process of the cetacean skull (Miller, 1923). Accordingly, the rostrum increased in size and in the number of specialized teeth to catch and grab small invertebrates and fishes (Armfield *et al.*, 2013) while the posterior portion of the upper jaw bones (maxillary and premaxillary bones) extended caudally and resulted in the rearrangement of the forehead muscles and soft tissues to open and occlude the nasal passage during diving behaviors (Geisler *et al.*, 2014; Heyning & Mead, 1990). Major changes occur during the morphogenesis of the cetacean skull (Klima, 1999; Kükenthal, 1889; Moran *et al.*, 2011) and are promoted primarily by the unique transformation of the nasal cartilages in fetal stages (**Fig. 1**) (Klima, 1999). In odontocetes, the main fetal transformations in the nasal cartilage development affect the soft nasal tissue morphology found in adults. Although many studies have attempted to analyze the prenatal development and the evolution of the cetacean skeleton (Moran *et al.*, 2011), few studies have addressed the ontogeny of the soft tissues and its macroevolutionary implications (Klima, 1999).

Extant cetaceans, i.e. baleen (suborder Mysticeti) and toothed (suborder Odontoceti) whales (**Fig. 10**), present similar patterns of rostrum formation since the *rostrum nasi* cartilage starts developing rostralwards during embryogenesis and is retained in all adult forms between the vomer, premaxilla and maxilla as the mesorostral cartilage (Klima, 1999). However, the two lineages differ in the development of individual parts of the nasal cartilage. Mysticetes retain the medial and caudal portion of the nasal cartilage in adults to sustain the inner margin of the blowhole (Buono *et al.*, 2015) while odontocetes present variable ontogenetic trajectories through which the posterior side wall structures are retained in adults (e.g. the left *tectum nasi* as the unilateral nasal roof cartilage in sperm whales), or are lost during postnatal development

(e.g. bursae cartilage in some odontocetes) (Klima, 1995; Prahl *et al.*, 2009). In addition, the skull formation differs between the two suborders mainly due to changes in the development of the skull (Moran *et al.*, 2011): Oelschläger (1990) proposed that the increased rostrum size in early odontocetes resulted in the dorsal anchoring of the premaxillary and maxillary bones to the frontal bone (i.e. instead of below the frontal bone in mysticetes). This in turn promoted the development of associated musculature and soft tissues surrounding the nasal passage capable of producing and transmitting sounds (Cranford *et al.*, 1996; Norris *et al.*, 1961).

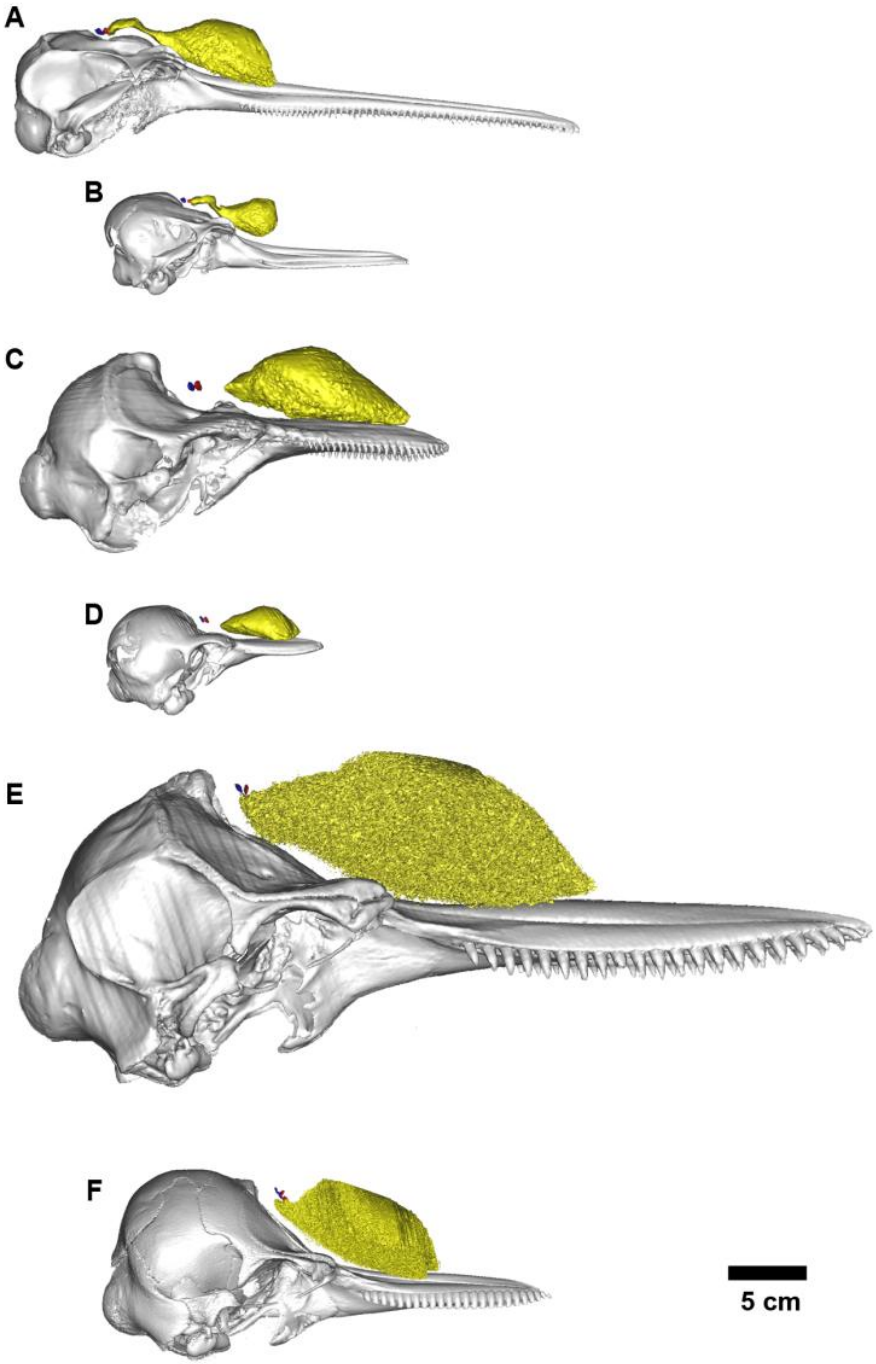

Fig. 7. 3D reconstructions of the main fat pathways (posterior dorsal bursae, **blue**; anterior dorsal bursae, **red**; melon and the "branches" of the melon, **yellow**) and the skull of (**A**-**B**) *Pontoporia blainvillei*, (**C**-**D**) *Phocoena phocoena*, and (**E**-**F**) *Tursiops* spp., in lateral view.

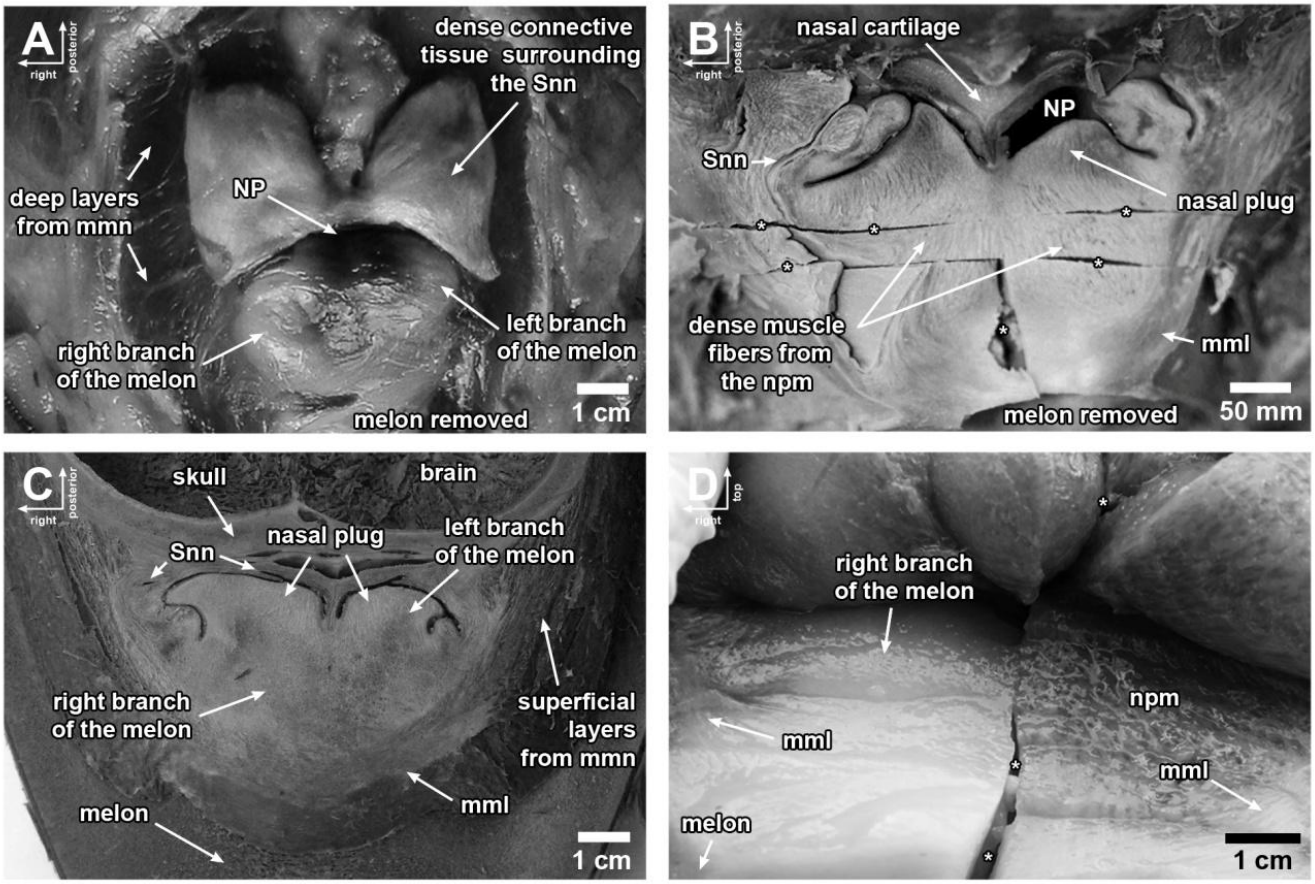

Fig. 8. Dorsal photographs of dissections (horizontal cuts) of epicranial complexes in (A) *Pontoporia blainvillei*, (B) *Phocoena phocoena*, (C) neonate *Tursiops truncatus*, and an (D) adult *Tursiops gephyreus* showing Interespecific variation in the main structures involved in sound modulation. *Musculus maxillolabialis*, **mml**; *Musculus maxillonasalis,* **mmn**; nasal passage, **NP**; nasal plug muscle, **npm,** *Saccus nasalis nasofrontalis,* **Snn**.

In this study, we demonstrated that ontogenetic-based transformations, as proposed in the Extended Evolutionary Synthesis (**EES**) (Laland *et al.*, 2015), were responsible for the morphological variation in the cetacean head, especially in odontocetes (**Fig. 9**, **Supplementary file - S1**). Body *bauplan* changes of Carnegie stages 16 through 19 combined with the development of the nasal cartilage may underlie the dorsoposterior movements of the external nasal passage to the vertex of the head (**Fig. 1**). Although Miller (1923) wrongly named a process (i.e. telescoping) (Churchill *et al.*, 2018) by comparing matured skulls of independently-evolved lineages, the transformation described by the author was, in part, perceived in the morphogenesis of the skull (Moran *et al.*, 2011, Fig. 1). Thus, the term will be used here to designate this ontogenetic-based transformation: the telescoping could be interpreted as a developmental process expressed in distinct transformational patterns among all cetaceans due to variable timing of the formation of nasal cartilages in early fetal life.

Morphological variation of the relative size of the nasal cartilage at early fetal stages might indicate accelerated ontogenetic timing in the formation of the *rostrum nasi* cartilage at early Carnegie stages in *P. blainvillei*, compared to *P. phocoena* and *L. albirostris* (**Fig. 3**). This seems to address the increased rostrum (i.e. premaxillary plus maxillary bones) size relative to the epicranial complex in adults (i.e. character 330, state=0) (**Fig. 6**, **Fig. 7, Fig. 9**). As perceived in the ancestral character reconstruction analsis (**Supplementary file - S1**), increased rostrum size relative to the ECL seems to represent a plesiomorphic

condition in odontocetes, after which two main convergent paedomorphic events have occurred (i.e. family Ziphiidae and Delphinoidea clade) with, at least, one reversion within each clade (i.e. *Ziphius cavirostris* and *Delphinus delphis*, respectively; **Supplementary file - S1**). Thus, the small size of the *rostrum nasi* in *P. phocoena* and *L. albirostris*, compared to *P. blainvillei*, might represent variable expression of regulatory mechanisms during early formation of the nasal cartilage in these groups (**Fig. 1, Fig. 3**) as observed in other parts of the body such as the hind-limb development (Thewissen *et al.*, 2006).

The presence of a pair of bursae cartilages (**bc**) found just posterior of each posterior dorsal bursa in dolphins (Cranford *et al.*, 1996) and neonate *P. phocoena* (Prahl *et al.*, 2009) were crucial to topographically determine the precursor tissues as posteriorly positioned relative to the nasal passage (**Fig. 1H**). Heyning (1989) also described a thin cartilage in the blowhole ligament (posterior to the nasal passage) of *D. leucas*. All specimens analysed in this study, including *M. monoceros* (Comtesse-Weidner, 2007), presented this cylindrical cartilage in parallel to the nasal passage associated with a loose connective tissue composed of mesenchymal cells at fetal stages (**Fig. 2**, **Fig. 3**, **Fig. 4A", B", C"**). Comtesse-Weidner (2007) proposed that the entire loose connective tissue from **TA1** may represent the precursor tissue of the bursae complex (i.e. posterior dorsal bursae). However, we suggest that the mentioned tissue together with the concentric collagen and muscle fibers, the *intrinsic muscle* (Heyning, 1989) (**Fig. 2**, **Fig. 3**, **Fig. 4**) may differentiate into the connective tissue surrounding the posterior nasofrontal air sacs (**Fig. 3C**). This is plausible because the precursor tissue of the posterior dorsal bursae seems to be restricted to the loose connective tissue between the bursae cartilage, posteriorly, and the nasal passage (**Fig. 2F**). Therefore, we assume that similar mesenchymal loose connective tissue (e.g. **TA1**) might originate fat (i.e. precursor tissue), soft or dense connective tissue.

Independently acquired features - i.e. homoplasies or repeated evolution - in isolated lineages may be due to convergent selection and/or developmental bias (Laland *et al.*, 2015). In this way, it would be plausible that the concentric and dense connective tissue surrounding the nasal diverticula in *Kogia*, the "vocal cap" (Thornton *et al.*, 2015) might represent a distinct ontogenetic derivation of the early loose connective tissue. This is composed of likewise concentrically arranged collagen and muscle fibers (i.e. posterior loose connective tissue in **TA1**) at early fetal stages in *Phocoena*, *Pontoporia*, *Lagenorhynchus* (**Fig. 2**, **Fig. 3**, **Fig. 4**) and *Monodon* (Comtesse-Weidner, 2007). Interestingly, the posterior nasofrontal air sacs in *Globicephala*, *Orcaella*, *Pontoporia* (Arnold & Heinsohn, 1996; Frainer *et al.*, 2015; Mead, 1975) and the "vocal cap" in *Kogia* (Thornton *et al.*, 2015) exhibit a similar trabecular structure associated with the dense connective tissue. However, further studies should address the topic in detail and investigate the early soft nasal tissues in *Physeter* and *Kogia*. Distinct trajectories of this connective tissue ontogeny might represent one among other adaptations for a narrow-band high frequency (**NBHF**) sound production (Kyhn *et al.*, 2010; Madsen *et al.*, 2005) (see below) as the connective tissue surrounding the posterior portion of the nasofrontal air sacs is highly developed in *P. blainvillei* and *P. phocoena* - i.e. the porpoise capsule (see Huggenberger *et al.*, 2009) - and presumably developed to a lesser degree in broadband species, such as *Globicephala* (Mead, 1975) and *Orcaella* (Arnold & Heinsohn, 1996).

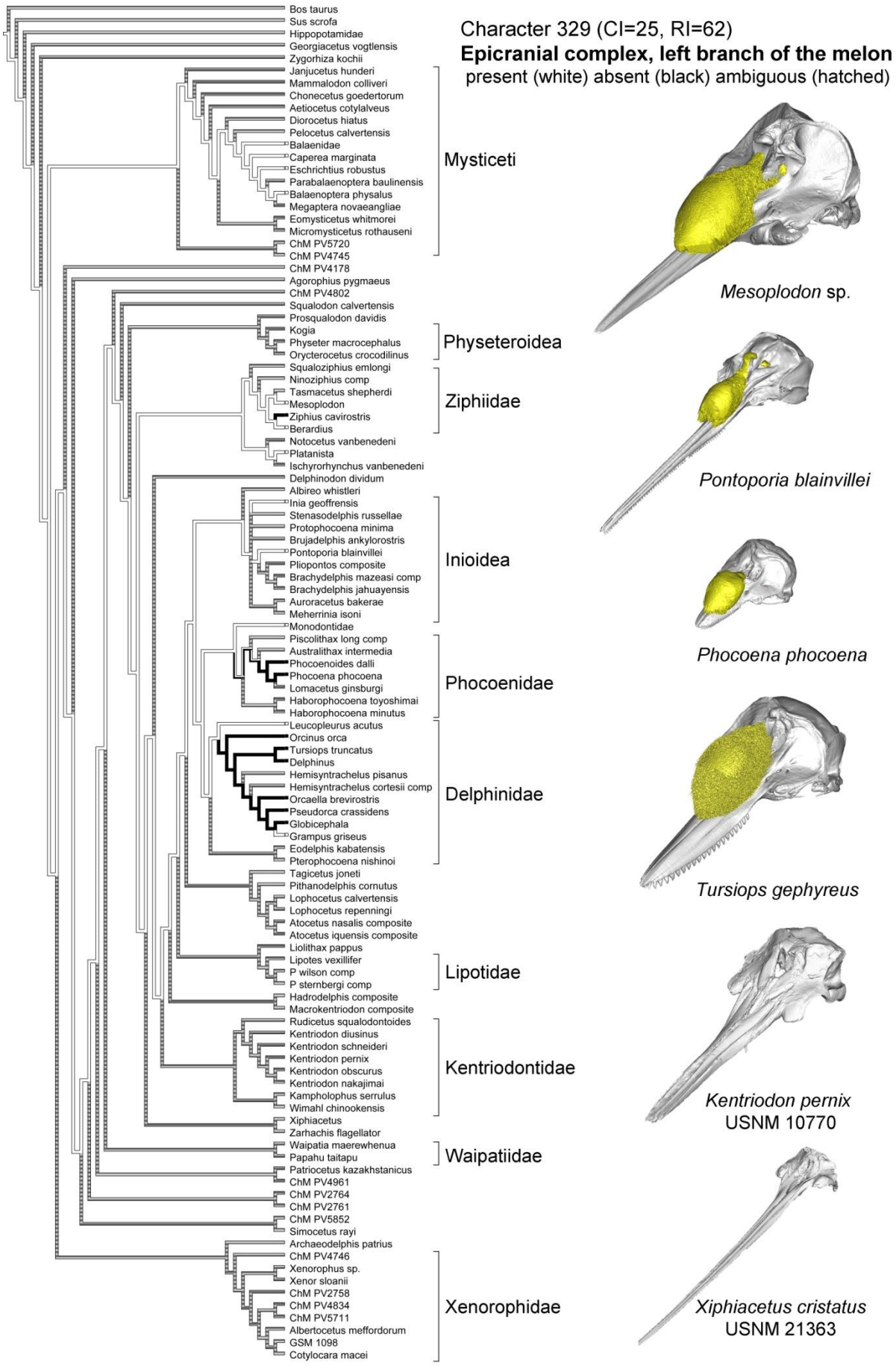
Character 329 (CI=25, RI=62)
Epicranial complex, left branch of the melon
present (white) absent (black) ambiguous (hatched)
Bos taurus
Sus scrofa
Hippopotamidae
Georgiacetus vogtlensis
Zygorhiza kochii
Janjucetus hunderi
Mammalodon colliveri
Chonecetus goedertorum
Aetiocetus cotylalveus
Diorocetus hiatus
Pelocetus calvertensis
Balaenidae
Caperea marginata
Eschrichtius robustus
Parabalaenoptera baulinensis
Balaenoptera physalus
Megaptera novaeangliae
Eomysticetus whitmorei
Micromysticetus rothauseni
ChM PV5720
ChM PV4745
Mysticeti
ChM PV4178
Agorophius pygmaeus
ChM PV4802
Squalodon calvertensis
Prosqualodon davidis
Kogia
Physeter macrocephalus
Orycterocetus crocodilinus
Physeteroidea
Squaloziphius emlongi
Ninoziphius comp
Tasmacetus shepherdi
Mesoplodon
Ziphius cavirostris
Berardius
Ziphiidae
Notocetus vanbenedeni
Platanista
Ischyrorhynchus vanbenedeni
Delphinodon dividum
Albireo whistleri
Inia geoffrensis
Stenasodelphis russellae
Protophocoena minima
Brujadelphis ankylorostris
Pontoporia blainvillei
Pliopontos composite
Brachydelphis mazeasi comp
Brachydelphis jahuayensis
Auroracetus bakerae
Meherrinia isoni
Inioidea
Monodontidae
Piscolithax long comp
Australithax intermedia
Phocoenoides dalli
Phocoena phocoena
Lomacetus ginsburgi
Haborophocoena toyoshimai
Haborophocoena minutus
Phocoenidae
Leucopleurus acutus
Orcinus orca
Tursiops truncatus
Delphinus
Hemisyntrachelus pisanus
Hemisyntrachelus cortesii comp
Orcaella brevirostris
Pseudorca crassidens
Globicephala
Grampus griseus
Eodelphis kabatensis
Pterophocoena nishinoi
Delphinidae
Tagicetus joneti
Pithanodelphis cornutus
Lophocetus calvertensis
Lophocetus repenningi
Atocetus nasalis composite
Atocetus iquensis composite
Liolithax pappus
Lipotes vexillifer
P wilson comp
P sternbergi comp
Lipotidae
Hadrodelphis composite
Macrokentriodon composite
Rudicetus squalodontoides
Kentriodon diusinus
Kentriodon schneideri
Kentriodon pernix
Kentriodon obscurus
Kentriodon nakajimai
Kampholophus serrulus
Wimahl chinookensis
Kentriodontidae
Xiphiacetus
Zarhachis flagellator
Waipatia maerewhenua
Papahu taitapu
Waipatiidae
Patriocetus kazakhstanicus
ChM PV4961
ChM PV2764
ChM PV2761
ChM PV5852
Simocetus rayi
Archaeodelphis patrius
ChM PV4746
Xenorophus sp.
Xenor sloanii
ChM PV2758
ChM PV4834
ChM PV5711
Albertocetus meffordorum
GSM 1098
Cotylocara macei
Xenorophidae
Mesoplodon sp.
Pontoporia blainvillei
Phocoena phocoena
Tursiops gephyreus
Kentriodon pernix
USNM 10770
Xiphiacetus cristatus
USNM 21363

Fig. 9. Ancestral character reconstruction using the parsimony method to infer the evolution of the posterior portion of the melon in odontocetes. Character 329 - Epicranial complex, left branch of the melon: present (white), absent (black), ambiguous (hatched). All 3D models contaning the main fat pathways (yellow) in the epicranial complex were provided in this study (see Material and Methods), while the remaining models were taken from Phenome10k library (http://phenome10k.org/). Classification followed Lambert et al. (2017).

The soft nasal tissues positioned just anterior to the nasal passage (i.e. **TA3**) at early fetal stages (**Fig. 1**) presented similar differentiation as **TA1**: the loose-like connective tissue composed of cells with large intercellular spaces surrounding the *septum nasi* cartilage is the origin of the fat and dense connective tissue in adults (Heyning, 1989) (**Fig. 8**). In most odontocetes, the right branch of the melon is mostly filled by fat and connects the right **MLDB** complex to the main body of the melon (Cranford *et al.*, 1996; Harper *et al.*, 2008; McKenna *et al.*, 2012).The shape and existence of melon's left branch is notably variable among species (**Fig. 9**). The left branch is developed and observed to be connecting its dorsocaudal portion to the left anterior dorsal bursa in *P. blainvillei*, *Stenella longirostris*, *Sousa plumbea*, *Grampus griseus* and *Lagenorhynchus obliquidens* (Cranford, 1988; Cranford *et al.*, 1996; Frainer *et al.*, 2015; Frainer *et al.*, 2018; McKenna *et al.*, 2012). In some species, the left branch of the **melon** is almost occluded by a dense connective tissue and muscle fibers from the nasal plug muscles such as in *Tursiops* (Cranford *et al.*, 1996; Harper *et al.*, 2008) and *Phocoena phocoena* (Huggenberger *et al.*, 2009; Prahl *et al.*, 2009) (**Fig. 8**). Interestingly, a pair of fat bodies embedded within the nasal plug muscles is described in some baleen whales (Buono *et al.*, 2015; Heyning & Mead, 1990) to presumably "... *allow the free movement of the nasal plugs as they are retracted by the nasal plug muscles during respiration*..." (Heyning & Mead, 1990). Heyning and Mead (1990) pointed out that the pair of fat bodies embedded within the nasal plug muscles are presumably homologous to the **melon** of odontocetes. If so, this structure should have originated in a common ancestor of both extant lineages (see below).

Cephalic adipose tissues in the human face are known to be derived from neural crest cells (Billon & Dani, 2012), which presumably give rise to chondrocytes and possibly other mesenchymal cells (Billon *et al.*, 2007). Accordingly, the adipose tissue depots in the human head constitute distinct small organs exhibiting functional differences and variable contribution to metabolic dysfunctions, such as obesity (Billon & Dani, 2012). Although the cellular and molecular mechanisms responsible for the formation of the fat tissues in the mammalian face are still unclear, we demonstrated that the evolution of odontocetes was remarkable for the great variation in the site-specific ontogenetic regulation of the cephalic adipose tissues (Billon & Dani, 2012). The morphological variation in the composition of the "posterior melon" (Harper *et al.*, 2008) (**Fig. 9**) may address specific adaptations to sound production among non-physeteroid odontocetes (Frainer *et al.*, 2018). Most non-physeteroids odontocetes exhibit the right branch of the **melon** connected to its main body (character 327, state=0) (**Fig. 5**, **Fig. 8D, Fig. 9**), except for *Globicephala*, *Cephalorhynchus* (Mead, 1975) and *Lagenorhynchus obliquidens* (Cranford *et al.*, 1996). In these species, the two structures are separated by dense connective tissue (character 327, state=1) which seems to represent hypertrophied *Musculus maxillolabialis* (**mml**) tendons and associated dense connective tissue derived from **TA2** in fetal development (Comtesse-Weidner, 2007) (**Fig. 1**, **Fig. 4**). In this study, we demonstrated that the branches of the melon, or the posterior melon (sensu Harper *et al.*, 2008), and the **melon** actually represent distinct structures derived from independent primordial tissues, under presumably distinct regulation factors according to the morphological variation found in odontocetes (**Fig. 9**). In this respect, we propose two new designations for

both right and left branch of the melon to address homology comparisons: *Corpus adiposum nasalis terminalis, partes posteriores dexter* (**Cand**) and *Corpus adiposum nasalis terminalis, partes posteriores sinister* (**Cans**), respectively.

Ontogenetically, the **melon** originates later than the nasal plug muscles and associated connective tissues since muscle fibers from the *Musculus maxillonasolabialis rostralis* (**mr**) start developing into **TA4** in late fetal stages (Carnegie stages F18-19) concomitant with increased differentiation of the blubber precursor tissues (**Fig. 1**). Increased fat production between **mr** layers rostral to the *Musculus maxillolabialis* (**mml**) started late in fetal stages and continued through the perinatal (**Fig. 5**) and postnatal development to form the melon (**Fig. 6**, **Fig. 7, Fig. 9**). The distinction between different main fat bodies positioned anterior to the nasal passage in odontocetes implemented in distinct cladistic interpretations for the origin of the **melon** in Cetacea (Heyning, 1989) was exclusive (autapomorphic) for odontocetes (**Supplementary file - S1**) and may be correlated to the acquisition of ultra-sound hearing in cetaceans (Churchill *et al.*, 2016; Galatius *et al.*, 2018). The existence and shape differences of the branches of the **melon** (i.e. **Cand** and **Cans**) presented great morphological variation into Delphinoidea: the **Cand** was commonly present in most non-physeteroid odontocetes except in phocoenids (**Fig. 8B**) (Huggenberger *et al.*, 2009; Prahl *et al.*, 2009) while the **Cans** exhibited variation within Delphinoidea (**Fig. 8**) and within the family Ziphiidae (**Fig. 9**). In some lineages (cited above), the left nasal plug muscle exhibits a smaller degree of development to dense muscle and collagen fibers, thus allowing the promordial loose connective tissue from **TA3** to give rise to **Cans** just below the anterior dorsal bursae (character 309, state=0). However, in phocoenids, most delphinids (**Fig. 8**) and *Ziphius cavirostris* (Heyning, 1989) the left-hand side nasal plug muscle was hypertrophied and completely replaced the pathway between the bursae complex (i.e. precursor tissue and anterior dorsal bursae) and the **melon** (character 329, state=1) (**Fig. 9**). The postnatal development of the left nasal plug muscle and the replacement of the **Cans** in *Tursiops* may polarize this ontogenetic-based transformation as it seems to represent paedomorphic events in delphinids that exhibit such a structure.

The development of the nasal air sacs exhibited distinct timing of formation, as they develop independently in a sequence of steps: first premaxillary air sacs and nasofrontal air sacs, and then the vestibular air sacs. Interestingly, the presence of premaxillary air sacs may represent a conserved condition in non-physeteroid odontocetes (Heyning, 1989; Mead, 1975; Schenkkan, 1973). The vestibular air sacs seem to represent the most variable nasal air sac in dolphin-sized species.In *Lipotes vexillifer* (Chen *et al.*, 1980), *I. geoffrensis* (Schenkkan, 1973), *P. blainvillei* (Frainer *et al.*, 2015), and *P. phocoena* (Huggenberger *et al.*, 2009) this structure exhibits larger dimensions than the premaxillary air sacs (character 328, state=0).In delphinids, on the other hand, the reverse size relation (premaxillary air sacs > vestibular air sacs) in the nasal diverticula (character 328, state=1) might represent distinct adaptations for sound production (see below). The ancestral character reconstruction analysis represented a cladistic method to presume the soft nasal morphology of extinct odontocetes and to map major changes linked with the evolution of the sound production and modulation structures in these complex echolocating and social mammals (**Supplementary file - S1**).

Echolocation and communication signals have evolved under the concomitant constraints of body size (Au, 1993), social (May-Collado *et al.*, 2007), and biosonar properties (Jensen *et al.*, 2018). The directional properties of a sound emission apparatus tend to increase the source level (dB) in the forward

direction where click energy exhibits elevated center frequency (kHz) and increasing target detection range (Finneran *et al.*, 2014; Jensen *et al.*, 2009; Koblitz *et al.*, 2012). In the dolphin head, the sound beam interacts with the skull, dense connective tissue theca (character 326, state=0) and the vestibular air sacs (Wei et al. 2017); and is collimated through the **Cand** (i.e. for navigation and hunting) or **Cans** (i.e. for communication) - or simultaneously (Ridgway *et al.*, 2015) - to the **melon** (Wei *et al.*, 2017). Since fat pathways are important for absorbing and collimating shorter wave lengths (i.e., high frequency) (Amundin & Andersen, 1983), the morphological variability in the composition of the nasal plug muscle might represent adaptations for high-frequency communication in some dolphin-sized odontocetes such as *S. longirostris*, *G. griseus, L. albirostris*, *P. blainvillei*, and *S. plumbea* (Frainer *et al.*, 2018). The **melon** collimates the sound and effectively transmits it into the aquatic environment by impedance matching (Harper *et al.*, 2008; McKenna *et al.*, 2012).

The general morphology of the sound generating structures in extant **NBHF** species revealed a distinct topographical arrangement (**Table 2**). However, presumably homoplasic conditions promoted by distinct ontogenetic trajectories may represent adapted biosonar apparatus for the production of highly directional sounds: *Kogia* species exhibit short rostra and a dense chamber of connective tissue in the right nasal passage involved in the sound production (Thornton *et al.*, 2015). As cited above, the dense connective tissue surrounding the nasofrontal air sacs in *P. blainvillei* and *P. phocoena* might address adaptation for high frequency sound production (Huggenberger *et al.*, 2009). Interestingly, the horizontal alignment of the bursae complex with the posterior portion of the **melon** (**Fig. 7**) (character 325, state=0) was perceived in *P. phocoena*, *P. blainvillei*, and *C. commersonii* and might represent a plesiomorphic character in Delphinida since it was observed in *Mesoplodon* and *P. gangetica* (not shown in figures). Galatius and Goodall (2016) reported comparatively less concave profile in the skulls of *Lagenorhynchus australis* and *Cephalorhynchus* dolphins, which might signify **NBHF** properties. On the other hand, the authors demonstrated that *L. cruciger*, which also produces **NBHF** clicks, presented a more concave skull profile compared to the other species. This might be an adaptation for modulating the sound beam, or may be related to the production of derived communication sounds, as *L. cruciger* shows increased social complexity compared to its closest relatives (Galatius *et al.*, 2018).

The morphology of the nasal tract in odontocetes evolved under several heterochronic processes linked to the development of main structures involved in the sound beam modulation (**Fig. 9**, **Supplementary file - S1**). Paedomorphic events related to decreasing rostrum size in adults may have occurred at least three times in odontocete evolution (i.e. Kogiidae, Ziphiidae and Delphinoidea clade), together with presumable changes in the directionality of the sound emitted. The increased rostrum length might represent an important component influencing sound modulation in some groups such as in *P. blainvillei* and *L. vexillifer* (Frainer *et al.*, 2018; Wei *et al.*, 2017). We did not consider rostrum size reduction in *P. macrocephalus* because in this species, the soft nasal tissue is hypertrophied due to specializations for highly directional, high-energy sounds (Møhl *et al.*, 2000). Most members of Delphinidae and Monodontidae are broad-band echolocators (Galatius *et al.*, 2018; Jensen *et al.*, 2018) with derived low-frequency modulated sounds for communication (i.e. whistles) besides pulsed calls (i.e. clicks for communication or burst clicks) (May-Collado *et al.*, 2007).

Morphological adaptations of Delphinoidea found in this study seem to have contributed to changes in the directional properties of the sound emission apparatus in comparison to other odontocetes. These morphological characters are: 1) the inverse size relation of the nasal diverticula (character 328, state=1)

(**Supplementary file - S1**); 2) the off-axis alignment of the dorsal bursae with the posterior portion of the **melon** (character 325, state=1, also observed in *Z. cavirostris*) (**Supplementary file - S1**) (Frainer *et al.*, 2018); 3) the development of muscle and dense collagen fibers in the nasal plug muscle with the loss of fat pathways (e.g. **Cans**) for a distinct timbre of lower frequencies in most delphinids (Frainer *et al.*, 2018); and 4) the decreased rostrum size (Wei *et al.*, 2014). Although in *P. phocoena* both nasal plug muscles are composed of muscle and collagen fibers, the arrangements of other structures are likely adaptations for the highly directional sonar, such as large vestibular air sacs, dense connective tissue surrounding the epicranial complex, and the alignment of the sound source with the posterior portion of the **melon** (**Fig. 9**, **Supplementary file - S1**). Topographical changes in the main fat pathways in *P. blainvillei* and *P. phocoena* (**Fig. 7**) are promoted by dorsal movements of the posterior portion of the premaxillary bone during the postnatal development, thus elevating the premaxillary air sacs and, consequently, the nasal plug muscle and anterior dorsal bursae tissues dorsally. In this way, the ancestral character reconstruction analysis provided cues to determine not only the soft nasal tissues of extinct organisms but also their presumable function.

Table 2. Comparative anatomy of the main structures involved in the sound modulation in the dolphin head. *See Ladegaard *et al.* (2015).

Genus	Rostrum size	Relative volume of the nasal diverticula	Branches of the melon	Connective tissue theca	Fat pads topography	Directional properties of the sound source
Pontoporia blainvillei	Long and narrow	Vestibular air sacs > premaxillary air sacs	Both present	Covering both lateral walls of the epicranial complex	The bursae complex is aligned horizontally to the melon	Narrow-band high frequency sounds
Inia geoffrensis	Long and narrow	Vestibular air sacs > premaxillary air sacs	Both present	Covering both lateral walls of the epicranial complex	The bursae complex is aligned horizontally to the melon	Broad-band low and high frequency sounds with highly directional properties*
Phocoena phocoena	short	Vestibular air sacs > premaxillary air sacs	Both absent	Covering both lateral walls of the epicranial complex	The bursae complex is aligned horizontally to the melon	Narrow-band high frequency sounds
Tursiops spec.	short	Vestibular air sacs < premaxillary air sacs	Right present and left absent	Covering only the dorsal portion of the epicranial complex	The bursa complex is dorsoposteriorly positioned relative to the melon	Broad-band sounds in lower frequency
Cephalorhynchus spec.	short	Vestibular air sacs > premaxillary air sacs	Right present and left absent	Covering both lateral walls of the epicranial complex	The bursae complex is aligned horizontally to the melon	Narrow-band high frequency sounds

Kentriodontids (Family Kentriodontidae) were small (approximately 2 m long) dolphin-like odontocetes living in neritic and shelf zones of the Pacific and Atlantic oceans, with a pan-tropical to temperate distribution

(Barnes, 1978; Ichishima *et al.*, 1994). The decline of kentriodontods is associated with changes in oceanic temperatures and the rising of recent lineages, such as delphinids, in the late Miocene (Ichishima *et al.*, 1994). Among this large group of echolocating fish-predators were the common ancestors of all known dolphins (Lambert *et al.*, 2017; Peredo *et al.*, 2018), thus functional interpretations based on kentriodontid morphology may elucidate the plesiomorphic condition of the sound emission apparatus. Galatius et al. (2018) found that *Kentriodon pernix* (**Fig. 9**) exhibited inner ear morphology similar to extant **NBHF** species, and, thus, it is plausible to assume such capabilities for *K. pernix*. The sound emission apparatus of *K. pernix* developed under a symmetric skull condition (Barnes, 1978) as in *P. blainvillei* and *P. phocoena* (**Fig. 9**), and with less concavity than in *C. commersonii*. By interpreting the ancestral character reconstruction analysis, the presumable soft nasal tissue morphology of *K. pernix* was surrounded by a dense connective tissue, and composed of larger vestibular air sacs compared to the premaxillary air sacs (character 328, state=0)**;** both **Cand** and **Cans** (character 329, state=0)**;** bursae complex, aligned (character 325, state=0) with the posterior portion of the **melon**; and a long rostrum compared to the size of the **melon** (character 330, state=0). Thus, the phylogenetic mapping of distinct structures involved in sound production (**Supplementary file - S1**) results in the interpretation that kentriodontids might have exhibited unique soft nasal tissue morphology adapted for highly directional sounds as previously proposed (Galatius *et al.*, 2018) and corroborate our hypothesis that extant broad-band vocalizing delphinids have evolved under more relaxed constraints regarding directionality of the sonar beam. The dependence on a narrow band of high frequencies which attenuate at rather short distances from the source would lead to a higher directionality to mitigate the reduced effective range of the biosonar.

In this study, a cladistic mapping of the evolution of the main structures involved in the sound generating structures in dolphins was performed and interpreted in the light of the Extended Evolutionary Synthesis (**EES**). The **EES** assumes that developmental mechanisms, operating through developmental bias (e.g. telescoping process in cetaceans) and inclusive inheritance (e.g. cultural transmission for echolocation and communication in toothed whales), along with natural selection (Darwin, 1859) share responsibility for the direction and rate of evolution, thus, contributing to organism-environment complementarity (Laland *et al.*, 2015). Additionally, Laland *et al.* (2015) pointed out that social (behavioral, e.g. echolocation) and cultural transmission may play a role by biasing phenotypic variants subject to selection, thus contributing to heritability. The evolution of odontocetes and their biosonar systems not only contributes to exemplifies evolutionary theory as didactic organisms (Thewissen *et al.*, 2006), but also promotes the future of systematics and comparative anatomy by adding the analysis of ontogenetic-based characters to determine the evolution of morphological traits. In this way, the research field of systematics and comparative anatomy should follow recent advances in the evolutionary theory. Following the ancestral character reconstruction analysis for the main structures involved in sound modulation, it is plausible to propose that extant coastal **NBHF** species represent highly specialized - and threatened (Frainer *et al.*, 2018; Reeves *et al.*, 2013) - sound generation and emission systems which evolved at least four times independently of each other.

ACKNOWLEDGMENTS

G.F. was supported by a PhD scholarship from CAPES (from 2015 to 2019) and CNPq (*Ciências Sem Fronteiras* - 201709/2015-5). We are thankful to the team of the Max-Planck for Metabolism Research by the assistance with the MRI scans, and to Tiago P. de Carvalho, Luiz R. Malabarba, Roberto E. dos Reis, Aldo M.

de Araújo and Cesar L. Schultz that helped to improve this study by their comments and suggestions. A special thanks to all integrants of the *Laboratório de Sistemática e Ecologia de Aves e Mamíferos Marinhos* (LABSMAR/UFRGS) and the Department II of Anatomy (University of Cologne). This is a contribution of the Research Group “Evolução e Biodiversidade de Cetáceos/CNPq”.

LITERATURE CITED

Alberch, P., Gould, S. J., Oster, G. F. & Wake, D. B. (1979) Size and shape in ontogeny and phylogeny. *Paleobiology,* **5**, 296-317. doi:10.1017/S0094837300006588.

Amundin, M. & Andersen, S. H. (1983) Bony nares air pressure and nasal plug muscle activity during click production in the harbour porpoise, *Phocoena phocoena*, and the bottlenosed dolphin, *Tursiops truncatus*. *Journal of Experimental Biology,* **105**, 275.

Armfield, B. A., Zheng, Z., Bajpai, S., Vinyard, C. J. & Thewissen, J. G. M. (2013) Development and evolution of the unique cetacean dentition. *PeerJ,* **1**, e24. doi:10.7717/peerj.24.

Arnold, P. W. & Heinsohn, G. E. (1996) Phylogenetic status of the Irrawaddy dolphin *Orcaella brevirostris* (Owen in Gray): a cladistic analysis. *Memoirs of the Queensland Museum,* **39**, 141-204.

Aroyan, J. L., Cranford, T. W., Kent, J. & Norris, K. S. (1992) Computer modeling of acoustic beam formation in *Delphinus delphis*. *The Journal of the Acoustical Society of America,* **92**, 2539-2545. doi:10.1121/1.404424.

Au, W. L. (2000) Hearing in whales and dolphins: An overview. In W. L. Au & R. F. Richard (eds) *Hearing by whales and dolphins*, 1-42. Springer, New York.

Au, W. W. L. (1993) *The sonar of dolphins*. Springer, new york.

Au, W. W. L., Houser, D. S., Finneran, J. J., Lee, W. J., Talmadge, L. A. & Moore, P. W. (2010) The acoustic field on the forehead of echolocating Atlantic bottlenose dolphins (*Tursiops truncatus*). *The Journal of the Acoustical Society of America,* **128**, 1426-1434. doi:10.1121/1.3372643.

Barnes, L. G. (1978) A review of *Lophocetus* and *Liolithax* and their relationships to the delphinoid family Kentriodontidae (Cetacea: Odontoceti). *Natural History Museum of Los Angeles County Science Bulletin,* **28**, 1-35.

Berta, A., Ekdale, E. G. & Cranford, T. W. (2014) Review of the cetacean nose: Form, function, and evolution. *The Anatomical Record,* **297**, 2205-2215. doi:10.1002/ar.23034.

Billon, N. & Dani, C. (2012) Developmental origins of the adipocyte lineage: New insights from genetics and genomics studies. *Stem Cell Reviews and Reports,* **8**, 55-66. doi:10.1007/s12015-011-9242-x.

Billon, N., Iannarelli, P., Monteiro, M. C., Glavieux-Pardanaud, C., Richardson, W. D., Kessaris, N., Dani, C. & Dupin, E. (2007) The generation of adipocytes by the neural crest. *Development,* **134**, 2283. doi:10.1242/dev.002642.

Buono, M. R., Fernández, M. S., Fordyce, E. R. & Reidenberg, J. S. (2015) Anatomy of nasal complex in the southern right whale, *Eubalaena australis* (Cetacea, Mysticeti). *Journal of Anatomy,* **226**, 81-92. doi:10.1111/joa.12250.

Chen , P., Lin, K. & Liu, R. (1980) Study of the anatomy and histology of the upper respiratory tract of Lipotes vexillifer Miller. *Acta Hydrobiologica Sinica,* **2**, 131-137 [In Chinese, English abstract].

Churchill, M., Geisler, J. H., Beatty, B. L. & Goswami, A. (2018) Evolution of cranial telescoping in echolocating whales (Cetacea: Odontoceti). *Evolution,* **72**, 1092-1108. doi:10.1111/evo.13480.

Churchill, M., Martinez-Caceres, M., de Muizon, C., Mnieckowski, J. & Geisler, J. H. (2016) The Origin of High-Frequency Hearing in Whales. *Current Biology,* **26**, 2144-2149. doi:https://doi.org/10.1016/j.cub.2016.06.004.

Comtesse-Weidner, P. (2007) Untersuchungen am Kopf des fetalen Narwals *Monodon monoceros*: Ein Atlas zur Entwicklung und funktionellen Morphologie des Sonarapparates. Universitätsbibliothek, Gießen.

Cranford, T. W. (1988) The anatomy of acoustic structures in the spinner dolphin forehead as shown by x-ray computed tomography and computer graphics. In P. E. Nachtigall & P. W. B. Moore (eds) *Animal Sonar: Processes and Performance*, 67-77. Springer US, Boston, MA.

Cranford, T. W., Amundin, M. & Norris, K. S. (1996) Functional morphology and homology in the odontocete nasal complex: implications for sound generation. *Journal of Morphology,* **228**, 223-285. doi:10.1002/(sici)1097-4687(199606)228:3<223::aid-jmor1>3.0.co;2-3.

Cranford, T. W., McKenna, M. F., Soldevilla, M. S., Wiggins, S. M., Goldbogen, J. A., Shadwick, R. E., Krysl, P., St. Leger, J. A. & Hildebrand, J. A. (2008) Anatomic Geometry of Sound Transmission and Reception in Cuvier's Beaked Whale (*Ziphius cavirostris*). *The Anatomical Record,* **291**, 353-378. doi:10.1002/ar.20652.

Darwin, C. (1859) *On the origin of the species*. Routledge, London.

de Pinna, M. C. C. (1991) Concepts and tests of homology in the cladistic paradigm. *Cladistics,* **7**, 367-394. doi:10.1111/j.1096-0031.1991.tb00045.x.

De Queiroz, K. (1985) The ontogenetic method for determining character polarity and its relevance to phylogenetic systematics. *Systematic Zoology,* **34**, 280-299. doi:10.2307/2413148.

Fink, W. L. (1982) The conceptual relationship between ontogeny and phylogeny. *Paleobiology,* **8**, 254-264. doi:10.1017/S0094837300006977.

Finneran, J. J., Branstetter, B. K., Houser, D. S., Moore, P. W., Mulsow, J., Martin, C. & Perisho, S. (2014) High-resolution measurement of a bottlenose dolphin's (*Tursiops truncatus*) biosonar transmission beam pattern in the horizontal plane. *The Journal of the Acoustical Society of America,* **136**, 2025-2038. doi:10.1121/1.4895682.

Fish, F. E. (2002) Balancing Requirements for Stability and Maneuverability in Cetaceans. *Integrative and Comparative Biology,* **42**, 85-93. doi:10.1093/icb/42.1.85.

Fox, K. C. R., Muthukrishna, M. & Shultz, S. (2017) The social and cultural roots of whale and dolphin brains. *Nature Ecology & Evolution,* **1**, 1699-1705. doi:10.1038/s41559-017-0336-y.

Frainer, G., Huggenberger, S. & Moreno, I. B. (2015) Postnatal development of franciscana's (*Pontoporia blainvillei*) biosonar relevant structures with potential implications for function, life history, and bycatch. *Marine Mammal Science,* **31**, 1193-1212. doi:10.1111/mms.12211.

Frainer, G., Plön, S., Serpa, N. B., Moreno, I. B. & Huggenberger, S. (2018) Sound generating structures of the humpback dolphin *Sousa plumbea* (cuvier, 1829) and the directionality in dolphin sounds. *The Anatomical Record,* **0**. doi:10.1002/ar.23981.

Galatius, A. & Goodall, N. P. (2016) Skull shapes of the Lissodelphininae: radiation, adaptation and asymmetry. *Journal of Morphology,* **277**, 776-785. doi:10.1002/jmor.20535.

Galatius, A., Olsen, M. T., Steeman, M. E., Racicot, R. A., Bradshaw, C. D., Kyhn, L. A. & Miller, L. A. (2018) Raising your voice: evolution of narrow-band high-frequency signals in toothed whales (Odontoceti). *Biological Journal of the Linnean Society,* **126**, 213-224. doi:10.1093/biolinnean/bly194.

Geisler, J. H., Colbert, M. W. & Carew, J. L. (2014) A new fossil species supports an early origin for toothed whale echolocation. *Nature,* **508**, 383-386. doi:10.1038/nature13086

https://www.nature.com/articles/nature13086#supplementary-information.

Goloboff, P. A., Farris, J. S. & Nixon, K. C. (2008) TNT, a free program for phylogenetic analysis. *Cladistics,* **24**, 774-786. doi:10.1111/j.1096-0031.2008.00217.x.

Gould, S. J. (1977) *Ontogeny and phylogeny*. Harvard University Press.

Harper, C. J., McLellan, W. A., Rommel, S. A., Gay, D. M., Dillaman, R. M. & Pabst, D. A. (2008) Morphology of the melon and its tendinous connections to the facial muscles in bottlenose dolphins (*Tursiops truncatus*). *Journal of Morphology,* **269**, 820-839. doi:10.1002/jmor.10628.

Heyning, J. E. (1989) Comparative facial anatomy of beaked whales (Ziphiidae) and a systematic revision among the families of extant Odontoceti. *Contributions in Science,* **405**.

Heyning, J. E. & Mead, J. G. (1990) Evolution of the nasal anatomy of cetaceans. In J. A. Thomas & R. A. Kastelein (eds) *Sensory Abilities of Cetaceans: Laboratory and Field Evidence*, 67-79. Springer US, Boston, MA.

Huggenberger, S. (2008) The size and complexity of dolphin brains - a paradox? *Journal of the Marine Biological Association of United Kingdom,* **88**, 1103-1108. doi:10.1017/s0025315408000738.

Huggenberger, S., André, M. & Oelschläger, H. H. A. (2014) The nose of the sperm whale: overviews of functional design, structural homologies and evolution. *Journal of the Marine Biological Association of the United Kingdom,* **96**, 783-806. doi:10.1017/S0025315414001118.

Huggenberger, S., Rauschmann, M. A., Vogl, T. J. & Oelschläger, H. H. A. (2009) Functional Morphology of the Nasal Complex in the Harbor Porpoise (*Phocoena phocoena* L.). *The Anatomical Record,* **292**, 902-920. doi:10.1002/ar.20854.

Huxley, J. (1942) *Evolution - The modern synthesis*. George Allen and Unwin, London.

Ichishima, H., Barnes, L. G., Fordyce, R. E., Kimura, M. & Bohaska, D. J. (1994) A review of kentriodontine dolphins (Cetacea; Deiphinoidea; Kentriodontidae): Systematics and biogeography. *Island Arc,* **3**, 486-492. doi:10.1111/j.1440-1738.1994.tb00127.x.

Jensen, F. H., Bejder, L., Wahlberg, M. & Madsen, P. T. (2009) Biosonar adjustments to target range of echolocating bottlenose dolphins (*Tursiops* sp.) in the wild. *Journal of Experimental Biology,* **212**, 1078. doi:10.1242/jeb.025619.

Jensen, F. H., Johnson, M., Ladegaard, M., Wisniewska, D. M. & Madsen, P. T. (2018) Narrow acoustic field of view drives frequency scaling in toothed whale biosonar. *Current Biology,* **28**, 3878-3885.e3873. doi:10.1016/j.cub.2018.10.037.

Kimura, T. & Hasegawa, Y. (2019) A new species of Kentriodon (Cetacea, Odontoceti, Kentriodontidae) from the Miocene of Japan. *Journal of Vertebrate Paleontology*, e1566739. doi:10.1080/02724634.2019.1566739.

Kleinenberg, S. C. & Yablokov, A. V. (1958) The morphology of the upper respiratory tract of whales. *Zoologichesk¨ zhurnal,* **37**, 1091-1099.

Klima, M. (1995) Cetacean phylogeny and systematics based on the morphogenesis of the nasal skull. *Aquatic Mammals,* **21**, 79-89.

Klima, M. (1999) *Development of the cetacean nasal skull*. Springer Berlin Heidelberg, Berlin, Heidelberg.

Klingenberg, C. P. (1998) Heterochrony and allometry: the analysis of evolutionary change in ontogeny. *Biological Reviews,* **73**, 79-123. doi:10.1111/j.1469-185X.1997.tb00026.x.

Kluge, A. G. (1985) Ontogeny and phylogenetic systematics. *Cladistics,* **1**, 13-27. doi:10.1111/j.1096-0031.1985.tb00408.x.

Koblitz, J. C., Wahlberg, M., Stilz, P., Madsen, P. T., Beedholm, K. & Schnitzler, H. U. (2012) Asymmetry and dynamics of a narrow sonar beam in an echolocating harbor porpoise. *The Journal of the Acoustical Society of America,* **131**, 2315-2324. doi:10.1121/1.3683254.

Kükenthal, W. G. (1889) *Vergleichend-anatomische und entwickelungsgeschichtliche Untersuchungen an Walthieren*. G. Fischer.

Kyhn, L. A., Jensen, F. H., Beedholm, K., Tougaard, J., Hansen, M. & Madsen, P. T. (2010) Echolocation in sympatric Peale's dolphins (*Lagenorhynchus australis*) and Commerson's dolphins (*Cephalorhynchus commersonii*) producing narrow-band high-frequency clicks. *The Journal of Experimental Biology,* **213**, 1940. doi:10.1242/jeb.042440.

Ladegaard, M., Jensen, F. H., de Freitas, M., Ferreira da Silva, V. M. & Madsen, P. T. (2015) Amazon river dolphins (*Inia geoffrensis*) use a high-frequency short-range biosonar. *The Journal of Experimental Biology,* **218**, 3091. doi:10.1242/jeb.120501.

Laland, K. N., Uller, T., Feldman, M. W., Sterelny, K., Müller, G. B., Moczek, A., Jablonka, E. & Odling-Smee, J. (2015) The extended evolutionary synthesis: its structure, assumptions and predictions. *Proceedings of the Royal Society B: Biological Sciences,* **282**, 20151019. doi:10.1098/rspb.2015.1019.

Lambert, O., Bianucci, G., Urbina, M. & Geisler, J. H. (2017) A new inioid (Cetacea, Odontoceti, Delphinida) from the Miocene of Peru and the origin of modern dolphin and porpoise families. *Zoological Journal of the Linnean Society,* **179**, 919-946. doi:10.1111/zoj.12479.

Lindberg, D. R. & Pyenson, N. D. (2007) Things that go bump in the night: evolutionary interactions between cephalopods and cetaceans in the tertiary. *Lethaia,* **40**, 335-343. doi:10.1111/j.1502-3931.2007.00032.x.

Maddison, W. P. & Maddison, D. R. (2018) Mesquite: a modular system for evolutionary analysis. **Version 3.51**, http://www.mesquiteproject.org.

Madsen, P. T., Carder, D. A., Bedholm, K. & Ridgway, S. H. (2005) Porpoise clicks from a sperm whale nose—convergent evolution of 130 khz pulses in toothed whale sonars? *Bioacoustics,* **15**, 195-206. doi:10.1080/09524622.2005.9753547.

Madsen, P. T., Lammers, M. O., Wisniewska, D. & Beedholm, K. (2013) Nasal sound production in echolocating delphinids (*Tursiops truncatus* and *Pseudorca crassidens*) is dynamic, but unilateral: clicking on the right side and whistling on the left side. *The Journal of Experimental Biology,* **216**, 4091-4102. doi:10.1242/jeb.091306.

Marino, L., McShea, D. & Uhen, M. D. (2004) The origin and evolution of large brains in toothed whales. *Anatomical Record-Advances in Integrative Anatomy and Evolutionary Biology,* **281A**, 1247–1255. doi:10.1002/ar.a.20128.

May-Collado, L. J., Agnarsson, I. & Wartzok, D. (2007) Phylogenetic review of tonal sound production in whales in relation to sociality. *BMC Evolutionary Biology,* **7**, 136. doi:10.1186/1471-2148-7-136.

McKenna, M. F., Cranford, T. W., Berta, A. & Pyenson, N. D. (2012) Morphology of the odontocete melon and its implications for acoustic function. *Marine Mammal Science,* **28**, 690-713. doi:10.1111/j.1748-7692.2011.00526.x.

Mead, J. G. (1975) Anatomy of the external nasal passages and facial complex in the Delphinidae (Mammalia: Cetacea). *Smithsonian Contributions to Zoology,* **207**, 1-35.

Mead, J. G. & Fordyce, R. E. (2009) The therian skull: a lexicon with emphasis on the odontocetes. *Smithsonian Contributions to Zoology*, 1-249. doi:https://doi.org/10.5479/si.00810282.627.

Miller, G. S. (1923) The telescoping of the cetacean skull. *Smithsonian Miscellaneous Collection,* **75**, 1-55.

Møhl, B., Wahlberg, M., Madsen, P. T., Miller, L. A. & Surlykke, A. (2000) Sperm whale clicks: Directionality and source level revisited. *The Journal of the Acoustical Society of America,* **107**, 638-648. doi:10.1121/1.428329.

Moran, M. M., Nummela, S. & Thewissen, J. G. M. (2011) Development of the Skull of the Pantropical Spotted Dolphin (*Stenella attenuata*). *The Anatomical Record,* **294**, 1743-1756. doi:10.1002/ar.21388.

Morisaka, T. & Connor, R. C. (2007) Predation by killer whales (*Orcinus orca*) and the evolution of whistle loss and narrow-band high frequency clicks in odontocetes. *Journal of Evolutionary Biology,* **20**, 1439-1458. doi:10.1111/j.1420-9101.2007.01336.x.

NAV. (2017) *Nomina Anatomica Veterinaria 6th ed*. World Association of Veterinary Anatomists, Hanover (Germany), Ghent (Belgium), Columbia, MO (U.S.A.), Rio de Janeiro (Brazil).

Norris, K. S., Prescott, J. H., Asa-Dorian, P. V. & Perkins, P. (1961) An experimental demonstration of echolocation behavior in the porpoise, *Tursiops truncatus* (Montagu). *The Biological Bulletin,* **120**, 163-176. doi:10.2307/1539374.

Nummela, S., Thewissen, J. G. M., Bajpai, S., Hussain, S. T. & Kumar, K. (2004) Eocene evolution of whale hearing. *Nature,* **430**, 776. doi:10.1038/nature02720

https://www.nature.com/articles/nature02720#supplementary-information.

Oelschläger, H. A. (1990) Evolutionary morphology and acoustics in the dolphin skull. In J. A. Thomas & R. A. Kastelein (eds) *Sensory Abilities of Cetaceans: Laboratory and Field Evidence*, 137-162. Springer US, Boston, MA.

Oelschläger, H. H. A., Ridgway, S. H. & Knauth, M. (2010) Cetacean Brain Evolution: Dwarf Sperm Whale (*Kogia sima*) and Common Dolphin (*Delphinus delphis*) – An Investigation with High-Resolution 3D MRI. *Brain Behavioral and evolution,* **75**, 33-62. doi:10.1159/000293601.

Peredo, C. M., Uhen, M. D. & Nelson, M. D. (2018) A new kentriodontid (Cetacea: Odontoceti) from the early Miocene Astoria Formation and a revision of the stem delphinidan family Kentriodontidae. *Journal of Vertebrate Paleontology,* **38**, e1411357. doi:10.1080/02724634.2017.1411357.

Prahl, S., Huggenberger, S. & Schliemann, H. (2009) Histological and ultrastructural aspects of the nasal complex in the harbour porpoise, *Phocoena phocoena*. *Journal of Morphology,* **270**, 1320-1337. doi:10.1002/jmor.10760.

Reeves, R. R., McClellan, K. & Werner, T. B. (2013) Marine mammal bycatch in gillnet and other entangling net fisheries, 1990 to 2011. *Endangered Species Research,* **20**, 71-97. doi: https://doi.org/10.3354/esr00481.

Ridgway, S. H., Dibble, D. S., Alstyne, V. K. & Price, D. (2015) On doing two things at once: dolphin brain and nose coordinate sonar clicks, buzzes and emotional squeals with social sounds during fish capture. *The Journal of Experimental Biology,* **218**, 3987. doi:10.1242/jeb.130559.

Rodionov, V. A. & Markov, V. I. (1992) Functional anatomy of the nasal system in the bottlenose dolphin. In J. A. Thomas, R. A. Kastelein & A. Y. Supin (eds) *Marine Mammal Sensory Systems*, 147-177. Springer US, Boston, MA.

Schenkkan, E. J. (1972) On the nasal tract complex of *Pontoporia blainvillei* Gervais and d'Orbigny 1844 (Cetacea, Platanistidae). *Investigations on Cetacea,* **4**, 83-90.

Schenkkan, E. J. (1973) On the comparative anatomy and function of the nasal tract in odontocetes (Mammalia, Cetacea). *Bijdragen tot de Dierkunde,* **43**, 127-159.

Sereno, P. C. (2007) Logical basis for morphological characters in phylogenetics. *Cladistics,* **23**, 565-587. doi:10.1111/j.1096-0031.2007.00161.x.

Thewissen, J. G. M., Cohn, M. J., Stevens, L. S., Bajpai, S., Heyning, J. & Horton, W. E. (2006) Developmental basis for hind-limb loss in dolphins and origin of the cetacean bodyplan. *Proceedings of the National Academy of Sciences,* **103**, 8414. doi:10.1073/pnas.0602920103.

Thewissen, J. G. M., Cooper, L. N., George, J. C. & Bajpai, S. (2009) From land to water: The origin of whales, dolphins, and porpoises. *Evolution: Education and Outreach,* **2**, 272-288. doi:10.1007/s12052-009-0135-2.

Thewissen, J. G. M. & Heyning, J. E. (2007) Embryogenesis and development in *Stenella attenuata* and other cetaceans. In D. L. Miller (ed) *Reproductive Biology and Phylogeny of Cetacea: Whales, Porpoises and Dolphins*, 305-327. Science Publishers, Enfield NH.

Thewissen, J. G. M. & Williams, E. M. (2002) The Early Radiations of Cetacea (Mammalia): Evolutionary Pattern and Developmental Correlations. *Annual Review of Ecology and Systematics,* **33**, 73-90. doi:10.1146/annurev.ecolsys.33.020602.095426.

Thornton, S. W., McLellan, W. A., Rommel, S. A., Dillaman, R. M., Nowacek, D. P., Koopman, H. N. & Ann Pabst, D. (2015) Morphology of the Nasal Apparatus in Pygmy (*Kogia Breviceps*) and Dwarf (*K. Sima*) Sperm Whales. *The Anatomical Record,* **298**, 1301-1326. doi:10.1002/ar.23168.

Wei, C., Au, W. W. L., Ketten, D. R., Song, Z. & Zhang, Y. (2017) Biosonar signal propagation in the harbor porpoise's (*Phocoena phocoena*) head: The role of various structures in the formation of the vertical beam. *The Journal of the Acoustical Society of America,* **141**, 4179-4187. doi:10.1121/1.4983663.

Wei, C., Zhang, Y. & Au, W. W. L. (2014) Simulation of ultrasound beam formation of baiji (*Lipotes vexillifer*) with a finite element model. *The Journal of the Acoustical Society of America,* **136**, 423-429. doi:10.1121/1.4883597.

Foto da capa: Ignacio Moreno/CECLIMAR-UFRGS

Supplementary file - S1

Character list added to Kimura and Hasegawa (2019):

325 - Epicranial complex, posterior portion of the melon and dorsal bursae, alignment: 0- the bursae complex is aligned horizontally to the melon's branches; 1- the bursa complex is dorsoposteriorly positioned relative to the melon's branches (CI=50, RI=80).

The position the bursae complex (i.e. **Cana** and **Canp**) is highly variable among odontocetes, since some groups presented alignment with the posterior portion of the main **melon** (state 0), as observed in *Mesoplodon* sp., *P. phocoena*, *P. blainvillei*, *Cephalorhynchus commersonii*. The bursae complex is dorsoposteriorly positioned (state 1) in most delphinids and in *Ziphius cavirostris* (Cranford et al., 2008). This character is ordered in the light of Fink (1982) due to the description of the ontogenetic-based transformation demonstrated in the results.

326 - Epicranial complex, dense connective tissue, shape: 0-covering both lateral walls of the epicranial complex; 1-covering just the upper portion of the epicranial complex (CI=33, RI=50).

Some toothed whales exhibited a dense connective tissue surrounding dorsally and along both lateral walls (state 0) as observed in *Physeter* (Huggenberger et al., 2014), *Kogia* (Thornton et al., 2015), most ziphiids (Heyning, 1989), phocoenids (Huggenberger et al., 2009), *P. blainvillei* (Frainer et al., 2015) and *Orcinus orca* (Mead, 1975). Most delphinids presented restricted dense connective tissue at the upper portion of the epicranial complex (state 1) (Mead, 1975), as observed in the specimens of this family analysed here.

327 - Epicranial complex, right branch of the melon, connection to the main melon: 0-connected to the main melon; 1-not connected to the main melon (CI=33, RI=33).

In most non-physeterid toothed whales, the right branch of the melon is connected to the main body of the **melon**, i.e. the **mml** is composed of muscle fibers embedded within fat tissue (state 0), while in *Globicephala*, *Cephalorhynchus* (Mead, 1975) and *Lagenorhynchus* (Cranford et al., 1996), both structures were separated by a dense connective tissue, i.e. the **mml** presented hypertrophied tendons and associated dense connective tissue (state 1).

328 - Epicranial complex, nasal diverticula: 0-vestibular air sacs (**Snv**) > premaxillary air sacs (**Snp**); 1-vestibular air sacs < premaxillary air sacs (CI=100, RI=100).

The **Snv** presented greater dimensions compared to the **Snp** (state 0) in *P. blainvillei*, *P. phocoena* and *C. commersonii* (not included in the matrix) the. On the other hand, most delphinids exhibit greater size of the **Snp** compared to the **Snv** (state 1) (Schenkkan, 1973). Information from *Lipotes vexillifer* was taken from Chen et al. (1980).

329 - Epicranial complex, left branch of the melon: 0-present; 1-absent (CI=25, RI=62).

The left branch of the melon is a fat pathway positioned anteriorly relative to the left **Vnv** and presenting great compositional variation among odontocetes. However, fat structures positioned topographically in the same place in baleen whales (Cetartiodactyla: Mysticeti) have been described in *Balaenoptera acutorostrata*, *Eubalaena glacialis*, *Eschrichtius robustus* (Heyning and Mead, 1990) as well as

in *Caperea* and *Eubalaena* (Buono et al., 2015) (state 0). Heyning (1989) described "...*small amount of isolated adipose tissue*..." in *Berardius* (state 0). *Tursiops, Delphinus, Steno*, *Orcinus* (Cranford et al., 1996, McKenna et al., 2012), *Globicephala*, *Pseudorca*, *Cephalorhynchus* (Mead, 1975) and *Z. cavirostris* (Heyning, 1989) do not exhibit the left branch of the melon (state 1), but in its place a dense connective tissue and muscle fibers from the nasal plug muscles. This character is ordered in the light of Fink (1982) due to the description of compositional changes from fat tissues to dense connective tissues.

330 - Epicranial complex, melon and rostrum, size proportion: 0- the rostrum anterior to the melon is of equal length or longer than the epicranial complex length; 1- the rostrum anterior to the melon is smaller than the epicranial complex length or absent (CI=25, RI=75).

Odontocetes exhibited remarkable variation in the rostrum size and in the shape of the **melon** as some groups presented elongated rostra as observed in baleen whales (Buono et al., 2015, Heyning and Mead, 1990), *Berardius*, *Mesoplodon* (Heyning, 1989), *Lipotes vexillifer* (Wei et al., 2014)*, Inia geoffrensis*, *P. gangetica*, *P. blainvillei* (state 0). However, most odontocetes exhibit a small rostrum in front of the **melon** such as in *T. gephyreus* and most other delphinids, while phocoenids (Huggenberger et al., 2009), monodontids (e.g. *D. leucas*) and only a few delphinid species such as *Cephalorhynchus* and *O. orca* exhibit the rostrum totally covered by the **melon** (Mead, 1975) (state 1).

331 - Epicranial complex, melon, development: 0-absent; 1-present (CI=100, RI=100).

The **melon** is the greatest fat structure in the epicranial complex of odontocetes and is directly involved in the modulation of the clicks. The junk in *P. macrocephalus* is homologous to the **melon** in other odontocetes, and was coded accordingly. Baleen whales exhibit an epicranial complex but the structure is not well developed as in most odontocetes. The morphogenesis of the melon occurred during late fetal stages in dolphins (Cetartiodactyla: Delphinoidea), thus, it was considered an ontogenetic-based transformation and the character is ordered as proposed by Fink (1982).

LITERATURE CITED

Buono MR, Fernández MS, Fordyce ER, Reidenberg JS (2015) Anatomy of nasal complex in the southern right whale, *Eubalaena australis* (Cetacea, Mysticeti). *Journal of Anatomy,* **226,** 81-92.

Chen P, Lin K, Liu R (1980) Study of the anatomy and histology of the upper respiratory tract of Lipotes vexillifer Miller. *Acta Hydrobiologica Sinica,* **2,** 131-137 [In Chinese, English abstract].

Cranford TW, Amundin M, Norris KS (1996) Functional morphology and homology in the odontocete nasal complex: implications for sound generation. *Journal of Morphology,* **228,** 223-285.

Cranford TW, McKenna MF, Soldevilla MS, et al. (2008) Anatomic Geometry of Sound Transmission and Reception in Cuvier's Beaked Whale (*Ziphius cavirostris*). *The Anatomical Record,* **291,** 353-378.

Fink WL (1982) The conceptual relationship between ontogeny and phylogeny. *Paleobiology,* **8,** 254-264.

Frainer G, Huggenberger S, Moreno IB (2015) Postnatal development of franciscana's (*Pontoporia blainvillei*) biosonar relevant structures with potential implications for function, life history, and bycatch. *Marine Mammal Science,* **31,** 1193-1212.

Heyning JE (1989) Comparative facial anatomy of beaked whales (Ziphiidae) and a systematic revision among the families of extant Odontoceti. *Contributions in Science,* **405**.

Heyning JE, Mead JG (1990) Evolution of the nasal anatomy of cetaceans. In *Sensory Abilities of Cetaceans: Laboratory and Field Evidence* (eds Thomas JA, Kastelein RA), pp. 67-79. Boston, MA: Springer US.

Huggenberger S, André M, Oelschläger HHA (2014) The nose of the sperm whale: overviews of functional design, structural homologies and evolution. *Journal of the Marine Biological Association of the United Kingdom,* **96,** 783-806.

Huggenberger S, Rauschmann MA, Vogl TJ, Oelschläger HHA (2009) Functional Morphology of the Nasal Complex in the Harbor Porpoise (*Phocoena phocoena* L.). *The Anatomical Record,* **292,** 902-920.

Kimura T, Hasegawa Y (2019) A new species of Kentriodon (Cetacea, Odontoceti, Kentriodontidae) from the Miocene of Japan. *Journal of Vertebrate Paleontology***,** e1566739.

McKenna MF, Cranford TW, Berta A, Pyenson ND (2012) Morphology of the odontocete melon and its implications for acoustic function. *Marine Mammal Science,* **28,** 690-713.

Mead JG (1975) Anatomy of the external nasal passages and facial complex in the Delphinidae (Mammalia: Cetacea). *Smithsonian Contributions to Zoology,* **207,** 1-35.

Schenkkan EJ (1973) On the comparative anatomy and function of the nasal tract in odontocetes (Mammalia, Cetacea). *Bijdragen tot de Dierkunde,* **43,** 127-159.

Thornton SW, McLellan WA, Rommel SA, et al. (2015) Morphology of the Nasal Apparatus in Pygmy (*Kogia Breviceps*) and Dwarf (*K. Sima*) Sperm Whales. *The Anatomical Record,* **298,** 1301-1326.

Wei C, Zhang Y, Au WWL (2014) Simulation of ultrasound beam formation of baiji (*Lipotes vexillifer*) with a finite element model. *The Journal of the Acoustical Society of America,* **136,** 423-429.

Ancestral character reconstruction analysis:

100 - Distal sacs**:** ☐ absent; ■ present, situated immediately distal to museau de singe (1) (modified from Heyning, 1989).

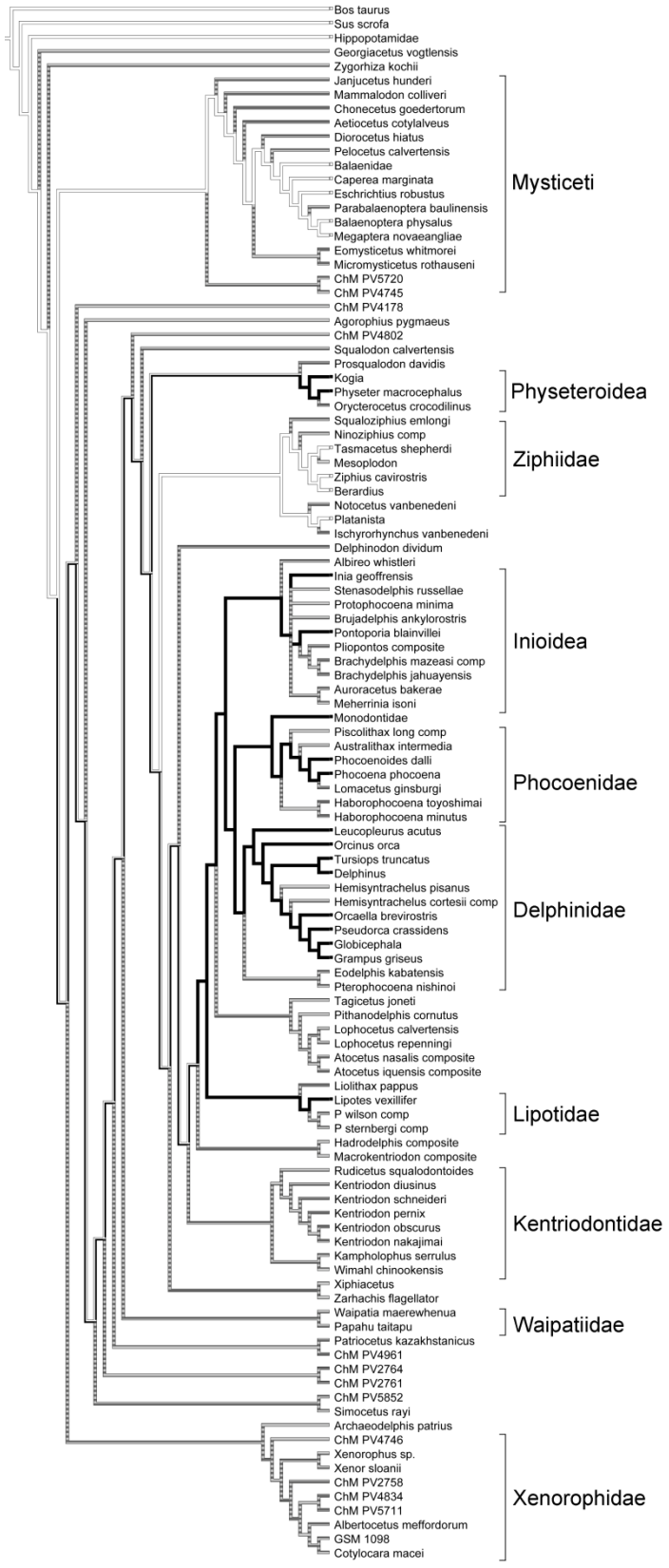

325 - Epicranial complex, posterior portion of the melon and dorsal bursae, alignment**:** ■ the bursae complex is aligned horizontally to the melon's branches; □ the bursa complex is dorsoposteriorly positioned relative to the melon's branches.

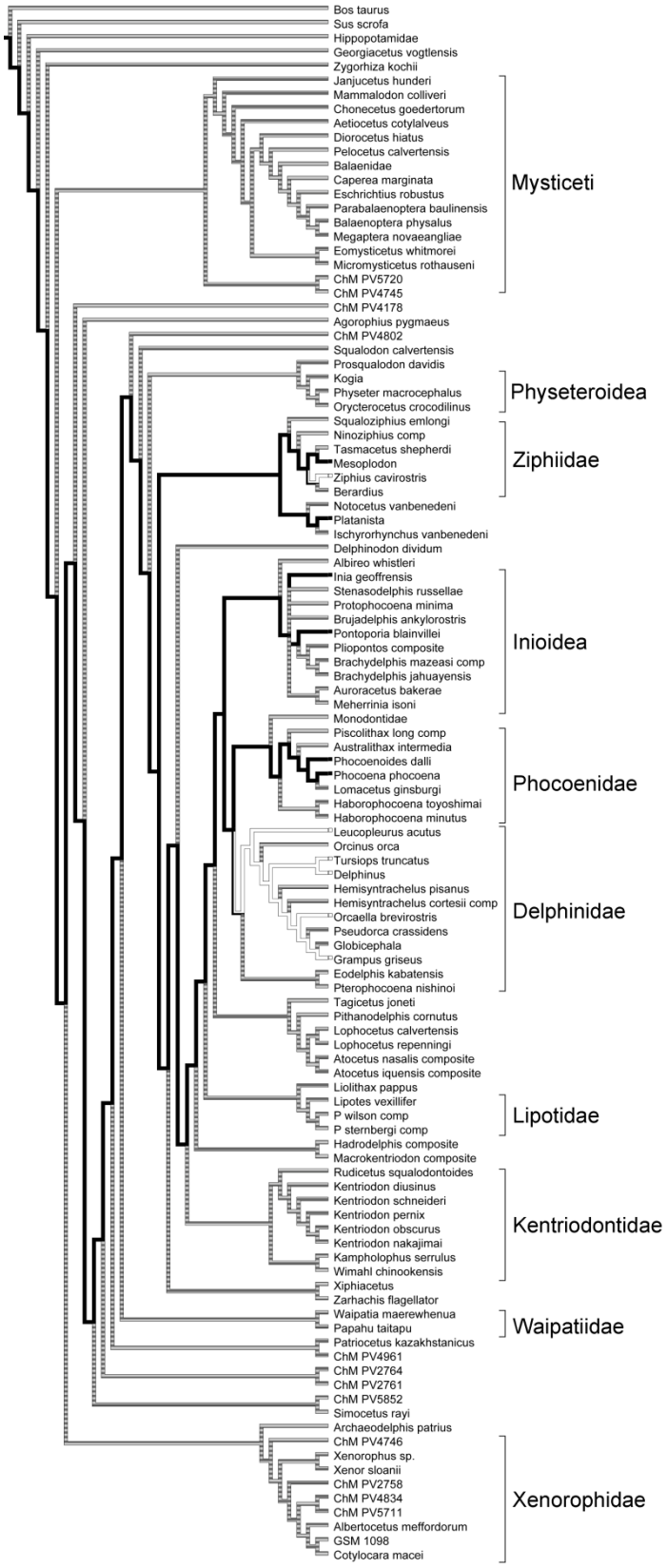

326 - Epicranial complex, dense connective tissue, shape**:** □ covering both lateral walls of the epicranial complex; ■ covering just the upper portion of the epicranial complex.

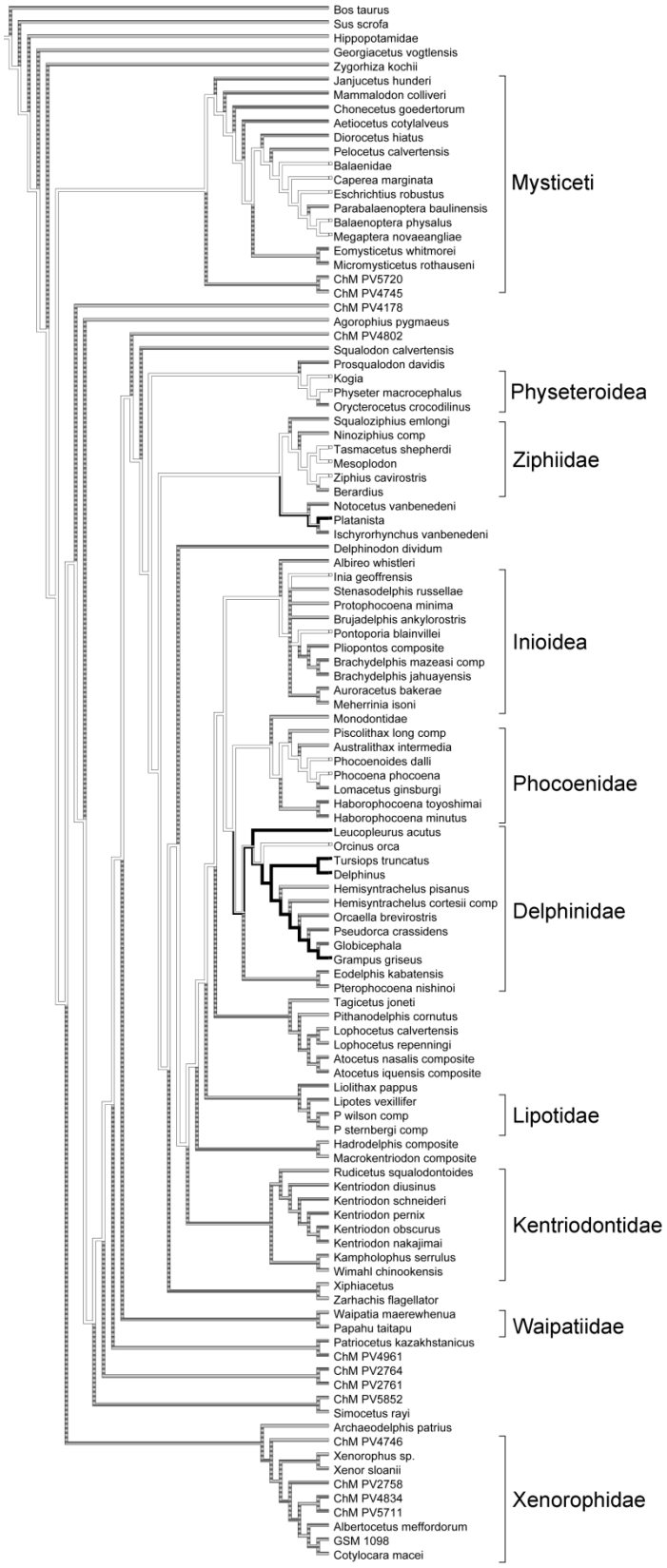

327 - Epicranial complex, right branch of the melon, connection to the main melon**:** □ connected to the main melon; ■ not connected to the main melon.

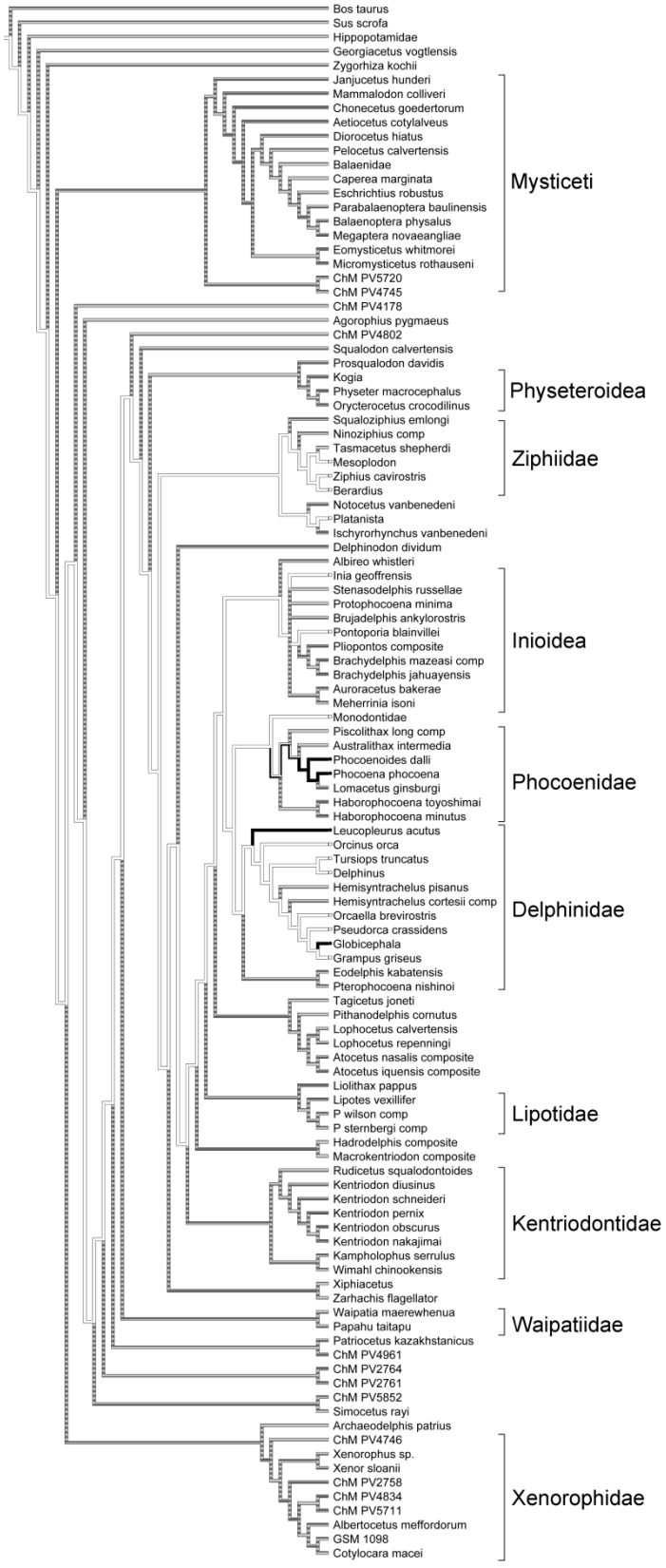

328- Epicranial complex, nasal diverticula**:** □ vestibular air sacs > premaxillary air sacs; ■ vestibular air sacs < premaxillary air sacs.

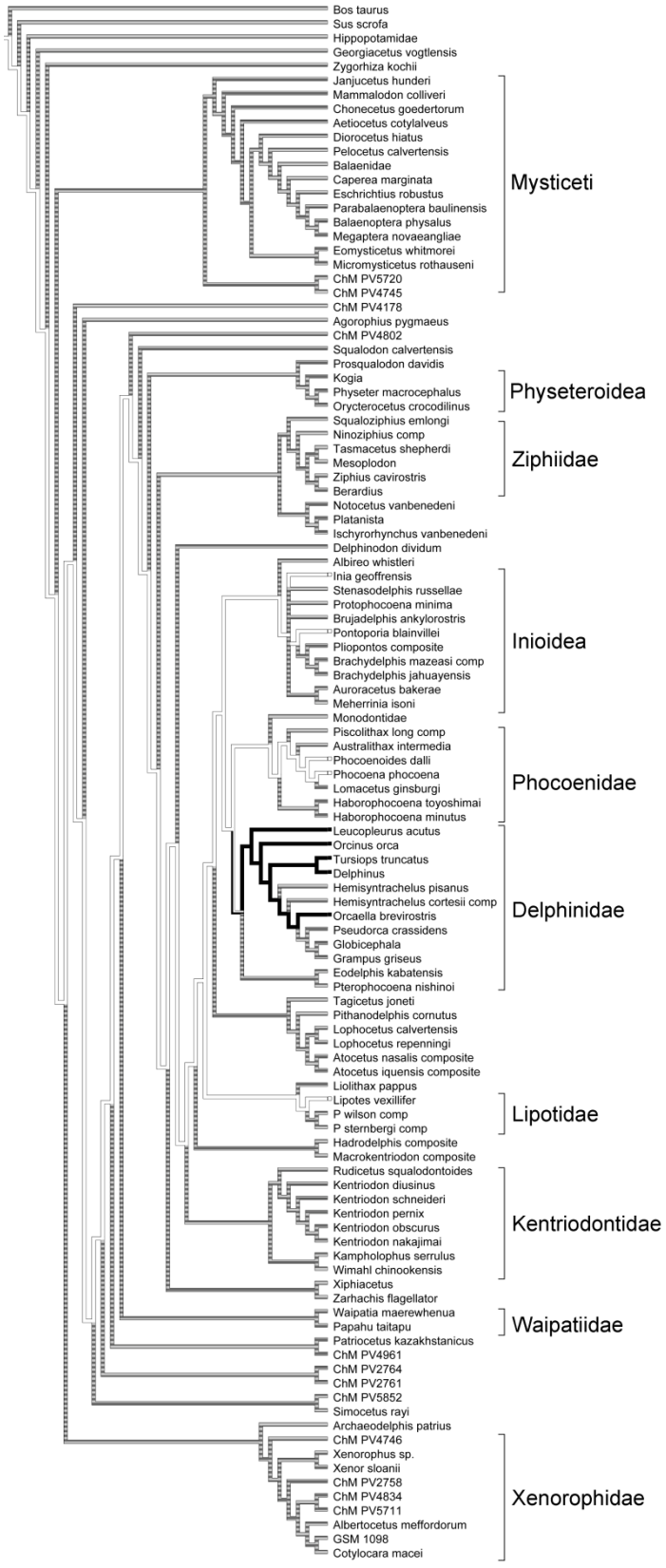

330- Epicranial complex, melon and rostrum, size proportion**:** ☐ the rostrum anterior to the melon is of equal length or longer than the epicranial complex length; ■ the rostrum anterior to the melon is smaller than the epicranial complex length or absent.

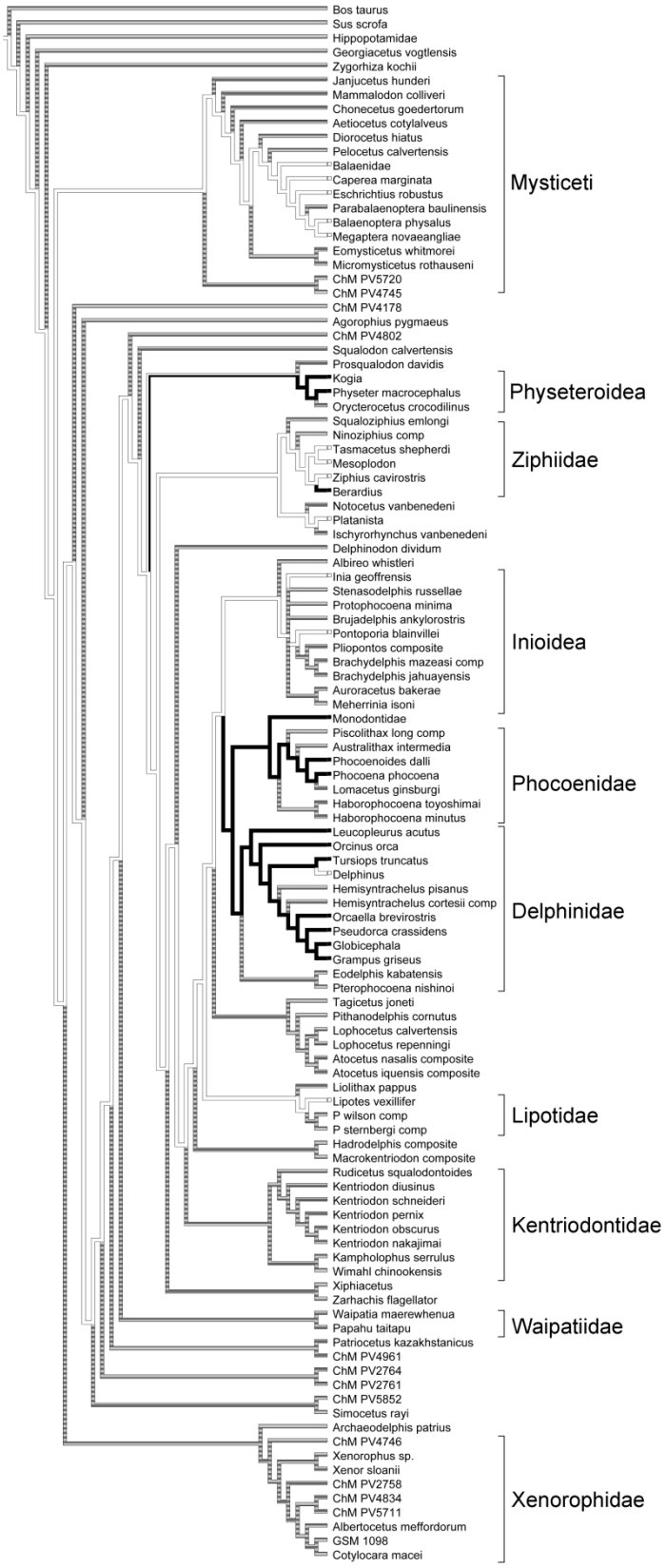

331- Epicranial complex, melon, development**:** □ absent; ■ present.

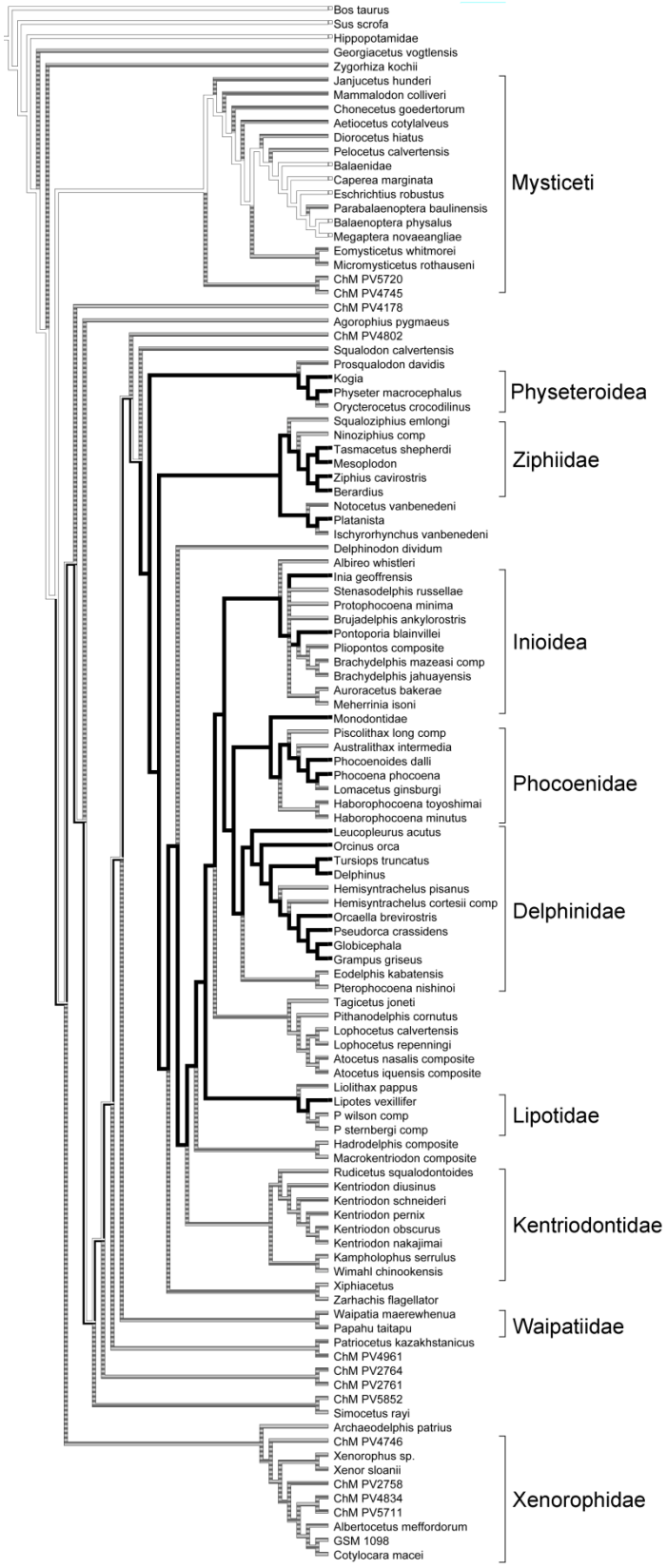

Supplementary file - S2

Bos taurus	??????0
Sus scrofa	??????0
Hippopotamidae	??????0
Caperea marginata	?0??000
Balaenidae	?0??000
Eschrichtius robustus	?0??000
Balaenoptera physalus	?0??000
Megaptera novaeangliae	?0???00
Physeter macrocephalus	?0???11
Kogia	?0???11
Tasmacetus shepherdi	?0???01
Ziphius cavirostris	000?101
Berardius	??0?011
Mesoplodon	100?001
Inia geoffrensis	1000001
Platanista	110?001
Lipotes vexillifer	???0?01
Pontoporia blainvillei	1000001
Monodontidae	??0?011
Phocoena phocoena	1010111
Phocoenoides dalli	1010111
Tursiops truncatus	0101111
Pseudorca crassidens	??0?111
Orcinus orca	?001111
Orcaella brevirostris	0?01111
Globicephala	??1?111
Grampus griseus	010?011
Leucopleurus acutus	0111011
Delphinus	0101101

Supplementary file - S3

Morphometric parameters of the specialized fat bodies (*Canp*, *Cana* and *melon*) in neonate and adult specimens of *Phocoena* (SNG 1903; CN 905), *Tursiops* (SAI no number, neonate; GEMARS 1447, adult), and *Pontoporia* (GEMM 220; GEMARS 1465), relative to the condylobasal length (CBL).

		Phocoena neonate			*Phocoena* adult			*Tursiops neonate*			*Tursiops* adult			*Pontoporia* neonate			*Pontoporia* adult		
Condylobasal length (CBL)		170.71	%CBL	%ECL	290.57	%CBL	%ECL	284.18	%CBL	%ECL	511.30	%CBL	%ECL	194.95	%CBL	%ECL	387.67	%CBL	%ECL
Distance between the *Canp* and the ventrolateral mesethmoid margin of the *ON*	right	7.93	4.65	10.17	18.73	6.45	12.86	13.81	4.86	13.22	18.55	3.63	8.31	3.39	1.74	5.78	4.58	1.18	3.89
	left	7.63	4.47	9.78	18.89	6.50	12.97	15.31	5.39	14.65	20.36	3.98	9.12	3.43	1.76	5.85	4.54	1.17	3.85
Maximum width of the *Canp*	right	6.93	4.06	8.88	12.64	4.35	8.68	9.93	3.49	9.50	20.22	3.95	9.06	4.77	2.45	8.14	6.91	1.78	5.86
	left	6.98	4.09	8.95	10.03	3.45	6.89	8.18	2.88	7.83	10.82	2.12	4.85	5.15	2.64	8.79	6.41	1.65	5.44
Height of the *Canp*	right	4.03	2.36	5.17	6.03	2.08	4.14	3.99	1.40	3.82	8.31	1.63	3.72	2.75	1.41	4.69	3.42	0.88	2.90
	left	3.27	1.92	4.19	4.06	1.40	2.79	2.53	0.89	2.42	6.30	1.23	2.82	2.64	1.35	4.51	3.23	0.83	2.74
Axial length of the *Canp*	right	2.06	1.21	2.64	3.53	1.21	2.42	1.29	0.45	1.23	3.70	0.72	1.66	3.74	1.92	6.38	4.25	1.10	3.61
	left	1.63	0.95	2.09	2.59	0.89	1.78	1.89	0.67	1.81	6.39	1.25	2.86	3.02	1.55	5.15	4.28	1.10	3.63
Maximum width of the *Cana*	right	6.46	3.78	8.28	11.21	3.86	7.70	9.95	3.50	9.52	20.67	4.04	9.26	3.08	1.58	5.26	6.08	1.57	5.16
	left	5.31	3.11	6.81	9.10	3.13	6.25	6.12	2.15	5.86	10.26	2.01	4.60	2.73	1.40	4.66	5.31	1.37	4.51
Height of the *Cana*	right	3.33	1.95	4.27	5.22	1.80	3.58	4.31	1.52	4.12	6.77	1.32	3.03	2.24	1.15	3.82	2.92	0.75	2.48
	left	2.88	1.69	3.69	3.93	1.35	2.70	3.19	1.12	3.05	5.48	1.07	2.46	2.13	1.09	3.63	3.09	0.80	2.62
Axial length of the *Cana*	right	2.90	1.70	3.72	4.29	1.48	2.95	1.38	0.49	1.32	2.36	0.46	1.06	2.25	1.15	3.84	3.28	0.85	2.78
	left	2.55	1.49	3.27	4.19	1.44	2.88	1.47	0.52	1.41	3.57	0.70	1.60	1.53	0.78	2.61	3.92	1.01	3.33
Largest width of the branches of the *melon*	right	-	-	-	-	-	-	39.05	13.74	37.37	69.90	13.67	31.32	9.01	4.62	15.38	14.60	3.77	12.39
	left	-	-	-	-	-	-	2.65	0.93	2.54	-	-	-	7.74	3.97	13.21	12.77	3.29	10.84
Maximum width of the *melon*		38.21	22.38	48.99	73.74	25.38	50.62	84.59	29.77	80.95	136.06	26.61	60.96	26.58	13.63	45.36	42.99	11.09	36.48
Length of the *melon* with its right fat branch		63.68	37.30	81.64	124.90	42.98	85.75	116.18	40.88	111.18	242.46	47.42	108.62	59.55	30.55	101.62	116.26	29.99	98.67
Epicranial complex length (ECL)	point to point	78.19	45.80	-	147.32	50.70	-	113.36	39.89	-	235.30	46.02	-	59.71	30.63	-	116.54	30.06	-
	in parallel	78.00	45.69	-	145.66	50.12	-	104.47	36.76	-	223.21	43.66	-	58.60	30.06	-	117.83	30.39	-
Elevation angle of the *Canp* and *Cana* complexes	right	16.39°	-	-	8.65°	-	-	22.96°	-	-	20.11°	-	-	18.90°	-	-	16.90°	-	-
	left	15.42°	-	-	7.00°	-	-	22.80°	-	-	19.51°	-	-	18.90°	-	-	16.90°	-	-
Height of the cranial vault		51.10	29.93	65.51	68.92	23.72	47.32	84.27	29.65	80.64	128.27	25.08	57.47	50.16	25.73	85.60	60.47	15.60	51.32

CAPÍTULO IV

A ORQUESTRA AMEAÇADA DOS GOLFINHOS

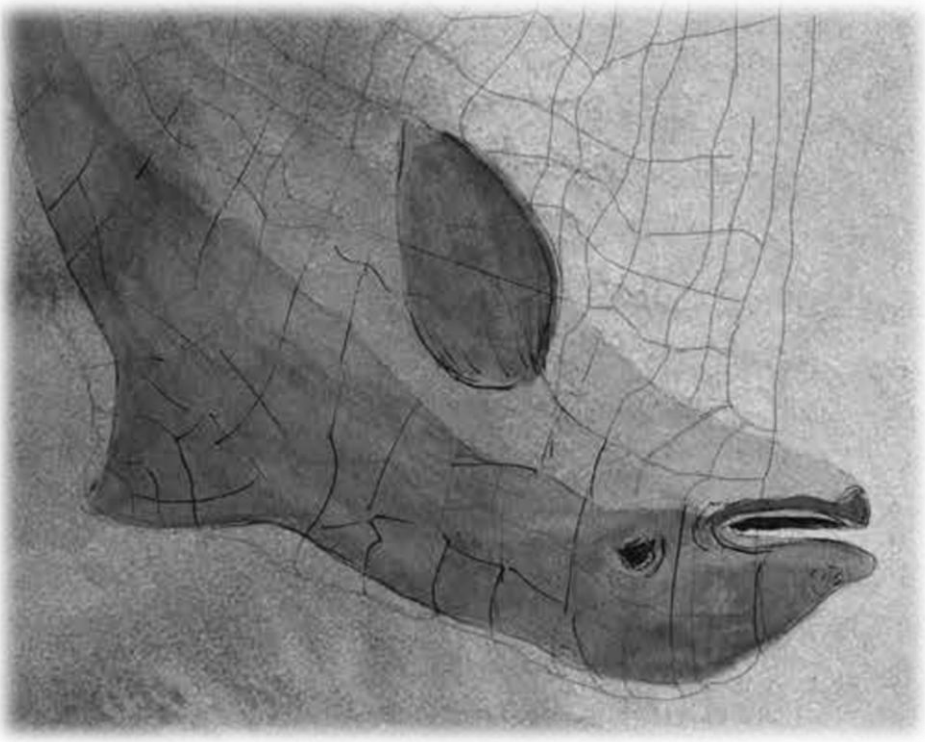

"*Se a educação sozinha não transforma a sociedade, sem ela tampouco a sociedade muda*."

Paulo Freire

*Manuscrito redigido para popularização da ciência nos formatos da revista Ciência Hoje

A ORQUESTRA AMEAÇADA DOS GOLFINHOS

Imagine que tu estás sentado na primeira fila de uma grande orquestra. Conseguimos perceber os diversos tipos de sons que compõem a obra a ser expressada pelos músicos: dos sons graves (i.e. baixa frequência - kHz) dos trombones e surdos, às notas mais agudas (i.e. maior frequência - kHz) das flautas e violinos. A composição de sons ao longo da interpretação de uma obra musical é resultado da sincronia de frases provindas de diferentes fontes sonoras com timbres únicos. O timbre dos instrumentos musicais, por sua vez, é caracterizado pela produção de inúmeros sons harmônicos resultado da interação da fonte sonora (e.g. cordas, sopro ou percussão) com o formato e composição de cada equipamento. A harmonicidade dos sons não apenas nos permite apreciar as vibrações que chegam aos nossos ouvidos, mas interpretar emocionalmente a mensagem de um compositor a partir de seus diferentes ritmos e tons. Da alegria Barroca em "*As quatro estações*" de Vivaldi (especialmente na primavera) ao romantismo único da sonata n 14 de Beethooven, o ouvido humano é capaz de perceber os sons mais agudos como violinos (~15kHz) e clarinetas (~12kHz), sendo possível perceber variações de pressão no ar (som) com frequências até 20 kHz.

Agora, imagine um grupo de mamíferos que não apenas evoluiu um instrumento biológico capaz de compor assinaturas e repertórios sonoros que ultrapassam os 150 kHz de frequência (~7,5 vezes maior do que o limite da audição humana), indispensável para a manutenção de uma sociedade complexa através da comunicação e que serve de principal ferramenta para a navegação e caça. A história evolutiva do sonar biológico dos golfinhos ajuda a compreender impactos de natureza humana devido à perturbações de seus ambientes naturais.

ADAPTAÇÕES MORFOLÓGICAS PARA VIVER E FAZER SOM DENTRO D'ÁGUA

Cetáceos são mamíferos adaptados exclusivamente ao ambiente aquático, mas descendem de formas quadrúpedes terrestres. As principais adaptações morfológicas do grupo para a essa transição foi a modificação das patas dianteiras em nadadeiras, redução das patas traseiras em ossos vestigiais, alongamento do corpo, aquisição de nadadeiras cartilaginosas dorsal e caudal, perda da olfação (i.e. evidente pela redução do bulbo olfatório), e a migração das narinas para o topo da cabeça.

Golfinhos (Fig. 1) são cetáceos odontocetos, grupo que inclui as cachalotes, baleias bicudas e outros pequenos golfinhos. A principal diferença entre os odontocetos e os misticetos (i.e. as baleias verdadeiras como a baleia-azul e a baleia-jubarte) se dá na transformação da cabeça ao longo do desenvolvimento fetal, resultando em distinta organização topográfica e estrutural do crânio e aparato alimentar na fase adulta. As modificações morfológicas são causadas, principalmente, pelos fatores reguladores do desenvolvimento em nível celular, modificando tecidos até a redução ou perda de estruturas (e.g. patas traseiras em cetáceos reduzidas aos ossos vestigiais, bulbo olfatório) como a aquisição de novidades evolutivas (e.g. nadadeiras cartilaginosas, orifício respiratório no top oda cabeça, etc.).

As baleias perdem os dentes e desenvolvem cerdas bucais queratinizadas na região do palato para a captura de pequenos invertebrados (e.g. krill) através da filtração. Odontocetos desenvolvem não apenas dentes especializados para a captura de presas como peixes e cefalópodes, como um sistema emissor e receptor de som que funciona como um sonar para navegação e forrageio (Fig. 1). Alguns autores sugerem que os odontocetes evoluíram com hábitos noturnos, de maneira a se alimentar de peixes e cefalópodes

(principalmente com conchas) demersais que se movimentam todas as noites em uma migração vertical da fauna bentônica para águas mais rasas. Isso explicaria o porquê de algumas espécies, como as baleias bicudas, mergulharem até mais de seis mil metros de profundidade onde essa fauna é abundante (i.e. é “noite o dia inteiro”).

O isolamento acústico do ouvido interno por um seio de ar e o desenrolamento da cóclea representam a adaptação a um tipo de audição direcional e de alta frequência em odontocetos primitivos (i.e. fósseis). Ainda, a musculatura facial e tecidos conjuntivos associados à passagem nasal se desenvolvem de forma que o nariz adquire não apenas a função de produção como de modulação do som produzido tanto para a comunicação quanto para a ecolocalização.

PRODUÇÃO E PERCEPÇÃO DE SONS DE ALTA FREQUÊNCIA

Somente comprovado no início da década de 60, o sonar biológico dos odontocetos é destinado à navegação e ao comportamento de forrageio. Consiste na percepção de ecos e/ou reverberações como informações do ambiente ou presa, a partir de sons gerados pelo próprio animal que os assimila. O som é produzido através da passagem do ar em um ponto específico da passagem nasal, os lábios-fônicos (*phonic lips*), que criam estalos (*clicks*) a partir da abertura e rápido fechamento dos músculos anteriores à passagem nasal. Os estalos são conduzidos por pares de corpos gordurosos (i.e. bursas dorsais posterior e anterior), adjacentes à passagem nasal, até o melão: um arranjo de tecido adiposo entre músculos e composto por fibras colágenas à frente da fonte produtora de som que tem a função de colimar (i.e. polarizar) as ondas para o ambiente à medida que diminui a impedância do som para que, assim, atravesse do tecido para o meio aquático com maior energia.

Os sons são refletidos pelo ambiente e percebidos pela mandíbula que, através dos corpos gordurosos presentes na janela mandibular, são conduzidos para a bula timpânica e codificados no cérebro. Estudos recentes sugerem que os dois lados da passagem nasal produzem sons independentes e de maneira simultânea, sendo os sons voltados para a ecolocalização exclusivamente pelo lado direito, e comunicação pelo lado esquerdo (Fig. 1, Fig. 4).

Odontocetos produzem, em geral dois tipos de som: os *clicks* explosivos (*burst clicks*), e os *clicks* voltados para a ecolocalização. Os *burst clicks* são clicks com um intervalos tão curtos que parecem sons contínuos, assim muitas vezes denominados "grunhidos". Os *clicks* voltados para a ecolocalização apresentam maior frequência de onda e são sempre seguidos de um segundo *click*, resultado da interação da fonte sonora com o crânio e as barreiras acústicas. Os assobios são mais comuns em golfinhos que apresentam sociedades complexas baseadas na fusão e fissão de grupos como os delfinídeos (Família Delphinidae), a família mais diversa dentre os odontocetos.

A estrutura física desses sons é única para cada espécie e está relacionada com a variabilidade morfológica encontrada nas estruturas produtoras do som no grupo. A direcionalidade no som dos golfinhos evoluiu tanto nos sons para comunicação como para a ecolocalização. Os sons voltados para a comunicação são em geral repletos de campos harmônicos atingindo até 22 oitavas em algumas espécies. Esses harmônicos são imprescindíveis para a caça em grupo, uma vez que outros golfinhos de um mesmo grupo podem localizar a fonte geradora de informação (i.e. outro golfinho) a partir da harmônico que chega às suas mandíbulas e, assim, se coordenarem durante uma caça em grupo.

A direcionalidade nos sons voltados para a ecolocalização evoluiu de tal maneira a projetar a distância de alcance máxima do sonar para frente, modulando o feixe de som a partir de sua interação com as estruturas que circundam a fonte de sonora, como os sacos de ar, os principais corpos gordurosos presentes no nariz e o crânio. Uma vez que as frequências maiores atenuam mais facilmente no ambiente, a evolução de grupos com produção de sons de maior frequência tendem a apresentar sonares biológicos com propriedades extremamente direcionais.

UMA ORQUESTRA AMEAÇADA

A variabilidade morfológica encontrada nas estruturas produtoras do som em odontocetos reflete os diferentes tipos de padrões acústicos encontrado no grupo. A maioria dos odontocetos, como o golfinho-nariz-de-garrafa ou boto (Fig. 1, Fig. 2), são ecolocalizadores com amplo espectro e alta intensidade (dB) comparado à pequenos odontocetos (veja abaixo). O boto (*Tursiops gephyreus*) faz parte de um grupo de golfinhos amplamente distribuído e apresenta um dos maiores cérebros do reino animal. Possui um dos maiores repertórios acústicos dentre todos os odontocetos, e suas atividades de caça vão desde perceber peixes enterrados no fundo do substrato até interações interespecíficas como a pesca cooperativa no sul do Brasil.

Alguns odontocetos como as cachalotes-anãs, focenídeos (Família Phocoenidae, sem nome popular na língua Portuguesa), golfinhos do gênero *Cephalorhynchus*, e a toninha (*Pontoporia blainvillei*) (Fig. 3) evoluíram padrões de *clicks* para comunicação e ecolocalização com frequência muito superior à maioria dos odontocetos (i.e. acima de 150 KHz) produzido em um feixe de som altamente direcional. A evolução de sons de alta frequência e direcionais parece ter evoluído nesses grupos em resposta a um ambiente mais ruidoso: nas zonas costeiras (no caso da toninha, golfinhos do gênero *Cephalorhynchus* e focenídeos), devido ao ambiente mais ruidoso e com predadores com ouvidos também sensíveis como orcas (*Orcinus orca*); e no oceano aberto (no caso das cachalotes-anãs e pigmeias), provocado por intensos ventos e agitação marítima durante a irradiação dessa linhagem.

Estudos recentes demonstram que a evolução de sonares extremamente direcionais em golfinhos (Cetartiodactyla: Delphinida), como o da toninha (Fig. 4), no ambiente costeiro surgiu de forma independente nos três grupos citados, ou seja, o som pode ter propriedades parecidas mas a forma como ele é produzido é totalmente diferente. No entanto, os três grupos apresentam muitas coincidências que podem estar relacionadas com a convergência na produção do som: além de ser costeiros e apresentarem produção de som particular comparado a outros golfinhos, os três grupos apresentam corpo reduzido, vivem em grupos pequenos, se comunicam primariamente por *burst clicks* e são extremamente ameaçados. A maior ameaça? A captura acidental em redes de emalhe.

Sonares direcionais, assim como animais com visão restrita, perdem informações que estão na periferia do alcance de seu sistema de navegação. Tanto os focenídeos (que inclui o cetáceo mais ameaçado do mundo por emalhamento em redes de pesca, a Vaquita *Phocoena sinus*) quanto os golfinhos do gênero *Cephalorhynchus* e a toninha apresentam alta mortalidade de animais juvenis em redes de emalhe. Uma vez que esses animais são conhecidos por apresentarem significativa troca na dieta (revelando amadurecimento comportamental) e mudanças na topografia das estruturas envolvidas na produção do som, é plausível que animais juvenis não consigam perceber as redes com seus sonares imaturos. Embora há evidência de

comportamento epimelético (i.e. quando outro indivíduo da mesma espécie tenta ajudar outro) evidenciando que talvez as mães possam perceber as redes, a mortalidade de adultos é muito maior que golfinhos que se diibuem no mesmo local como os botos (Fig. 2). A complexidade do sonar biológico desses pequenos odontocetos pode estar relacionado com a maior vulnerabilidade desses grupos.

A interação negativa com a pesca de emalhe tanto da toninha no Brasil (Fig. 4), Uruguai e Argentina, quanto da Vaquita no Golfo do México também é complexa: comunidades que dependem de um recurso que está a caminho do colapso e animais que, acidentalmente, morrem nas redes de pesca. A criação de áreas de proteção integral não será (e talvez não foi no caso da Vaquita) suficiente para conter essa interação negativa que tende a crescer. Além da criação de áreas permanentes de exclusão de pesca, tecnologias baseadas nas particularidades do som de cada espécie inseridas em aparatos pesqueiros ainda são escassas ou inexistentes (embora o capital internacional gire em torno de *air-guns* que são sonares em navios de sísmica em busca de combustíveis fósseis, os quais são conhecidos por causar perturbações extremas no ambiente marinho e até encalhes em massa de organismos com ouvidos ultra-sensíveis como baleias-bicudas).

A orquestra dos golfinhos e demais odontocetos, e como funciona cada tipo de instrumento produtor de som nesse grupo, ainda é muito pouco conhecida, e, talvez, seus compositores e instrumentistas mais complexos não estão suportando a platéia que cresce.

Imagem da Capa:Sebastian Grote/Universidade de Colônia-Alemanha

Fig. 1. O boto ou golfinho-nariz-de-garrafa, *Tursiops gephyreus*, na barra do rio Tramandaí, Rio Grande do Sul, Brasil. Modelos em 3D do crânio e das principais gorduras envolvidas na modulação do som dessa espécie foram sobrepostos à imagem. Foto: Ignacio Moreno/CECLIMAR-UFRGS.

Fig. 2. Botos na barra do rio Tramandaí, Rio Grande do Sul, Brasil. A harmonicidade na comunicação dos golfinhos, promovida pelo timbre de seus instrumentos produtores de som e pela forma como é manipulado, é crucial para a caça em grupo. Os golfinhos são coordenados em movimento pelo líder do grupo, o qual produz sons com múltiplos harmônicos a fim de demonstrar sua posição para os outros membros do grupo. Foto: Ignacio Moreno/CECLIMAR-UFRGS.

Fig. 3. A toninha, *Pontoporia blainvillei*, na Baía da Babitonga, Santa Catarina, Brasil, é o golfinho mais ameaçado do Atlântico devido à mortalidade acidental em redes de pesca. Foto: Projeto Toninhas/UNIVILLE.

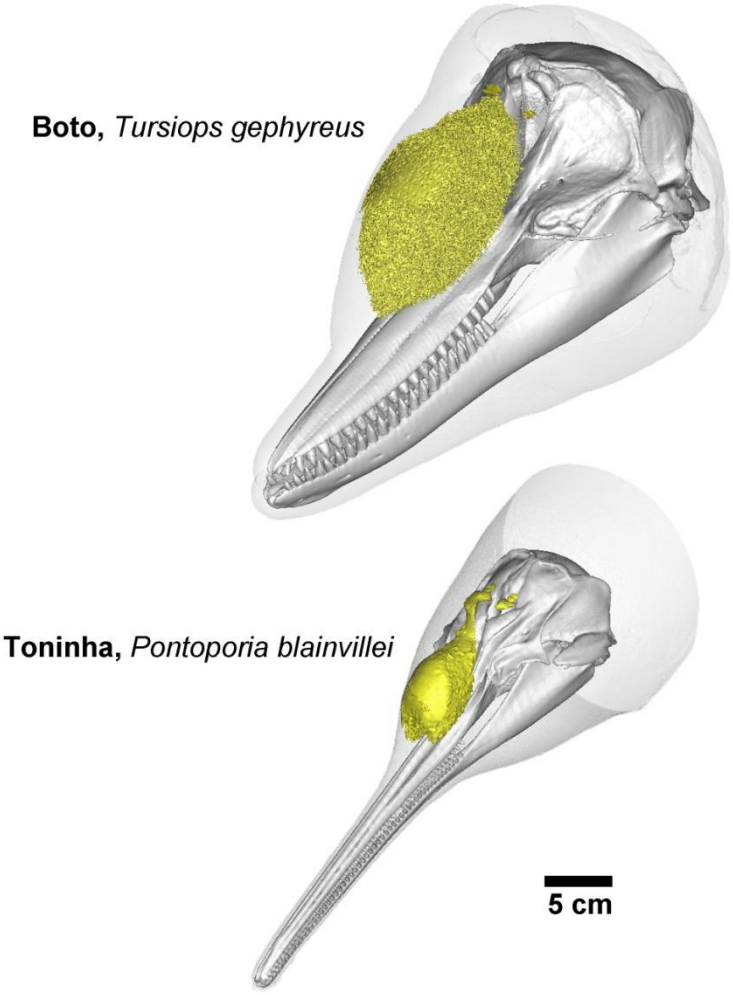

Fig. 4. Modelos em 3D gerados a partir de imagens de tomografia computadorizada caracterizando os principais corpos gordurosos (em amarelo) envolvidos na modulação do som no boto, *Tursiops gephyreus* (acima), e na toninha, *Pontoporia blainvillei* (abaixo).

Fig. 5. Toninhas (*Pontoporia blainvillei*) capturadas acidentalmente em uma rede de pesca na costa do Rio Grande do Sul na década de 90. Foto: Ignacio Moreno/CECLIMAR-UFRGS.

CAPÍTULO V

CONCLUSÃO

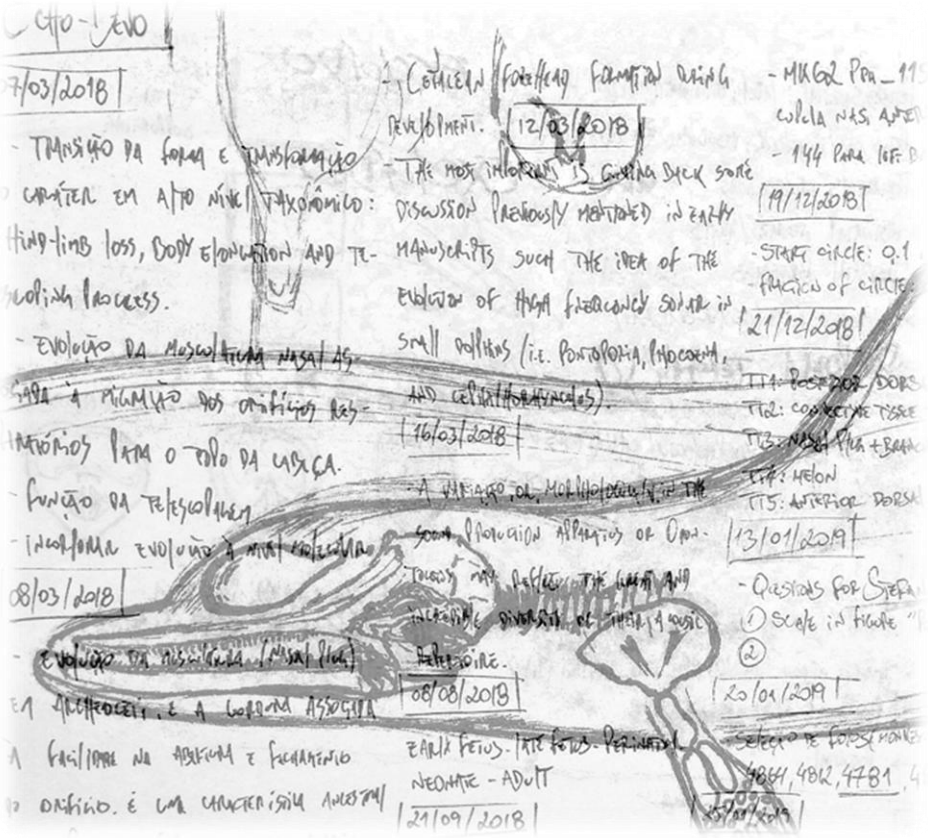

"*Nothing in biology makes sense except in the light of evolution*."

Theodosius Dobzhansky (1964) *American Zoologist*, 4: 443-452

CONSIDERAÇÕES FINAIS

A investigação da variação morfológica do complexo epicranial dos odontocetos (Cetartiodactyla: Odontoceti), incluindo as principais transformações ao longo da ontogenia em golfinhos, foi útil para propor não apenas como o órgão produtor de som surgiu durante a evolução da linhagem, mas como se aperfeiçoou em cada grupo frente às adaptações ao ambiente e à seus padrões comportamentais. O resultado de maior valor dessa tese é que a adaptação morfológica de golfinhos que produzem sons de alta frequência em banda estreita (espécies NBHF, *narrow-band high frequency species*) se dá pela combinação de características únicas para cada grupo, as quais derivaram de deprocessos heterocrônicos independentes durante a evolução de Delphinida (Cetartiodactyla: Odontoceti). A forma como os resultados foram obtidos reflete a interdisciplinaridade metodológica aplicada tanto no âmbito prático, a partir da utilização de diversas técnicas em morfologia para investigar tecidos moles; como teórico, uma vez que resgata conceitos antigos aplicados às transformações ontogenéticas à luz da sistemática filogenética para integrar à análise cladística aos conceitos da síntese evolutiva estendida. A identificação de distintos padrões ontogenéticos para a porção posterior do melão e do melão, bem como as distintas origens dessas estruturas, implicou na separação da estrutura em três partes: "melão posterior direito" (*Corpus adiposum nasalis terminalis, partes posteriores dexter*), "melão posterior esquerdo" (*Corpus adiposum nasalis terminalis, partes posteriores sinister*), e melão (*Corpus adiposum nasalis terminalis*). A morfogenia do saco de ar vestibular é descrita pela primeira vez, bem como a comparação interespecífica de toda a ontogenia em três grupos de cetáceos. De maneira mais específica, foi possível discutir as adaptações morfológicas das estruturas moduladoras do som em golfinhos frente às novas descobertas sobre a funcionalidade do órgão produtor de som. A partir da reconstrução ancestral de caracteres, foi possível inferir que grupos ancestrais a todos os golfinhos atuais provavelmente apresentavam sonares com características parecidas com àquelas espécies NBHF. Assim, tanto as características morfológicas quanto comportamentais são resultado dos processos heterocrônicos pedomórficos (e.g. redução do saco de ar vestibular e lento desenvolvimento da porção posterior (nasal) do osso pré-maxilar em Delphinidae; redução do rostro em Delphinoidea) e hipermórficos (e.g. aquisição do melão em odontocetos; migração da passagem nasal para posterior ao osso frontal de forma independente em Mysticeti e Odontoceti). A síntese de idéias sobre o tema abordado nessa tese pode ser útil como uma ferramenta educacional uma vez que exemplifica um método prático, nunca antes utilizado, para a determinação de homologias e investigar a evolução da forma biológica. O estudo da evolução dos organismos e a exemplificação didática desse fenômeno é de extrema relevância em um período em que a sociedade vive na condição do surgimento de revisionismos a partir da distorção de fatos. O negacionismo da teoria evolutiva, bem como outros assuntos já muito esclarecidos cientificamente, é uma realidade na sociedade atual que vivemos sendo a biologia - e principalmente a teria evolutiva em si - uma ferramenta para o desenvolvimento do senso crítico em estágios iniciais de desenvolvimento escolar. Os golfinhos são utilizados aqui como modelos biológicos úteis (i.e. carismáticos) uma vez que suas ameaças impactam de forma negativa aos olhos de quem observa (principalmente na sociedade oidental). A mortalidade de espécies com sonares mais direcionais pode ser fruto da natureza do órgão responsável pela navegação e orientação desses organismos, que representam resquícios evolutivos de sonares complexos que evoluíram a 18 milhões de anos atrás. Imagem: caderno de notas do autor.